GEORGIA
DEPARTMENT OF NATURAL RESOURCES
ENVIRONMENTAL PROTECTION DIVISION

Final 2017 Ozone Exceedance Report for Atlanta, Georgia

Prepared by:
Data and Modeling Unit
Planning and Support Program
Air Protection Branch
Environmental Protection Division

July 25, 2018

Executive Summary

Ozone concentrations in Georgia have decreased over the past 25 years. On October 1, 2015, the 8-hour ozone National Ambient Air Quality Standard (NAAQS) was lowered from 75 ppb to 70 ppb. In 2017, only two Metropolitan Statistical Areas (MSAs) experienced ozone exceedance days where the measured 8-hour average ozone concentration was above 70 ppb. In comparison, there were six MSAs with ozone exceedances in 2016. For each ozone exceedance day, the Data and Modeling Unit developed an initial exceedance report with preliminary analyses of air quality, meteorological, and emission data to aid in determining the cause of the ozone exceedance. If ozone exceedances occur frequently, the design value (3-year average of annual 4th highest daily maximum 8-hour average ozone concentrations) can exceed the ozone NAAQS, and EPA can classify the area as nonattainment. The recently certified 2017 ozone measurements show that Atlanta is the only area in Georgia currently violating the 2015 ozone NAAQS.

A final, in-depth ozone exceedance report was developed for the Metro Atlanta area to identify causes of the 2017 ozone exceedances. The report includes: trend analysis of ozone concentrations and meteorological conditions in Atlanta during 1990-2017; multiple linear regression (MLR) analysis and classification and regression tree (CART) analysis to understand the relationship between ozone and environmental variables; Hybrid Single Particle Lagrangian Integrated Trajectory (HYSPLIT) back trajectory analysis to determine the origin of air masses and establish source-receptor relationships on ozone exceedance days; animation of ozone and wind conditions to illustrate ozone formation and transport; and analysis of VOC and NOx measurements to understand the impacts of precursors on ozone formation. Also, a preliminary investigation of traffic congestion impacts on ozone exceedances was performed.

In summary, the following factors likely contributed to 2017 ozone exceedances in Atlanta:

1) Low relative humidity in the afternoon;
2) High daily maximum air temperature;
3) Low cloud coverage;
4) High ozone on previous days;
5) Low wind speed;
6) NOx emissions, mainly from local on-road mobile sources;
7) VOC emissions, mainly from biogenic sources in the summer months with additional contributions from local on-road mobile sources in the evening and morning hours; and
8) Local transport of emissions from the Atlanta urban core to monitors outside the urban core.

This final ozone exceedance report can be used to guide future air quality management practices in Georgia to aid in preventing future ozone exceedances.

List of Acronyms

aNMOC	Anthropogenic Non-Methane Organic Carbon
AQI	Air Quality Index
AQS	Air Quality System
CAMD	Clean Air Markets Division
CART	Classification and Regression Tree
CAS	Chemical Abstract Service
CASTNET	Clean Air Status and Trends Network
CO	Carbon Monoxide
EBIR	Equal Benefit Incremental Reactivity
ENSO	El Niño–Southern Oscillation
EPA	U.S. Environmental Protection Agency
EPD	Environmental Protection Division
GIF	Graphics Interchange Format
HCHO	Formaldehyde
HYSPLIT	Hybrid Single Particle Lagrangian Integrated Trajectory
IDL	Interactive Data Language
IR	Incremental Reactivity
LIDAR	Light Detection and Ranging
LT	Local Time
MAE	Mean Absolute Error
MB	Mean Bias
mb	millibar (=10^{-3} bar)
MDA8O3	Maximum Daily 8-hour Average Ozone Concentrations
MIR	Maximum Incremental Reactivity
MLR	Multiple Linear Regression
MOIR	Maximum Ozone Incremental Reactivity
MSAs	Metropolitan Statistical Areas
NAAQS	National Ambient Air Quality Standards
NAM	North American Mesoscale
NCEI	National Centers for Environmental Information
NEI	National Emissions Inventory
NMB	Normalized Mean Bias
NME	Normalized Mean Error
NOAA	National Oceanic and Atmospheric Administration
NOx	Oxides of Nitrogen
OMI	Ozone Monitoring Instrument
PAMS	Photochemical Assessment Monitoring Stations
PBL	Planetary Boundary Layer
QA	Quality Assurance
RH	Relative Humidity
RMSE	Root Mean Square Error
RWC	Reactivity-weighted concentrations
SEARCH	Southeastern Aerosol Research and Characterization
VOC	Volatile Organic Compounds

Table of Contents

1. Introduction

Ozone pollution can impair lung function and cardiovascular health. Ground-level ozone is formed in the atmosphere by chemical reactions of volatile organic compounds (VOCs) and oxides of nitrogen (NOx) in the presence of sunlight. Sources of VOCs include fuel combustion, fuel evaporation, paints, solvents, and vegetation. NOx emissions are primarily from the combustion of fuels. The U.S. Environmental Protection Agency (EPA) lowered the National Ambient Air Quality Standards (NAAQS) for ground-level ozone from 75 ppb (2008 ozone NAAQS) to 70 ppb (2015 ozone NAAQS) to better protect public health and welfare.

Ozone concentrations in Georgia have decreased over the years (Figure 1) in various Metropolitan Statistical Areas (MSAs). The Metro Atlanta area was the only area in Georgia designated nonattainment for the 2008 ozone standard and was redesignated to attainment in June 2017. On April 30, 2018, EPA designated seven counties (Bartow, Clayton, Cobb, DeKalb, Fulton, Gwinnett, and Henry) as nonattainment for the 2015 ozone standard.

In 2017, only two MSAs (Atlanta-Sandy Springs-Marietta and Augusta) experienced ozone exceedances where the measured 8-hour average ozone concentration was above 70 ppb. In comparison, there were six MSAs with ozone exceedances in 2016. For each ozone exceedance day, the Data and Modeling Unit developed an initial exceedance report with a preliminary analysis of air quality, meteorological, and emission data to help understand the cause of the ozone exceedance. If ozone exceedances occur frequently, the design value (3-year average of annual 4th highest daily maximum 8-hour average ozone concentrations) can exceed the ozone NAAQS and EPA can classify the area as nonattainment. Based on 2015-2017 ozone data, Atlanta has four monitors with design values above 70 ppb (Table 1 and Figure 3). Only one monitor had a 4th highest concentration above 70 ppb in 2017 (Figure 2).

The ten ozone monitors in the Metro Atlanta area have altogether experienced 11 ozone exceedance days in 2017, much less than the 29 ozone exceedance days in 2016. Detailed ozone exceedance days by monitor are displayed in Figure 4 and summarized by month in Table 2. In addition, ozone concentrations by ozone monitors in Atlanta on ozone exceedance days during 2017 are summarized in Table 3. Most of the 2017 ozone exceedances occurred at the Confederate Ave. monitor located in downtown Atlanta (Figure 4). There were three exceedance days (May 15, July 21, and August 19) when ozone exceedances occurred at several Atlanta monitors on the same day and eight exceedance days when the ozone exceedances only occurred at one monitor (Figure 5).

A final in-depth ozone exceedance report was developed for the Metro Atlanta area to identify causes of the 2017 ozone exceedances. The report includes: trend analysis of ozone concentrations and meteorological conditions in Atlanta during 1990-2017; multiple linear regression (MLR) analysis and classification and regression tree (CART) analysis to understand the relationship between ozone and environmental variables; Hybrid Single Particle Lagrangian Integrated Trajectory (HYSPLIT) back trajectory analysis to determine the origin of air masses and establish source-receptor relationships on ozone exceedance days; animation of ozone and wind conditions to illustrate ozone formation and transport; and analysis of NOx and VOCs measurements to understand the impacts of precursors on ozone formation. Also, a preliminary

investigation of traffic congestion impacts on ozone exceedances was performed. This final ozone exceedance report can be used to guide future air quality management practices in Georgia to help prevent future ozone exceedances.

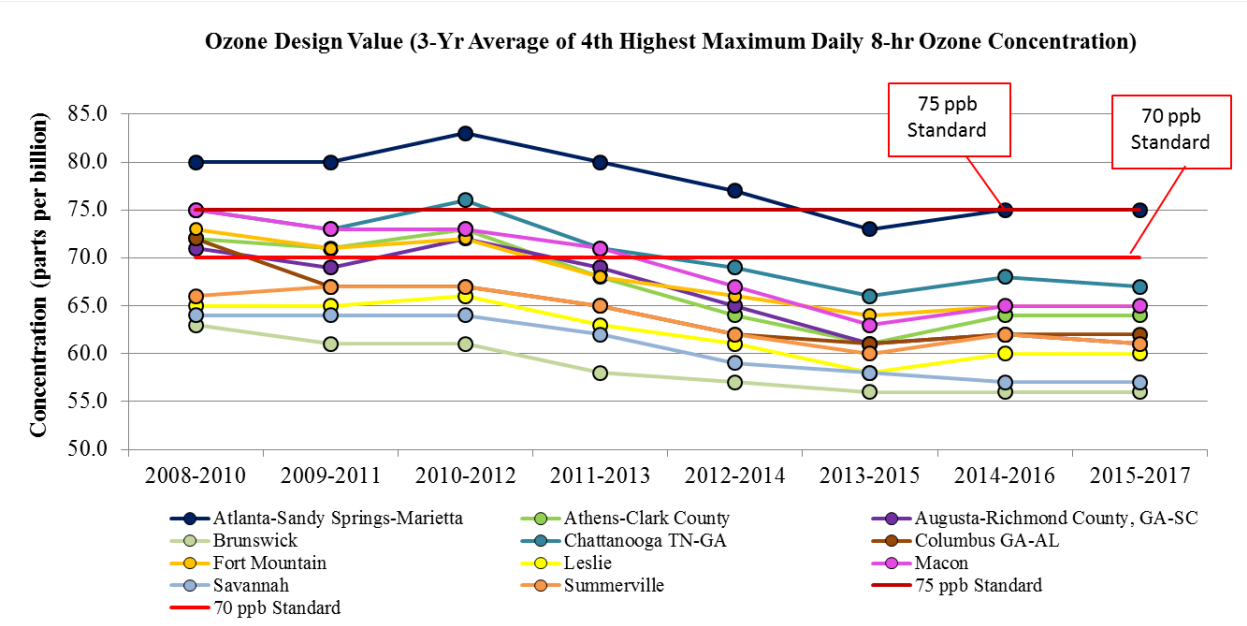

Figure 1. Trend of ozone design values by various MSAs in Georgia.

Table 1. Annual 4th highest daily maximum 8-hour average ozone concentrations (ppb) and design value for ten ozone monitors in the Metro Atlanta area during 2013-2017.

			4th Highest (ppb)					Design Value (ppb)		
Site ID	**County**	**Site Name**	**2013**	**2014**	**2015**	**2016**	**2017**	**2015**	**2016**	**2017**
130670003	Cobb	Kennesaw	67	63	66	70	65	65	66	67
130770002	Coweta	Newnan	53	67	66	66	57	62	66	63
130850001	Dawson	Dawsonville	63	66	63	67	65	64	65	65
130890002	DeKalb	South DeKalb	62	70	71	74	68	67	**71**	**71**
130970004	Douglas	Douglasville	63	65	70	71	66	66	68	69
131210055	Fulton	Confederate Ave.	69	73	77	75	74	**73**	**75**	**75**
131350002	Gwinnett	Gwinnett Tech	69	68	71	78	65	69	**72**	**71**
131510002	Henry	McDonough	70	75	70	78	67	**71**	**74**	**71**
132319991	Pike	CASTNET	64	66	68	71	62	66	68	67
132470001	Rockdale	Conyers	71	79	68	76	65	**72**	**74**	69

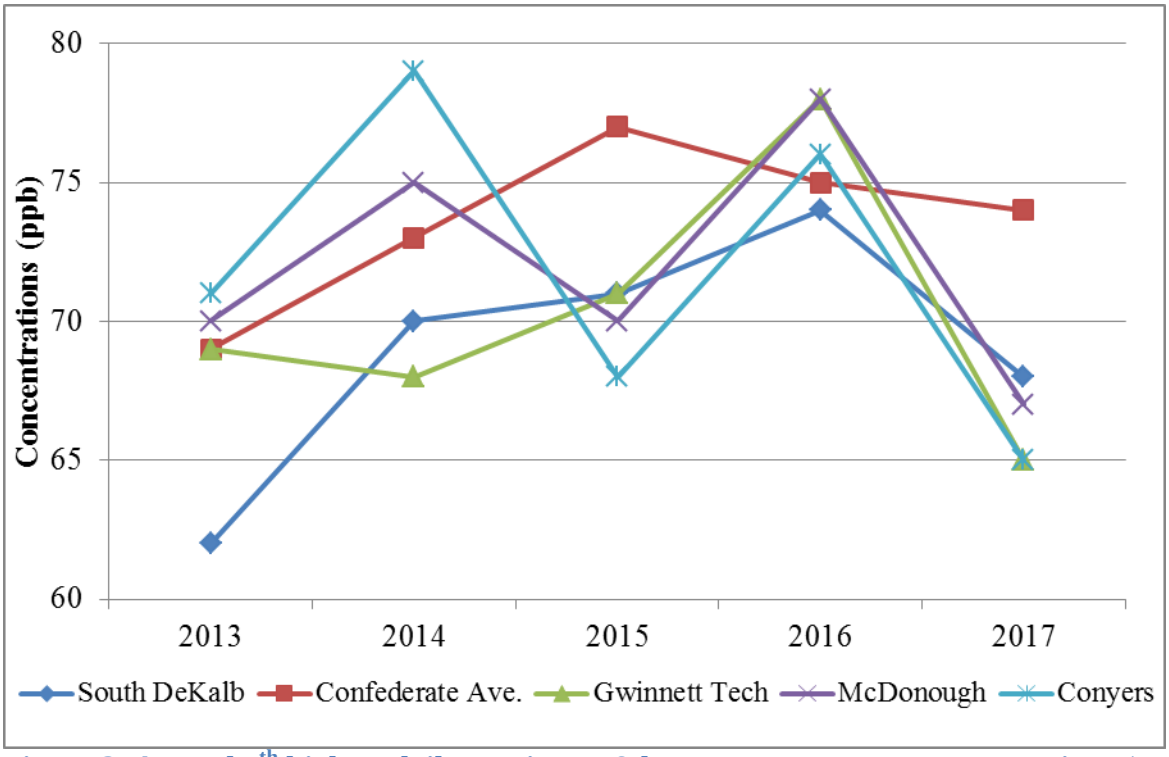

Figure 2. Annual 4th highest daily maximum 8-hour average ozone concentrations (ppb) for five high ozone monitors in the Metro Atlanta area during 2013-2017.

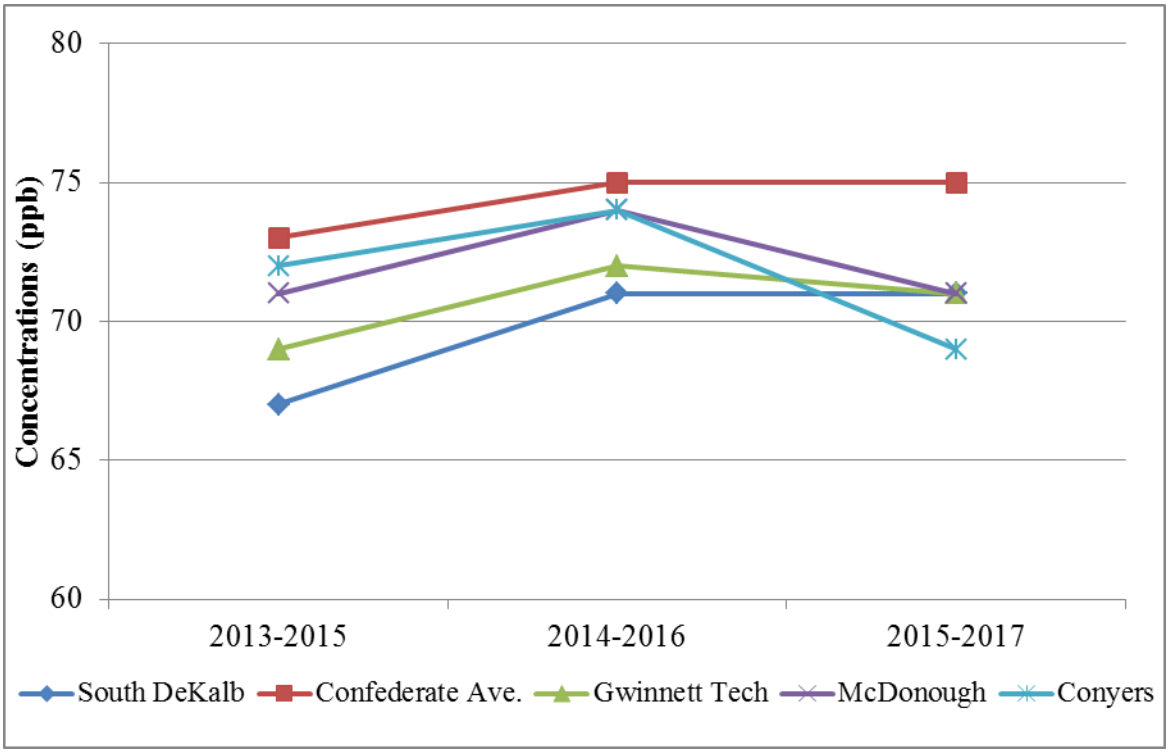

Figure 3. Ozone design values for five high ozone monitors in the Metro Atlanta area.

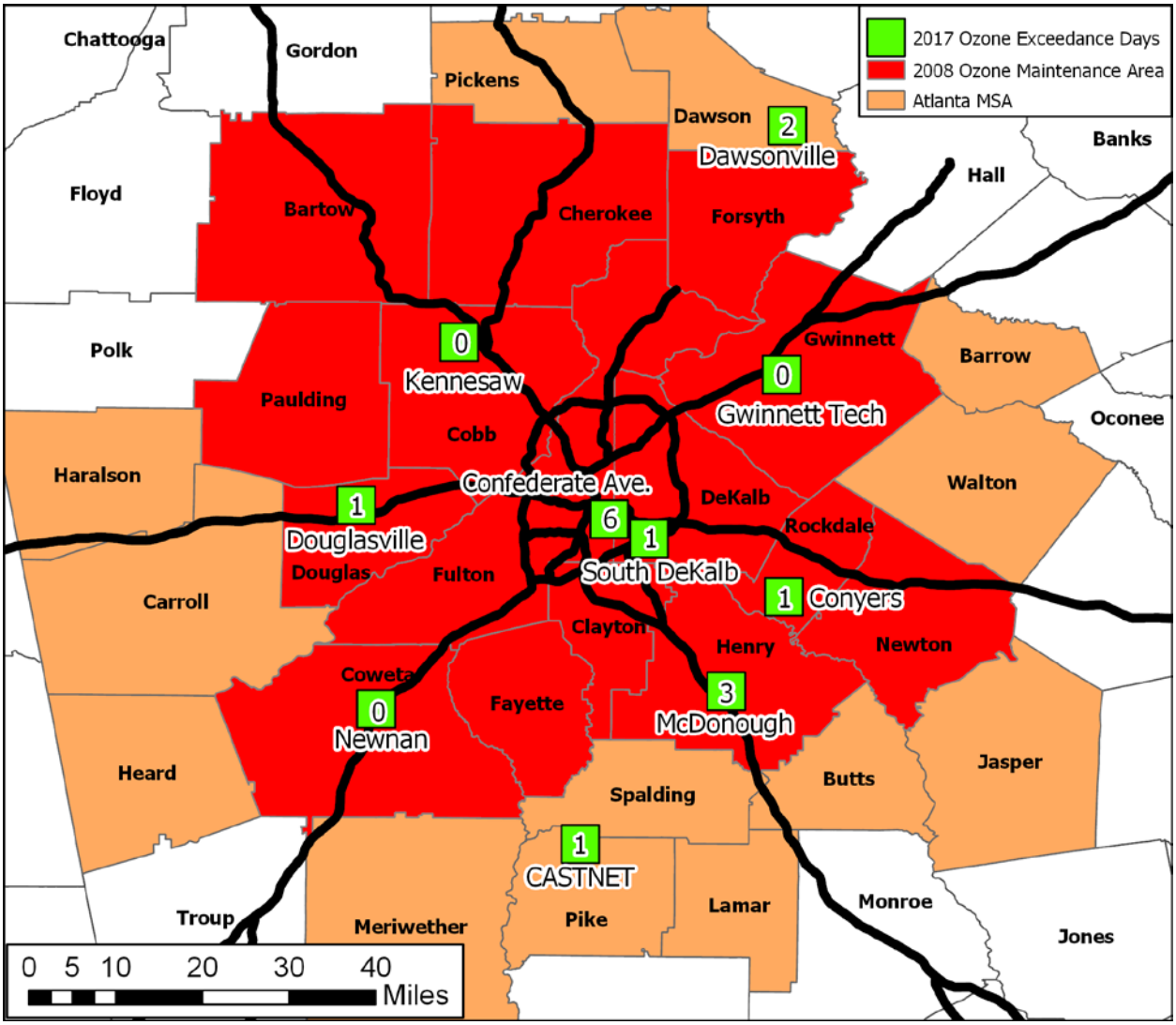

Figure 4. Locations of ozone monitors and the number of 2017 ozone exceedance days in the Metro Atlanta area.

Table 2. Summary of 2017 ozone exceedances for ten ozone monitors in the Metro Atlanta area.

ID	Site Name	April	May	June	July	August	September	October	Total
131210055	Confederate Ave.		1		2	2	1		6
131510002	McDonough				2	1			3
130850001	Dawsonville	1	1						2
130890002	South DeKalb		1						1
132470001	Conyers		1						1
130970004	Douglasville					1			1
132319991	CASTNET					1			1
131350002	Gwinnett Tech								
130670003	Kennesaw								
130770002	Newnan								
	Total	**1**	**4**	**0**	**4**	**5**	**1**	**0**	**15**

Table 3. Ozone concentrations (ppb) for ten ozone monitors in the Metro Atlanta area on exceedances days during 2017.

Month	Day	Day of Week	Confederate Ave.	McDonough	Dawsonville	South DeKalb	Conyers	Douglasville	CASTNET	Gwinnett Tech	Kennesaw	Newnan
April	**10**	Monday	60	56	**71**	59	57	57	55	59	57	53
May	**15**	Monday	**81**	65	49	**83**	**78**	54	55	69	62	53
May	**16**	Tuesday	60	55	**74**	58	59	55	54	67	61	51
July	**19**	Wednesday	62	**79**	36	60	67	44	57	51	54	46
July	**21**	Friday	**77**	**73**	39	68	58	61	35	64	64	55
July	**26**	Wednesday	**73**	56	43	63	57	58	62	59	51	62
August	**1**	Tuesday	62	49	53	55	50	**85**	56	59	67	50
August	**19**	Saturday	**74**	**76**	42	69	63	53	54	58	59	49
August	**20**	Sunday	**76**	51	52	69	51	56	64	55	59	55
August	**24**	Thursday	68	61	41	67	53	53	**76**	52	47	52
September	**28**	Thursday	**72**	63	45	68	55	54	52	61	50	49

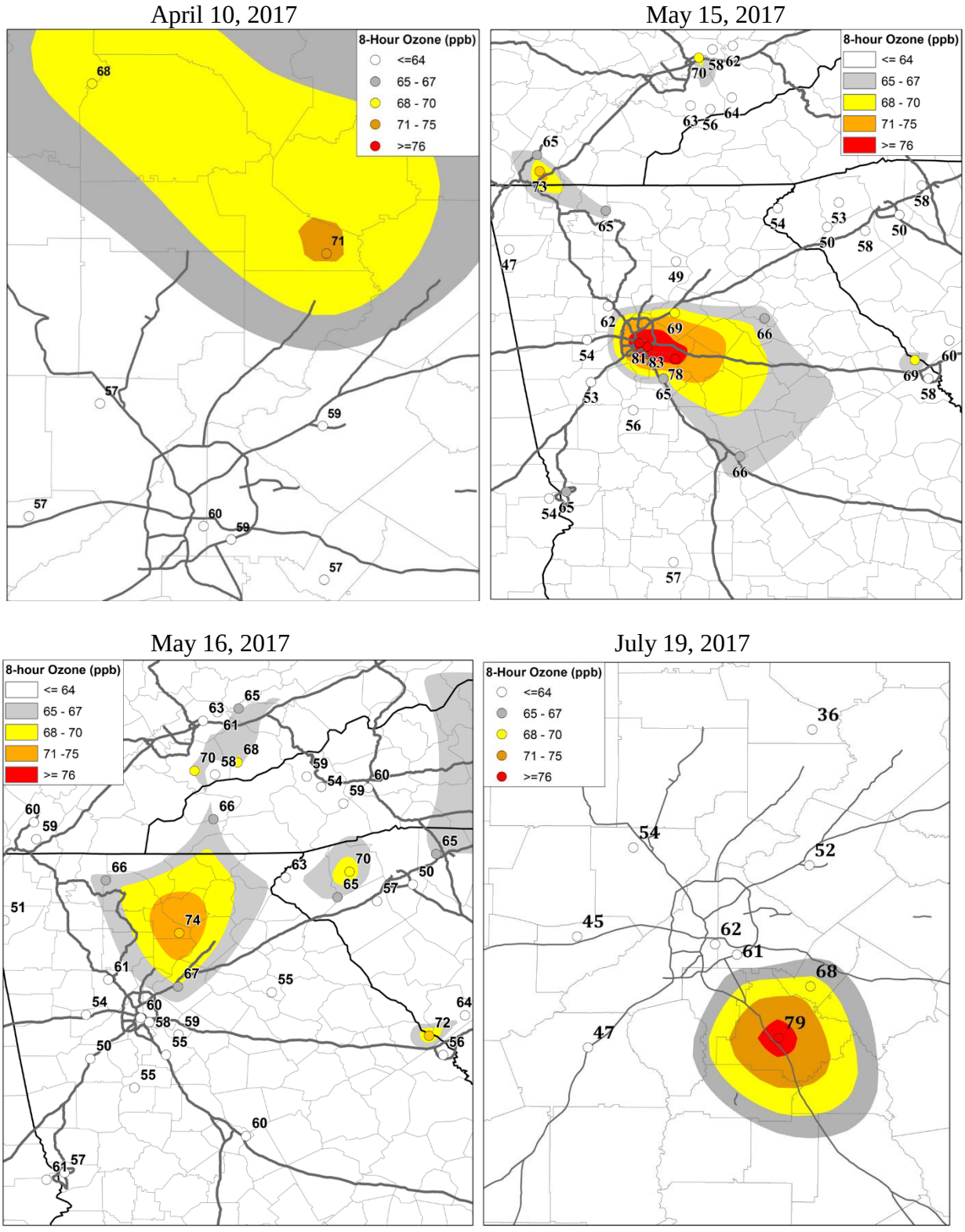

Figure 5. Daily maximum 8-hour ozone concentrations at monitors in and around the Metro Atlanta area on exceedance days.

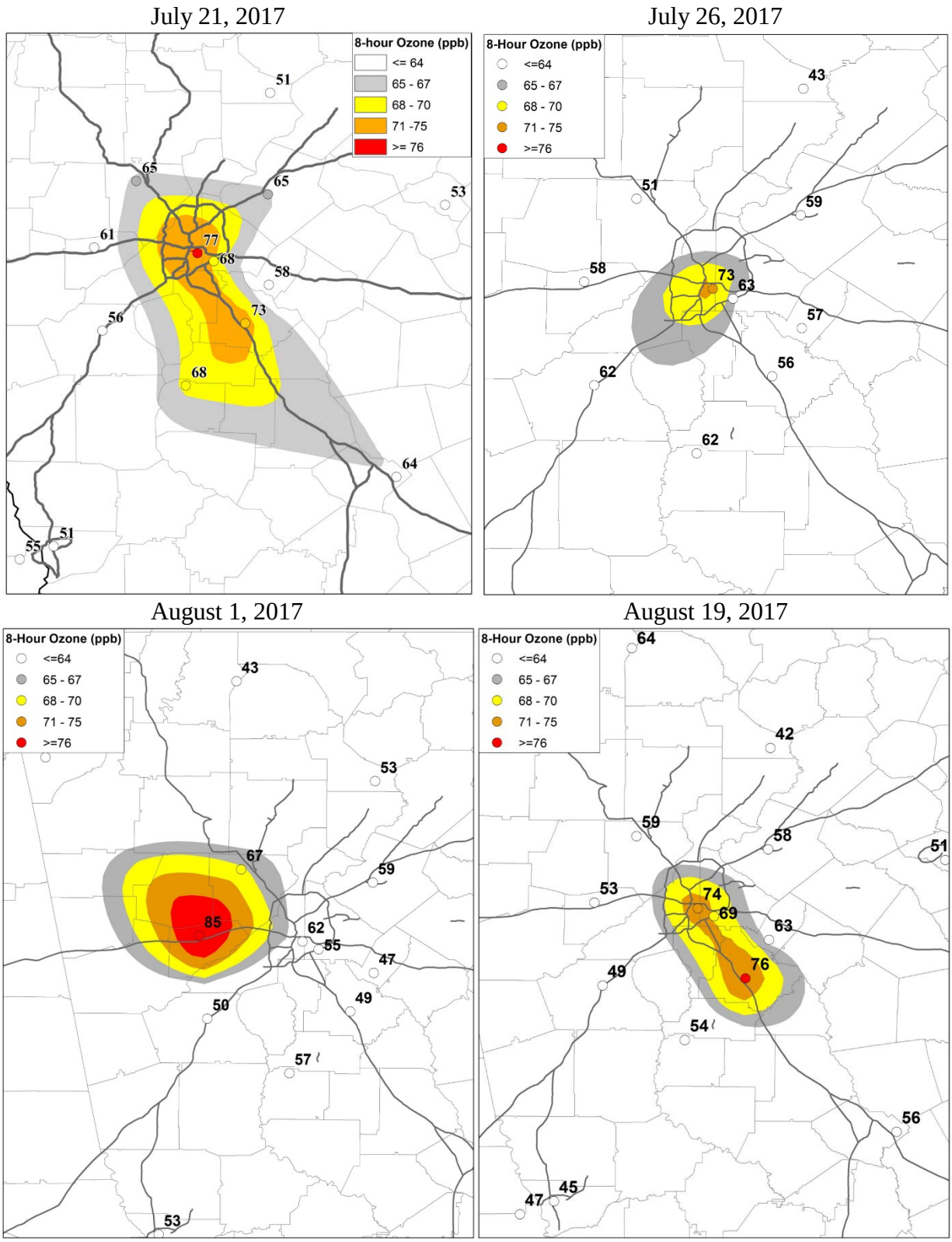

Figure 5 (Continued). Daily maximum 8-hour ozone concentrations at monitors in and around the Metro Atlanta area on exceedance days.

August 20, 2017

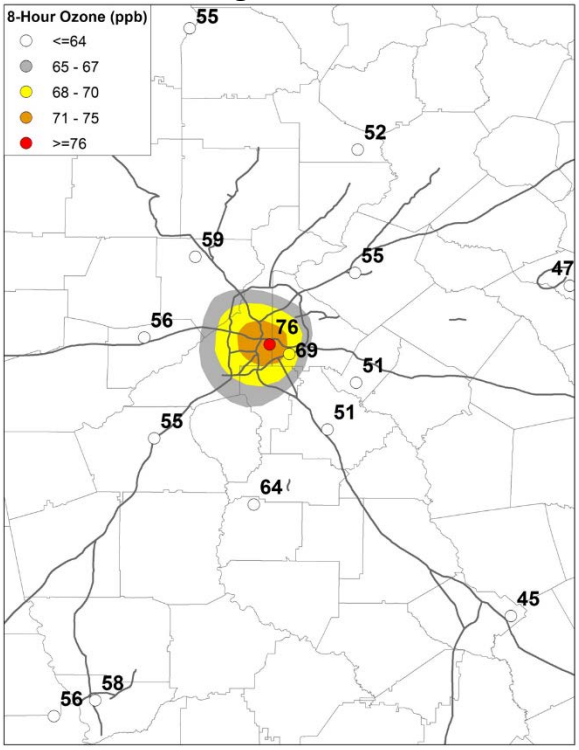

August 24, 2017

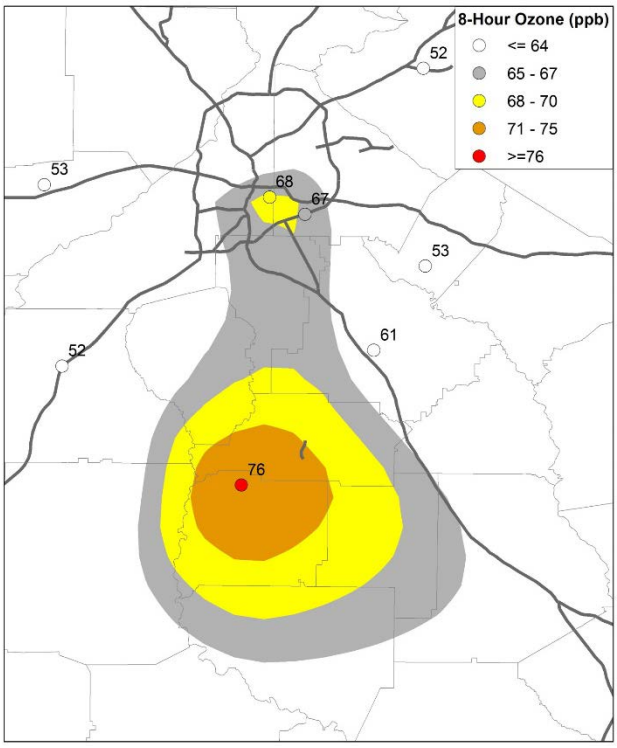

September 28, 2017

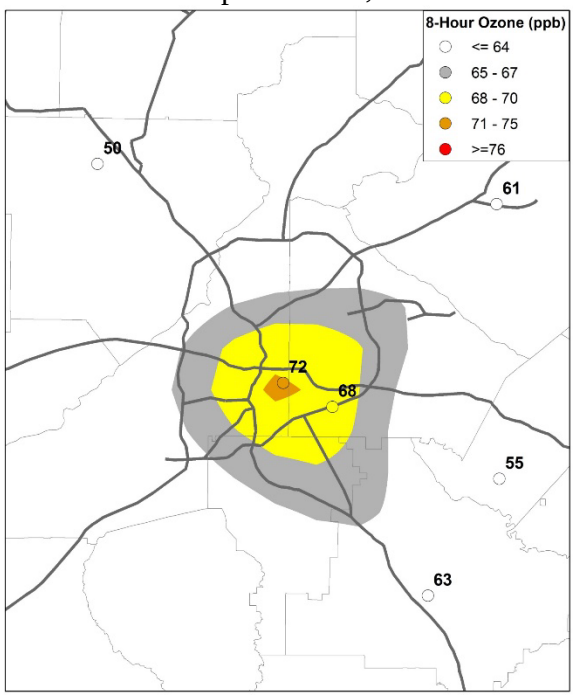

Figure 5 (Continued). Daily maximum 8-hour ozone concentrations at monitors in and around the Metro Atlanta area on exceedance days.

2. Ozone Exceedance Trends in the Metro Atlanta Area during 1990-2017

Ozone exceedance trends in Atlanta during 1990-2017 were analyzed using ozone concentrations measured at ten ozone monitors in the Metro Atlanta area, including nine Georgia EPD-operated ozone monitors (eight located in the Atlanta 2008 ozone maintenance area and one located in Dawsonville), as well as one EPA-operated monitor (CASTNET) outside the Atlanta 2008 ozone maintenance area (Figure 4 and Table 4). Note that the Yorkville monitor used in the 2016 Final Ozone Exceedance Report was discontinued in 2017. The 1990-2017 ozone data were downloaded from EPA's Air Quality System (AQS).

Table 4. Ten ozone monitors in the Metro Atlanta area.

ID	Site Name
130670003	Kennesaw
130770002	Newnan
130890002	South DeKalb
130970004	Douglasville
131210055	Confederate Ave
131350002	Gwinnett Tech
131510002	McDonough
132470001	Conyers
130850001	Dawsonville
132319991	CASTNET

Maximum daily 8-hour average ozone concentrations (MDA8O3) in Atlanta were calculated as the maximum MDA8O3 for the ten ozone monitors in Atlanta. The annual maximum, mean, and median MDA8O3 from April to October in 1990-2017 shows the inter-annual variability with a slight downward trend through the years (Figure 6). The annual mean MDA8O3 in 1999 is the highest at 71.8 ppb, and decreases to the lowest in 2013 with 47.6 ppb. This generally coincides with Georgia NOx (Figure 7) and VOC (Figure 8) emission reductions over the same period of time. The annual mean MDA8O3 dropped slightly to 48.7 ppb in 2017, which was the second lowest after 2013. Although the maximum MDA8O3 decreases through the years, the minimum MDA8O3 increased as a result of less ozone removal through NOx titration[1].

The MDA8O3 were compared with the 2015 ozone NAAQS (70 ppb) to identify ozone exceedance days. The number of exceedance days during the 1990-2017 ozone seasons shows a similar pattern. There were less than 20 ozone exceedance days during 2013-2015. The number increased to 29 days in 2016, but dropped to 11 days in 2017. We see a high number of ozone days above 70 ppb in 1993, 1999, 2006, 2011, and 2016. There seems to be a 5-7 year period between these occurrences. It is similar to the 2-7 year period of El Niño–Southern Oscillation (ENSO), but not peaking in the same year. Further work is needed to determine if there is a potential connection between ozone concentrations and climate patterns.

[1] The removal of ozone through the reaction of $O_3 + NO \rightarrow O_2 + NO_2$.

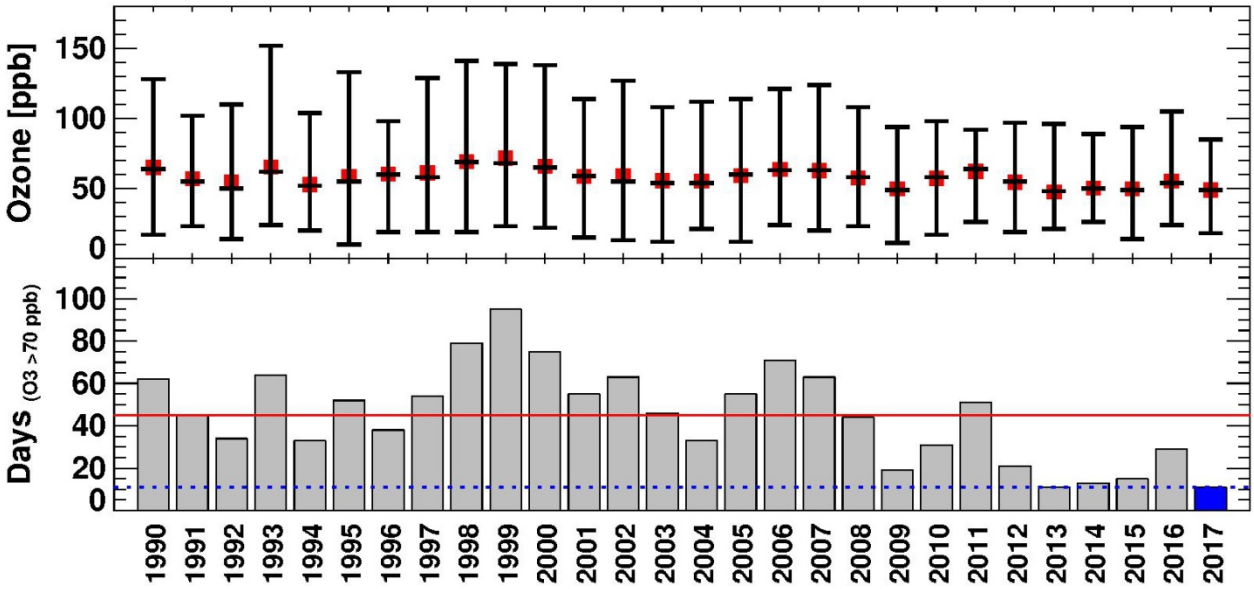

Figure 6. Mean MDA8O3 concentrations (top) and the number of ozone exceedance days (bottom) in April to October in 1990-2017 in the Metro Atlanta area. 2017 value is highlighted in blue and drawn in blue dotted line. The red solid line is the average for 1990-2017.

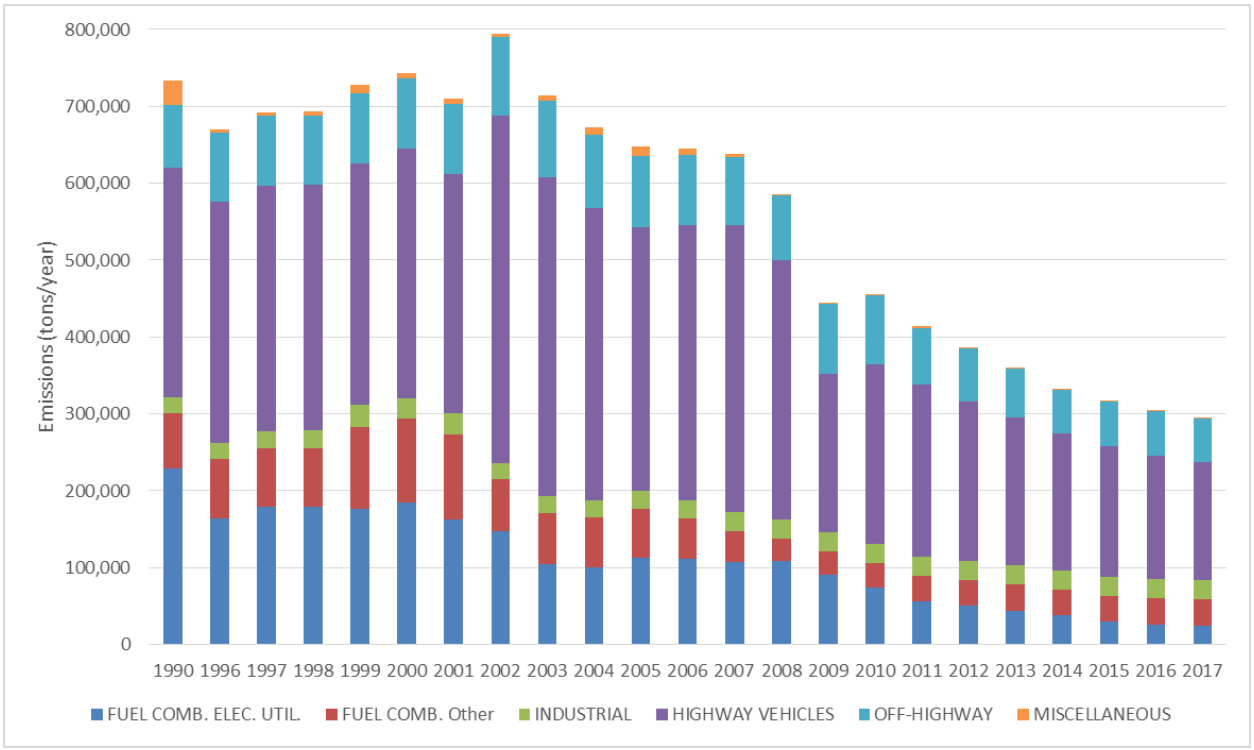

Figure 7. Georgia NOx emission trends by source sectors during 1990-2017.

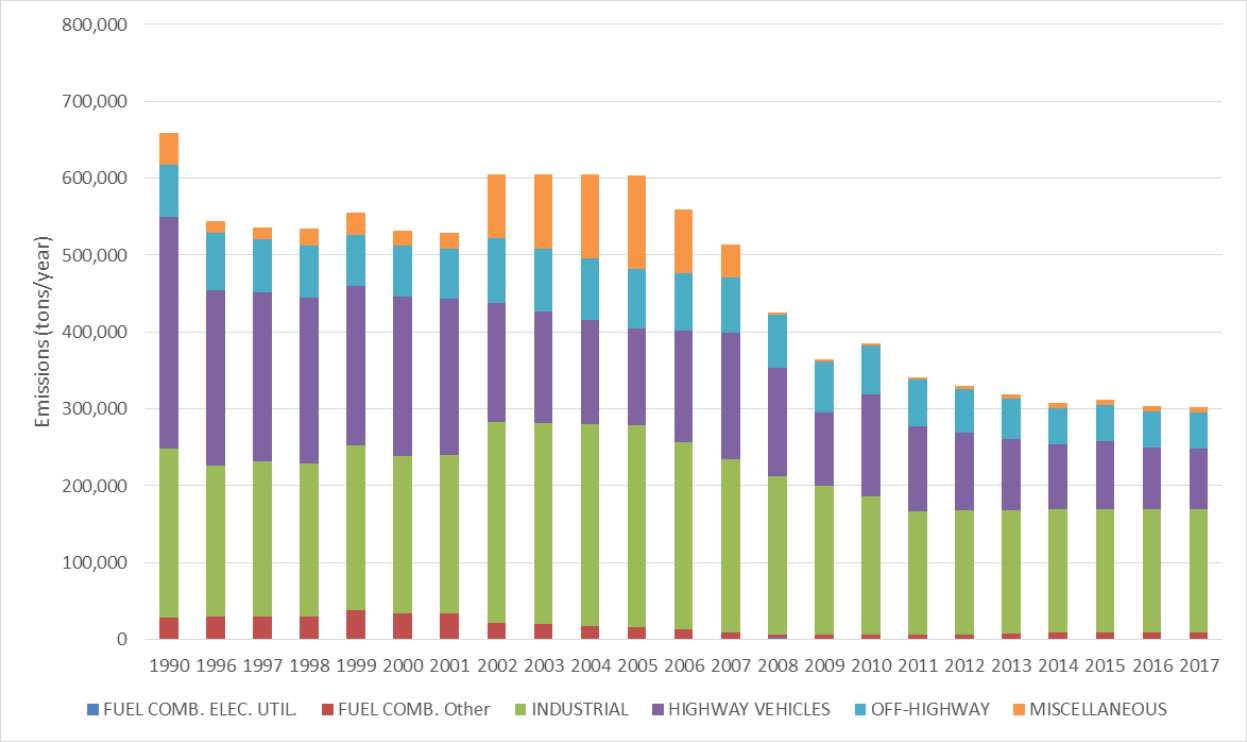

Figure 8. Georgia VOCs emission trends by source sectors during 1990-2017.

The monthly average ozone exceedance days and percentage of exceedance occurring in each month are summarized by different time periods during 1990-2017 in the Metro Atlanta area (Figure 9). Typically, more than 70% of the ozone exceedances occur during June, July, and August when temperature is higher and sunlight is stronger, and less than 10% of the ozone exceedances occur in April and October when air temperature is relatively low. In 2017, most of exceedances occur in May, July and August (no exceedances occurred in June or October).

Also, daily patterns of ozone exceedances were investigated (Figure 10). Generally, more ozone exceedances occur during weekdays than weekends in recent years, but this difference is small before 2010. This is likely due to large emission reduction for industrial sources which have less daily emission variation compared with mobile sources.

The mean ozone increases on exceedance days were calculated by subtracting ozone concentrations on one day or two days before exceedance days from ozone concentrations on exceedance days (Figure 11). During 2017, ozone increased by an average of 19.7 ppb compared to two days before and 14.5 ppb compared to one day before. It was the largest one-day increase during 1990-2017 and the third largest two-day increase ranking after 1992 and 2013.

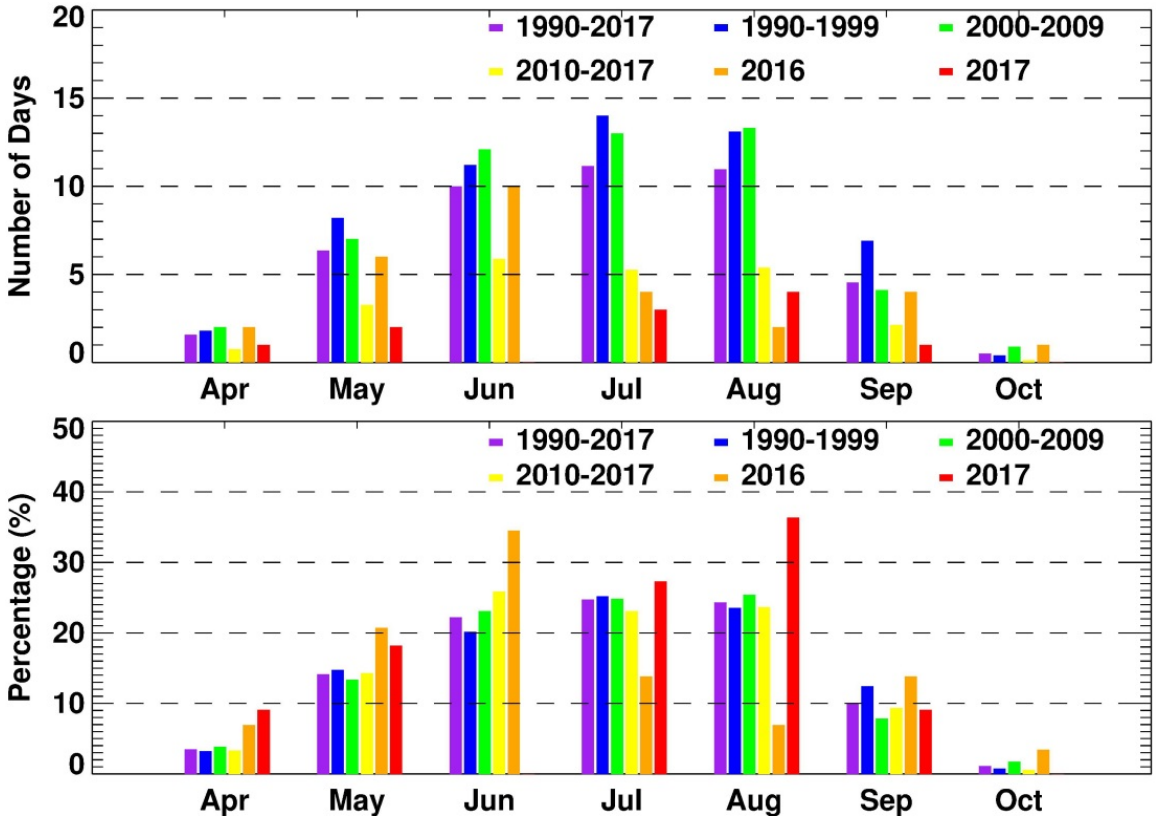

Figure 9. Monthly average number of ozone exceedance days (top) and percentage of exceedances occurring in that month (bottom) in ozone season by different time periods during 1990-2017 in the Metro Atlanta area.

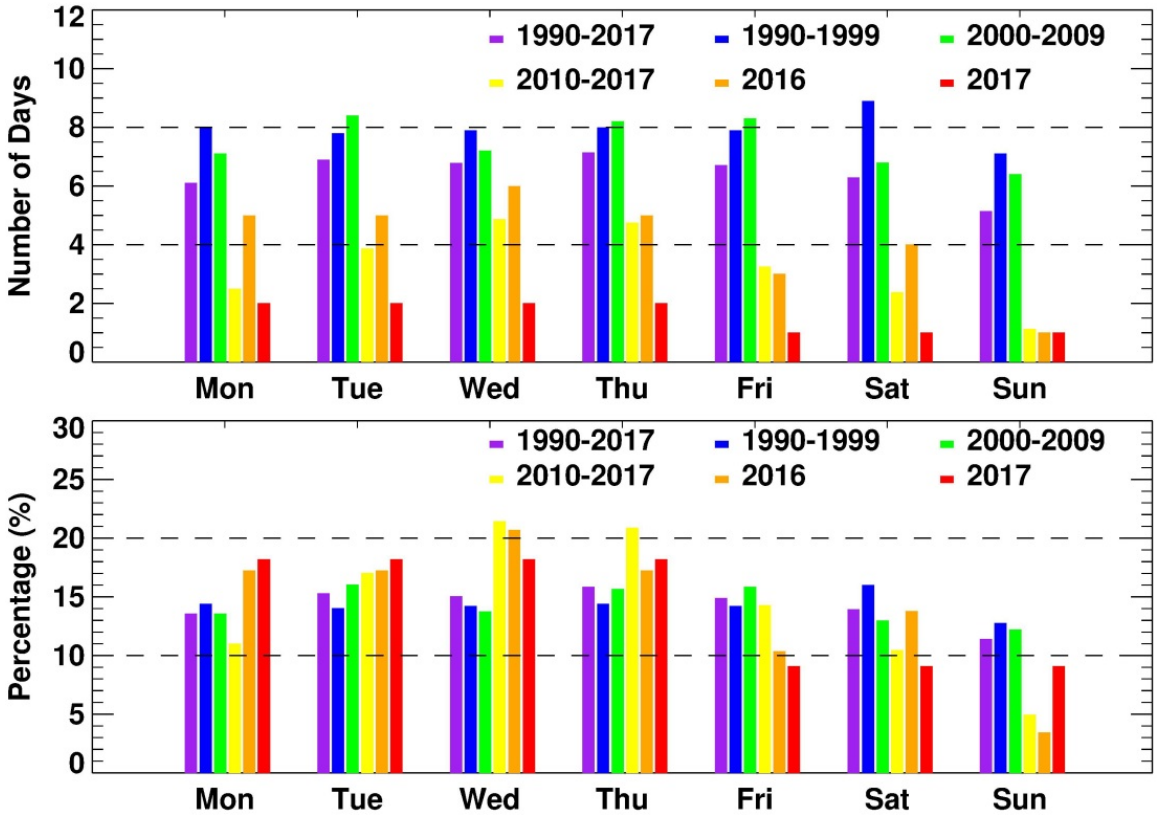

Figure 10. The number (top) and percentage (bottom) of ozone exceedance days by days of week for different periods during 1990-2017 in the Metro Atlanta area.

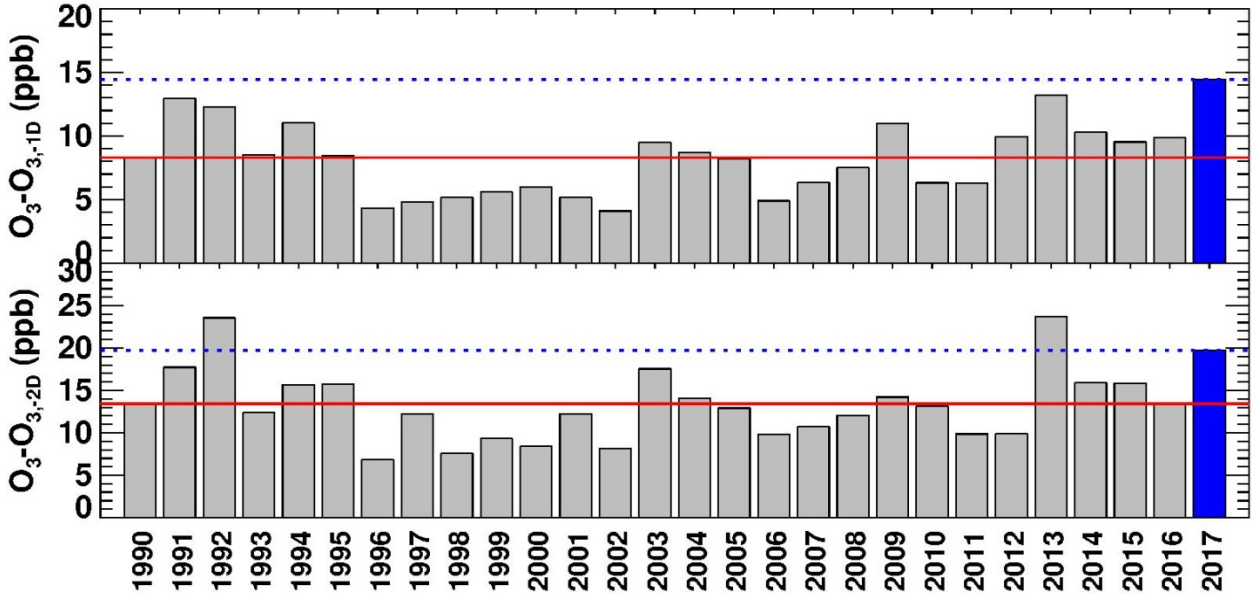

Figure 11. The mean ozone increases (ppb) from one day before (top) and two days before (bottom) the ozone exceedance days during 1990-2017 in the Metro Atlanta area. 2017 value is highlighted in blue and drawn in blue dotted line. The red solid line is the average for 1990-2017.

3. Meteorological Conditions in the Metro Atlanta Area during 1990-2017

Trends of meteorological conditions in Atlanta during 1990-2017 were analyzed using meteorological observations at Atlanta International Airport (Table 5) downloaded from https://mesonet.agron.iastate.edu/request/download.phtml?network=GA_ASOS. The observational intervals varied from one hour to several minutes depending on variables.

Table 5. Observed meteorological variables at Atlanta International Airport

Variables	Definition	Unit
tmpf	Air Temperature, typically @ 2 meters	degree of Fahrenheit
dwpf	Dew Point Temperature, typically @ 2 meters	degree of Fahrenheit
relh	Relative Humidity	%
drct	Wind Direction	degree from north
sknt	Wind Speed	knots
p01i	One hour precipitation for the period from the observation time to the time of the previous hourly precipitation reset.	inches
alti	Pressure altimeter	inches
mslp	Sea Level Pressure	millibar
vsby	Visibility	miles
gust	Wind Gust	knots
skyc1	Sky Level 1 Cloud Coverage	%
skyc2	Sky Level 2 Cloud Coverage	%
skyc3	Sky Level 3 Cloud Coverage	%
skyc4	Sky Level 4 Cloud Coverage	%

Mean meteorological conditions in ozone season were calculated for each year (Figure 12). Most variables have significant inter-annual variations, except pressure and wind direction. In 2017, AM and PM cloud coverages (defined as the percentage of sky covered by clouds) are much less than the 1990-2017 average cloud coverages. Other meteorological conditions in 2017 are similar to the 1990-2017 average conditions. Temperatures in 2017 were compared with 1930 to 2017 trends (Figure 13) and showed slightly above average temperatures. In summary, meteorological conditions in 2017 were not as favorable for ground level ozone formation as those in 2016.

The meteorological conditions are investigated further for the 11 ozone exceedance days in 2017. The relative humidity, cloud fraction, wind speed in the morning and afternoon, and daily maximum and minimum temperatures on the day before and after each exceedance are compared to those on the exceedance day (Figure 14). For the days without observations, the data from two days before or after are used. Continuous exceedances lasting more than one day are considered as one event. In general, the ozone exceedance days feature relatively lower RH, less cloud coverage, lower wind speed, and higher daily max temperature. Other meteorological variables such as dew point temperature, pressure, and wind direction do not show a clear pattern with ozone exceedances. This is consistent with the analysis of meteorological and air quality data during the period from 1990-2017 mentioned above.

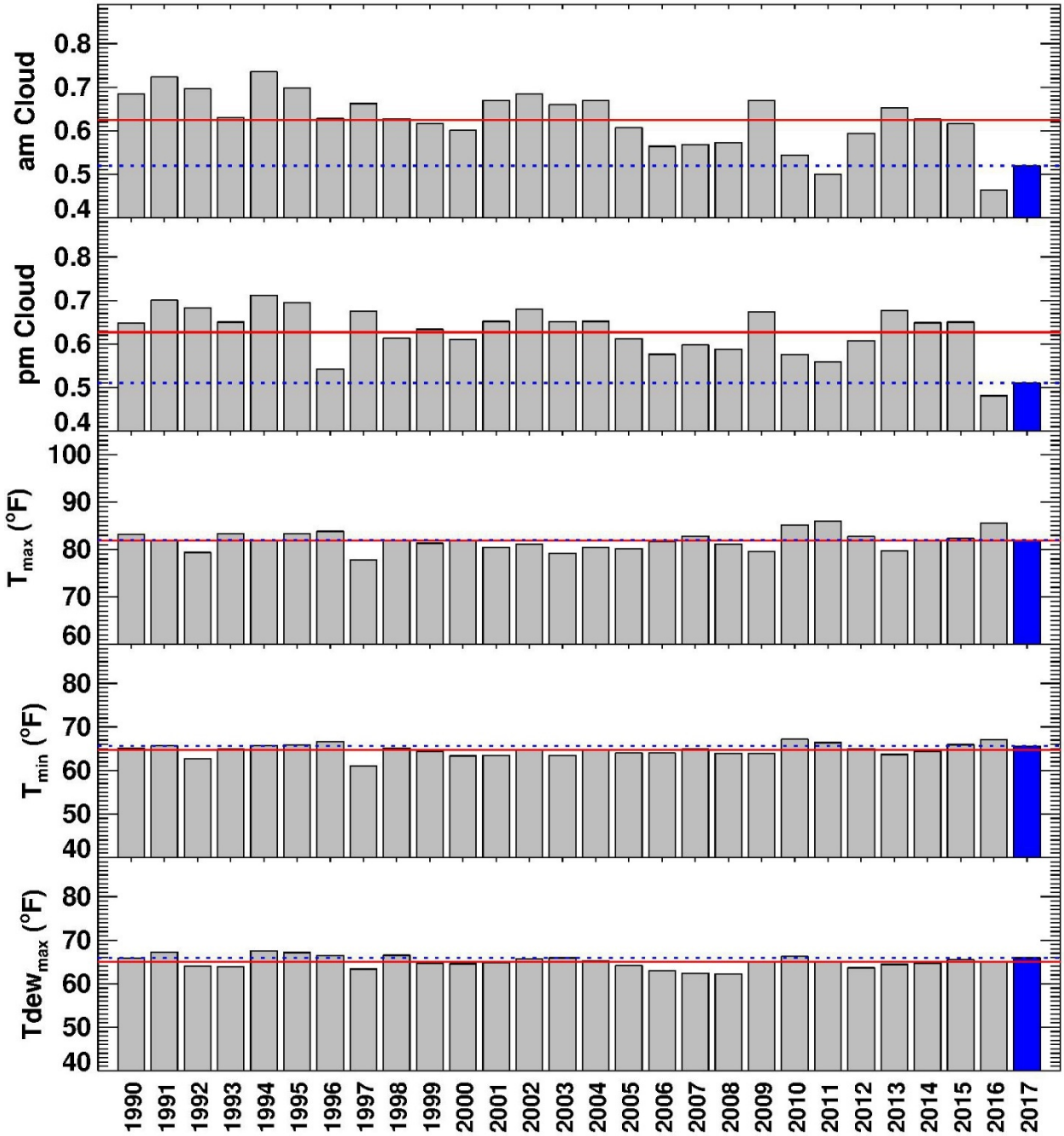

Figure 12. Atlanta ozone season mean meteorological conditions during 1990-2017. 2017 values are highlighted in blue and also represented by the blue dotted line, and 1990-2017 average values are represented by the red solid line to facilitate comparison.

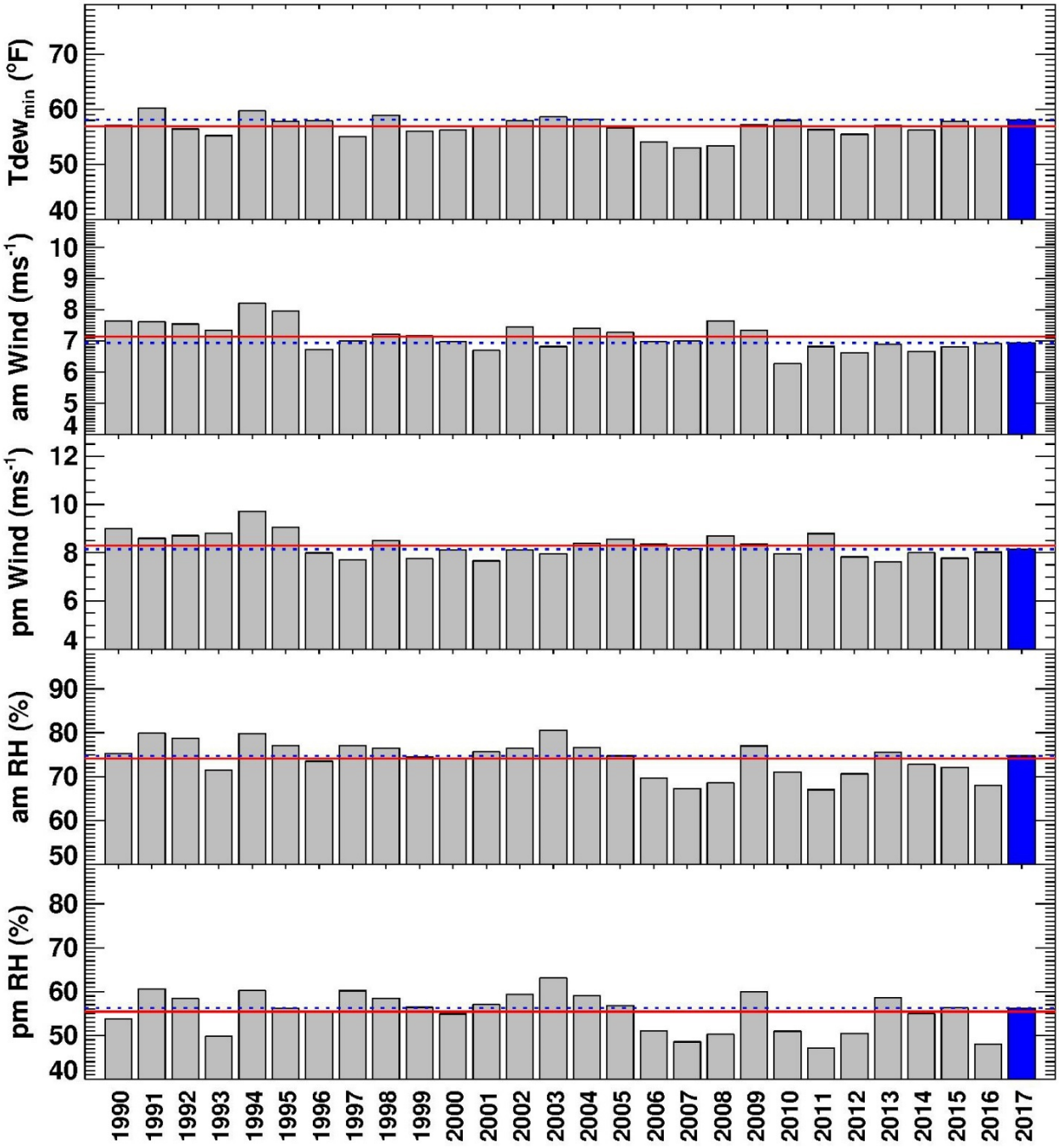

Figure 12. (continued). Atlanta ozone season mean meteorological conditions during 1990-2017. 2017 values are highlighted in blue and also represented by the blue dotted line, and 1990-2017 average values are represented by the red solid line to facilitate comparison.

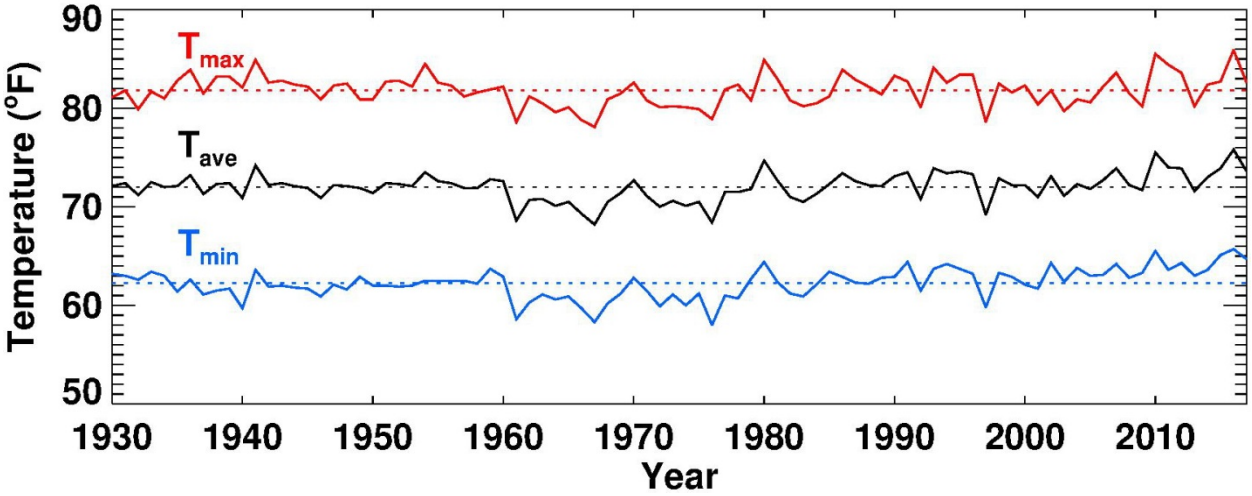

Figure 13. Mean maximum temperature (red), mean average temperature (black), and mean minimum temperature (blue) during the ozone season (April 1 – October 31) in Atlanta from 1930 to 2017. Data is downloaded from NOAA/NCEI (https://www.ncdc.noaa.gov/).

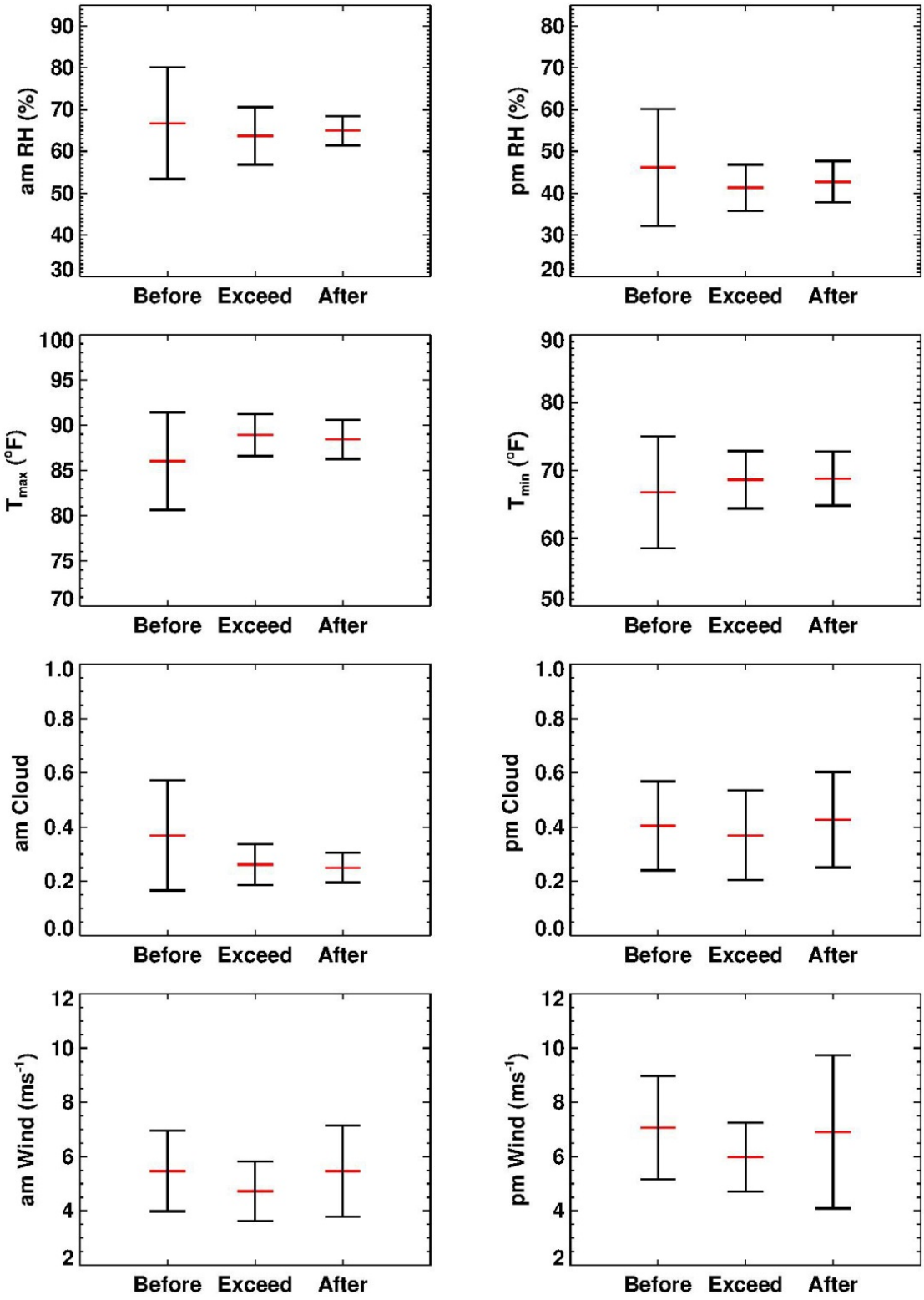

Figure 14. Comparison of meteorological variables in 2017 on the ozone exceedance day, and the day before and after the exceedance. The red bar is the mean, and the upper and lower bars (black) represent the standard deviations.

4. Ozone Regression Model

Multiple linear regression (MLR) analysis was previously used to quantify the relationship between Atlanta MDA8O3 and environmental variables in a previous study (Cardelino, 2011). In this 2011 study, 15 environmental variables (12 meteorological variables and O_3-day2, weekday, and Julian day) were used (Table 6). O_3-day2 is used to represent chemical production background assuming slow changes, weekday is for emission variation due to human activities, and Julian day is to represent the variations of solar radiation throughout the ozone season. In the 2016 final ozone exceedance report, two additional environmental variables (relh1 and relh2) were added in the MLR analysis. In this 2017 report, Julian day (which shows very poor correlation with ozone in the 2016 MLR analysis) is replaced by the daily maximum solar elevation angle (SunAngle) to better represent the intensity of solar radiation (Table 6).

For this analysis, daily data of MDA8O3 and 17 environmental factors are used in the MLR to build a linear relationship of Atlanta MDA8O3 and environmental factors assuming independency among these environmental factors:

$$y = \alpha_0 + \sum_{i=1}^{i=17} \alpha_i x_i$$

where, y stands for MDA8O3, x_i stands for the environmental factor, α_0 is an adjustment factor, and α_i is a weighting factor.

Table 6. Daily variables used for the MLR analysis and CART analysis

Name	Meaning	Formula	Unit
T_{max}	Daily maximum temperature	max(tmpf)	degree of Fahrenheit
T_{min}	Daily minimum temperature	min(tmpf)	degree of Fahrenheit
TD_{max}	Daily maximum dew point temperature	max(dwpf)	degree of Fahrenheit
TD_{min}	Daily minimum dew point temperature	min(dwpf)	degree of Fahrenheit
pres1	Mean surface pressure in the morning (6-12 pm)	mean(mlsp $_{(6\text{-}12)}$)	millibar
pres2	Mean surface pressure in the afternoon (12-6 pm)	mean(mlsp $_{(12\text{-}18)}$)	millibar
wdir1	Mean wind direction in the morning (6-12 pm)	mean(drct $_{(6\text{-}12)}$)	degree from north
wdir2	Mean wind direction in the afternoon (12-6 pm)	mean(drct $_{(12\text{-}18)}$)	degree from north
wsp1	Mean wind speed in the morning (6-12 pm)	mean(sknt $_{(6\text{-}12)}$)	m/s
wsp2	Mean wind speed in the afternoon (12-6 pm)	mean(sknt $_{(12\text{-}18)}$)	m/s
sky1	Mean cloud coverage in the morning (6-12 pm)	mean(max(skyc1,skyc2,skyc3,skyc4) $_{(6\text{-}12)}$)	%
sky2	Mean cloud coverage in the afternoon (12-6 pm)	mean(max(skyc1,skyc2,skyc3,skyc4) $_{(12\text{-}18)}$)	%
O_3-day1	Daily Maximum 8-hr average ozone one day ago (CART only)	-	ppbv
O_3-day2	Daily Maximum 8-hr average ozone two days ago (MLR only)	-	ppbv
wkday	Day of week	Weekday(date)	n/a
SunAngle	Daily maximum solar elevation angle	See equations (1) and (2) below	degree
relh1*	Mean relative humidity in the morning (6-12 pm)	mean(relh $_{(6\text{-}12)}$)	%
relh2*	Mean relative humidity in the afternoon (12-6 pm)	mean(relh $_{(12\text{-}18)}$)	%

(1) Solar declination, $\delta = 23.45^o sin\left[\frac{Julian\ Day+284}{365} \times 360^o\right]$

(2) Daily maximum solar elevation angle, $\propto = asin(\cos(latitude)\cos\delta + \sin(latitude)\, sin\delta)$

Correlation Analysis

The correlation coefficients of MDA8O3 and the 17 environmental variables during ozone season were calculated for different years during 1990-2017 in Atlanta (Table 7 and Figure 15). The difference of correlation coefficients among different years illustrates how the relationships between Atlanta MDA8O3 and environmental variables changed through the years. The ranking of correlation coefficients is similar for different years. The top 6 most correlated environment variables (i.e. variables with the top 6 highest absolute r) are AM and PM relative humidity, AM and PM cloud coverage, daily max temperature, and ozone level 2 days ago. Daily max temperature is the most correlated environmental variable before 2000, and PM relative humidity is the most correlated environmental variable after 2000. The newly introduced variable, daily maximum solar elevation angle, ranks right after the 6 most important variables (r=0.342) in the case using 1990-2017. In 2017, relative humidity and cloud coverage for both AM and PM are the top 4 variables, followed by the daily max temperature and daily maximum 8-hour average ozone two days ago (O_3-Day2). The correlation for the daily maximum solar elevation angle and daily minimum temperature is insignificant in 2017.

In general, the ozone exceedance days were associated with the following meteorological conditions:

1. Low relative humidity (dry)
2. High daily temperature (hot)
3. Low cloud coverage (high solar radiation)
4. High ozone on previous days (persistence)
5. Relatively low wind speed (calm)

The above meteorological conditions favor the chemical production of ozone in the lower troposphere. Low relative humidity may reduce the ozone loss through the reaction with water vapor (Seinfeld and Pandis, 1998). Ozone formation increases with higher temperatures and low cloud coverage due to higher solar radiation, leading to more active ozone production. High ozone on previous days indicates that the ozone buildup was a multiple-day process. Calm conditions correspond to poor dispersion and less regional transport, indicating that the local ozone production is important for ozone exceedances in Atlanta.

Updated MLR Ozone Model

The MLR ozone model was first updated using 2011-2016 observation data, and then used to predict 2017 ozone conditions. Performance of the updated MLR ozone models were evaluated by comparing the predictions with 2017 ozone observations (Table 8). The updated MLR ozone model can explain about 65% of the ozone variance (or R^2). The mean bias (MB) and normalized mean bias (NMB) decreases significantly by using recent data (i.e. MB and NMB for 2013-2016 are less than those for 2012-2016 and 2011-2016), while the Mean Absolute Error (MAE), Normalized Mean Error (NME), and Root Mean Square Error (RMSE) are similar among the updated MLR ozone models. The MLR model based on the 2011-2017 data is recommended to be used for future ozone forecast. The coefficients of the MLR ozone model with 2011-2017 dataset are listed in Table 9.

Table 7. Correlation coefficients of MDA8O3 and environmental variables during ozone season by time periods during 1990-2017 in the Metro Atlanta area.

Name	1990-2017	1990-1999	2000-2009	2010-2017	2016	2017
O3-day2	0.494	0.48	0.496	0.413	0.3	0.324
sky1	-0.503	-0.559	-0.554	-0.534	-0.379	-0.615
sky2	-0.462	-0.515	-0.488	-0.497	-0.451	-0.53
tmax	0.538	**0.592**	0.587	0.488	0.342	0.399
tmin	0.263	0.317	0.3	0.18	0.063	0.022
tdmax	0.067	0.136	0.055	-0.038	-0.146	-0.187
tdmin	0.058	0.128	0.048	-0.051	-0.126	-0.172
SunAngle	0.344	0.346	0.413	0.266	0.125	0.065
pres1	0.033	-0.027	0.07	0.077	0.152	0.194
pres2	0.011	-0.056	0.049	0.056	0.11	0.179
wdir1	0.137	0.231	0.1	0.094	0.026	0.113
wdir2	0.15	0.25	0.111	0.092	0.039	-0.007
wspd1	-0.26	-0.316	-0.272	-0.266	-0.271	-0.291
wspd2	-0.235	-0.266	-0.241	-0.271	-0.372	-0.318
relh1	-0.475	-0.475	-0.536	-0.574	-0.515	-0.654
relh2	**-0.568**	-0.573	**-0.616**	**-0.636**	**-0.597**	**-0.685**
wkday	-0.027	-0.011	-0.035	-0.044	-0.174	-0.039

Note: Top 6 absolute values are highlighted in red. The highest absolute value is in bold.

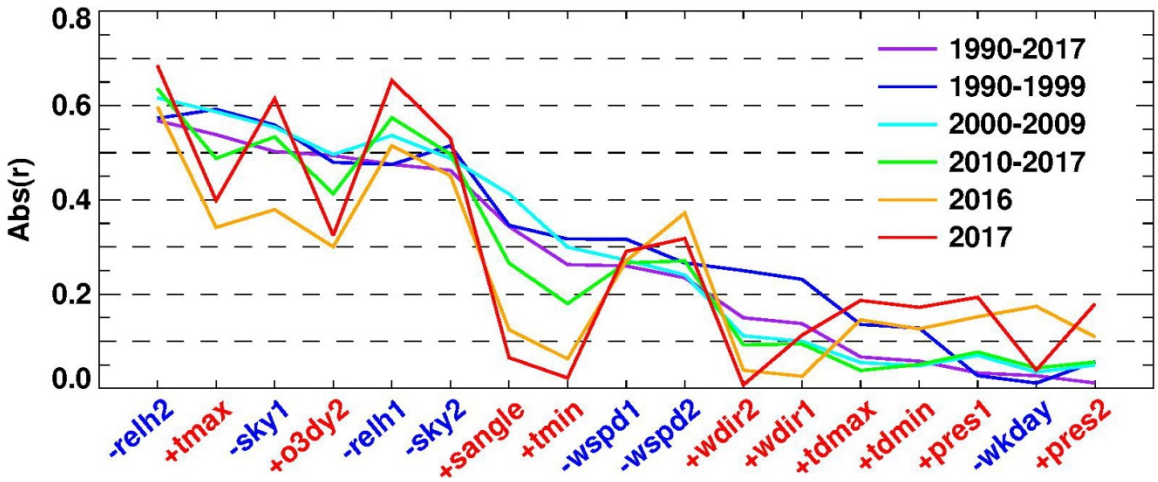

Figure 15. Correlation coefficients of MDA8O3 and environmental variables during ozone season by time periods during 1990-2017 in Atlanta. Variables with positive correlation with MDA8O3 are labeled in red, and variables with negative correlation are labeled in blue.

Table 8. Performance of updated MLR ozone model using various datasets during 2011-2016.

Data range	R	R^2	MB[a]	MAE[a]	NMB[a]	NME[a]	RMSE[a]
2011 - 2016	0.789	0.623	1.109	6.612	2.3%	13.6%	8.612
2012 - 2016	0.792	0.627	0.730	6.553	1.5%	13.4%	8.490
2013 - 2016	0.79	0.623	0.447	6.550	0.9%	13.4%	8.511
2011 - 2017	0.802	0.644	0.758	6.405	1.6%	13.1%	8.301
2012 - 2017	0.806	0.649	0.454	6.342	0.9%	13.0%	8.198
2013 - 2017	0.807	0.651	0.258	6.332	0.5%	13.0%	8.169

[a] MB is Mean Bias, MAE is Mean Absolute Error, NMB is Normalized Mean Bias, NME is Normalized Mean Error, RMSE is Root Mean Square Error.

Table 9. The coefficients of the MLR ozone model using dataset during 2011-2017.

Variable	Coefficient
Constant	502.491
O_3-day2	0.190632
sky1	-2.66874
sky2	-2.77572
T_{max}	0.575724
T_{min}	-0.0393645
TD_{max}	-0.0267983
TD_{min}	-0.233327
SunAngle	0.215487
pres1	-1.06601
pres2	0.615537
wdir1	-0.0104419
wdir2	-0.00352686
wspd1	-0.0843647
wspd2	-1.0357
relh1	-0.175021
relh2	-0.306425
wkday	-0.475764

5. CART Analysis

Classification and regression tree (CART) analysis was used to understand the relationship between Atlanta MDA8O3 and environmental variables. CART (Breiman et al., 1984) is a non-parametric statistical tool which can estimate the hierarchs of the importance of each variable, especially when the relationship between these variables is complicated and nonlinear. Since linearity has been assumed in MLR ozone model as discussed above, CART analysis was performed to further investigate the causes of ozone exceedance using the CART package for R which is a free statistical software available online[2].

CART uses similar regression techniques as the MLR model, although it fits the model locally at each split instead of globally. A sequence of questions related to different variables (or attributes) are asked, and the answer is either "yes" or "no". At each node, a large group is split into two distinct sub-groups based on a single variable. The recursive partition will divide a dataset into a binary tree chart. There are two types of trees, regression and classification trees. In regression trees, the response variable (MDA8O3) is continuous and the final nodes feature the mean values of the response variables. In classification trees, the response variable (MDA8O3) is categorical and the final nodes are assigned to different categories (classes). Both regression tree and classification tree analysis were conducted in this study.

The same 2011-2017 dataset used in MLR analysis was also used for both CART analyses, except that the ozone on previous one day (O3 Day-1) was used for the CART analyses to study the ozone persistence instead of ozone on previous two days used in MLR analysis. In comparison to the actual MDA8O3 concentrations used for regression CART analysis, MDA8O3 concentrations for the classification CART analysis were divided into 4 categories (Table 10) following the definition used in EPA's air quality index (AQI) for the 2015 ozone NAAQS.

Table 10. Four ozone categories used for the classification CART analysis.

Category	Ozone (ppbv)
1	0-54
2	55-70
3	71-85
4	> 85

Regression tree CART analysis

The best split of regression tree CART analysis finds 22 nodes which represent ozone clusters grouped after a sequence of filters with various conditions. The mean ozone concentrations generally increase from left to right (Figure 16). There are three nodes with mean ozone concentrations higher than 70 ppb and three nodes with mean ozone concentrations ranging from 60 to 70 ppb (Figure 17). Six "critical" nodes with mean ozone concentrations were investigated to understand the patterns of environmental conditions on high ozone days (Table 11).

The six "critical" nodes are always associated with two environmental variables (PM RH and O3 Day-1). Five of the six nodes are associated with daily maximum solar elevation angle

[2] https://www.r-project.org/

(SunAngle). PM wind shows association only in two nodes and PM pressure in three nodes. The environmental variables with the higher number of associated nodes for high ozone days are more responsible for the high ozone days. In addition, the importance of variables decreases from the top of the tree to the bottom (Figure 16). Therefore, PM relative humidity (PM RH) is the most critical variable, followed by ozone on previous one day (O_3 Day-1) for the nodes with high ozone concentrations. Six levels of splits are shown in the best regression CART tree (Figure 16).

The number of both days and exceedance days in the 6 'critical' nodes were summarized by years (Figure 18) showing a large inter-annual variation. The number of both days and exceedance days during 2011 in the node 21 representing dry condition and high ozone concentrations on a previous day is the highest. Similar conditions represented by node 21 caused much less exceedances in 2017. Ten out of the eleven ozone exceedances in 2017 falls in the six "critical" nodes (mostly in node 18 and 19). For these two nodes representing typical conditions in 2017, the PM RH is less than 56.4%, indicating high correlation of high ozone days with low relative humidity (relatively dry conditions). A drier condition represented in node 21 and 22 (PM RH < 43.2%) can cause even higher ozone concentrations. The PM wind speeds for the two nodes are less than 8.5 m/s, and solar elevation angle is higher than 61.6 degree. A high solar elevation angle can cause high solar radiation and thus a stronger photochemical production of ozone. In addition, high ozone days in 2017 are less associated with high ozone concentrations on a previous day. All these findings are consistent with the MLR analysis. Interestingly, high ozone days in 2017 are not associated with high temperatures. However, this result may be due to the strong correlation between solar elevation angle and the daily maximum temperature (T_{max}). The contribution from daily maximum temperature may be mixed with the contribution from solar elevation angle. In summary, the ozone exceedance days in 2017 are usually associated with dry and calm meteorological conditions with relative high solar elevation angles.

Table 11. Conditions for top 6 high ozone nodes of the regression tree CART analysis

Node Number	14	18	20	19	21	22
Mean O_3 (ppb)	63.3	64.4	66.6	70.9	75.2	85.3
O_3 exceedances in 2017	1	4	1	3	1	0
PM RH (%)	< 56.4	< 56.4	56.4-43.2	< 56.4	< 43.2	< 43.2
PM wind (m/s)		< 8.5		< 8.5		
O_3 Day-1 (ppb)	<56.5	55.5-71.5	>71.5	55.5-71.5	> 71.5	> 71.5
PM Pressure (mb)	≥ 1016	≥ 1016		< 1016		
SunAngle	> 52.6	> 61.6		> 61.6	< 79.2	> 79.2
AM Sky	< 0.38					

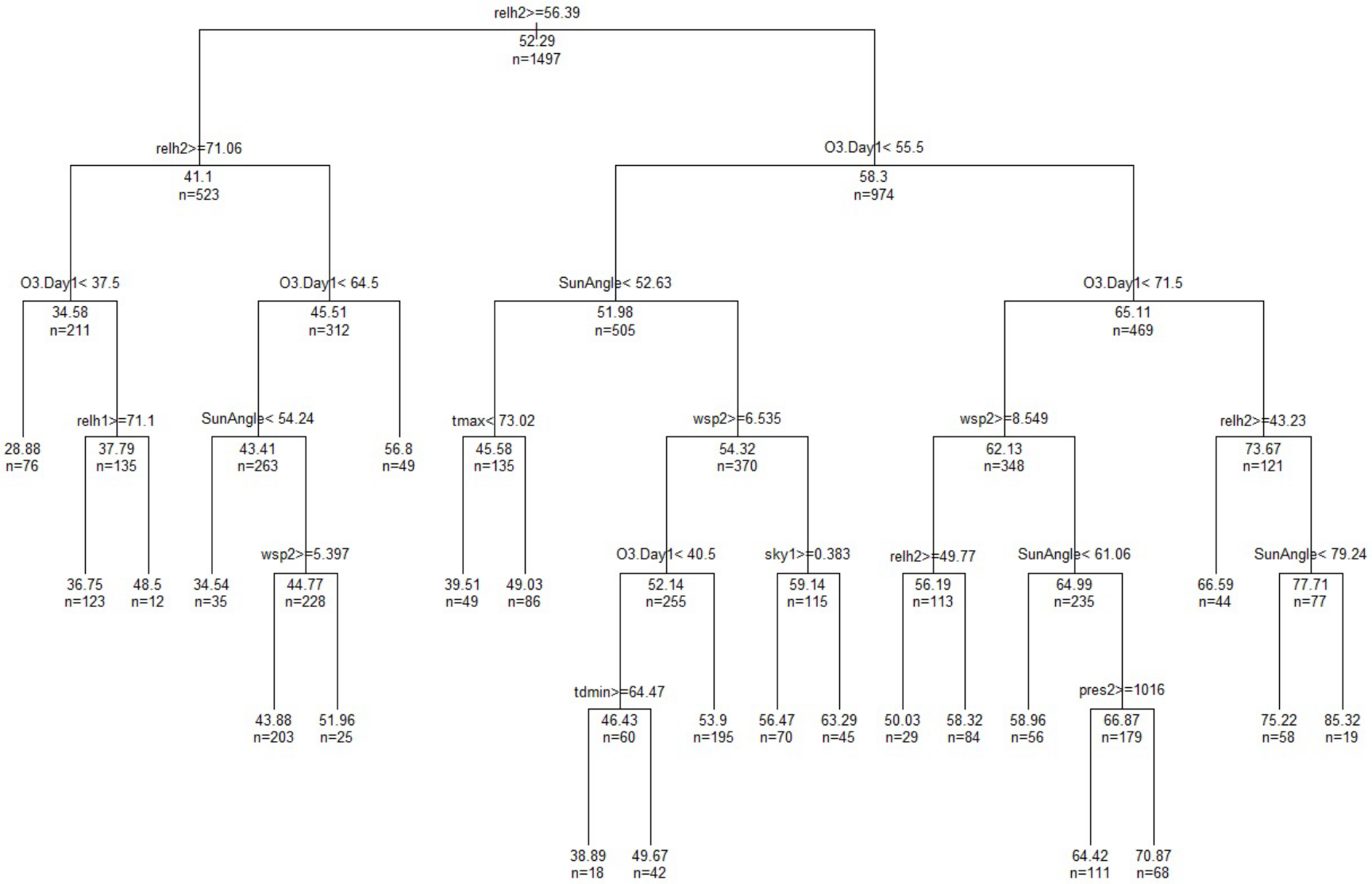

Figure 16. Best split for the regression tree CART analysis for Atlanta ozone during 2011-2017. Tree splits to the left meet the specified criteria and tree splits to the right do not meet the specified criteria.

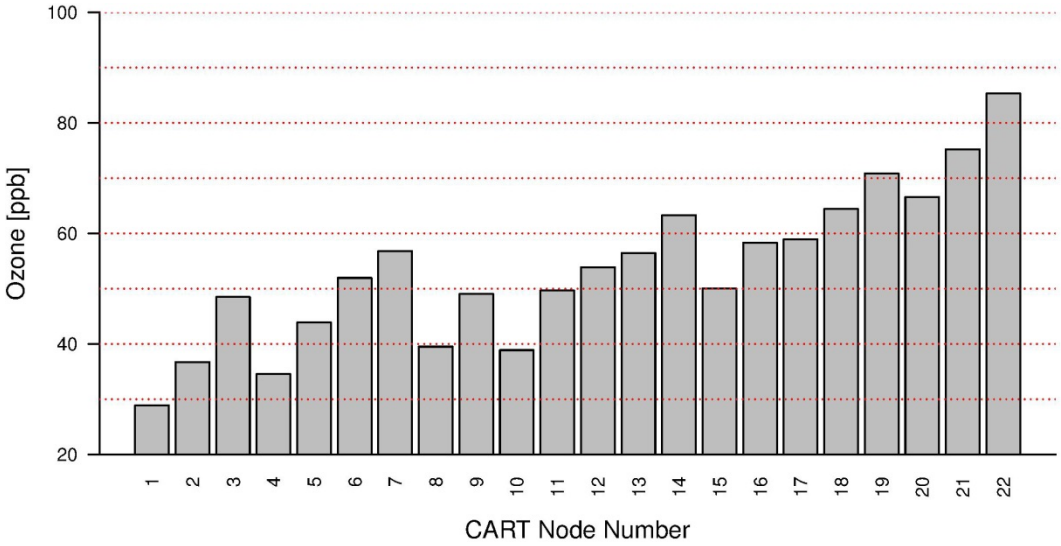

Figure 17. Mean ozone concentrations for 22 nodes found in the regression tree CART analysis.

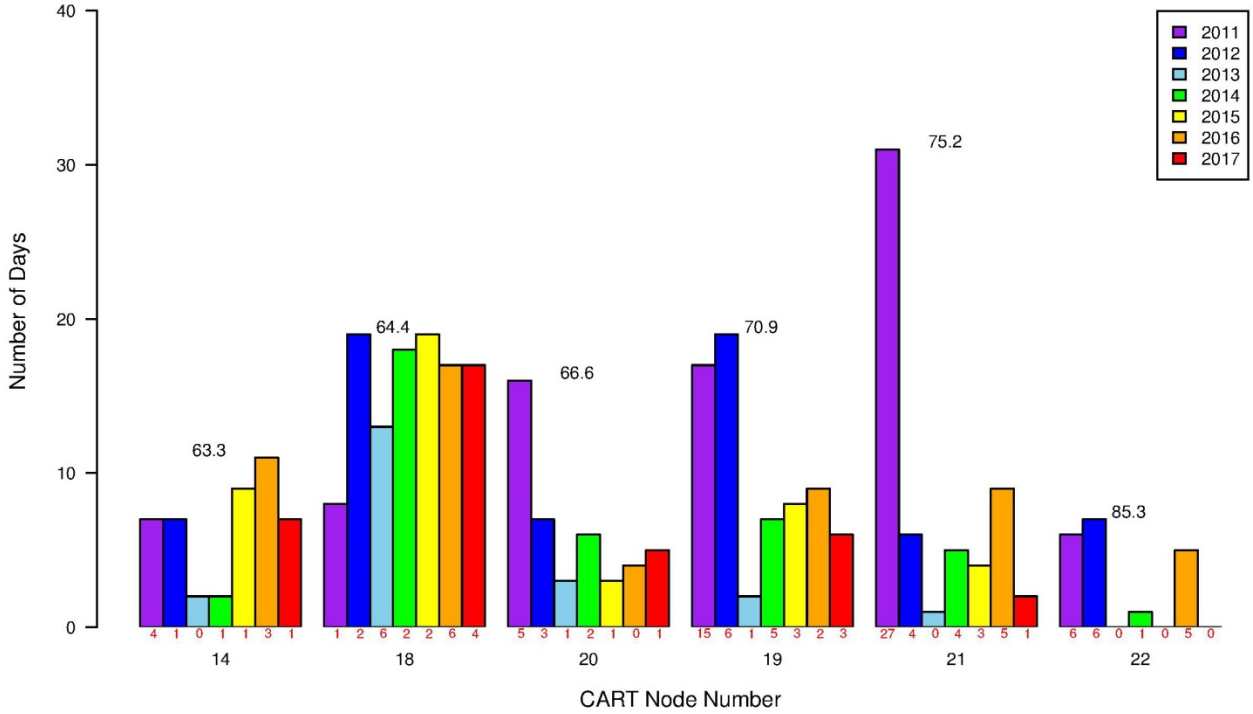

Figure 18. Number of days in 2011-2017 in the 6 high ozone nodes found in the regression tree CART analysis. Average ozone concentrations (black numbers on top) and number of ozone exceedance days (red numbers on bottom) are labeled for each node.

Classification tree CART analysis

The best split of classification tree CART analysis finds 17 nodes which represent ozone clusters grouped after a sequence of filters with various conditions. The mean ozone concentrations generally increase from left to right (Figure 14). There are two nodes with mean ozone concentrations higher than 70 ppb and six nodes with mean ozone concentrations ranging from 60 to 70 ppb (Figure 15). Six "critical" nodes with high mean ozone concentrations were investigated to understand the patterns of environmental conditions on high ozone days (Table 11), similar to the regression tree CART analysis conducted above.

The six "critical" nodes in the classification tree CART analysis are always associated with two environmental variables (PM RH and T_{max}). Four of the six critical nodes are also associated with ozone on previous one day (O_3 Day-1), similar to the regression tree CART analysis. PM wind is associated with four of the six critical nodes in this analysis. The maximum dew point temperature (Td_{max}) appears only in one node, indicating less association with the nodes for high ozone days and thus less responsibility for the high ozone days. The daily maximum solar elevation angle is not in association with any of the six "critical" nodes with high ozone levels, different than the results from regression CART analysis. The environmental variables with the higher number of associated nodes for high ozone days are more responsible for the high ozone days. In addition, the importance of variables decreases from the top of the tree to the bottom (Figure 19). Therefore, PM relative humidity (PM RH) is the most critical variable, followed by ozone on previous one day (O_3 Day-1) for the nodes with high ozone concentrations. Eight levels of splits are shown in the best classification CART tree (Figure 19).

The number of both days and exceedance days in the 6 'critical' nodes were summarized by years (Figure 21) showing a large inter-annual variation. The number of exceedance days during 2011 in the node 17 representing dry condition and high ozone concentrations on a previous day is the highest. Similar conditions represented by node 17 caused much less exceedances in 2017. Ten out of the eleven ozone exceedances in 2017 falls in the six "critical" nodes (mainly nodes 14, 15, 16 and 17). For these four nodes, the PM RH is less than 51.4%, indicating high correlation of high ozone days with low relative humidity (relatively dry conditions). A drier condition represented in node 16 (PM RH < 40.2%) can cause even higher ozone concentrations. High ozone days in 2017 are also associated with high temperatures, which can increase chemical reaction rates resulting in faster ozone production. The T_{max} is higher than 87.1 ^{o}F for four critical nodes. Low PM wind speeds are also linked to high ozone days. In addition, high ozone days in 2017 are less associated with high ozone concentrations on a previous day. The ozone concentrations on the day before exceedance are higher than 55 ppb. Interestingly, high ozone days in 2017 are not impacted by the solar elevation angle as found in the regression CART analysis. The contribution from solar elevation angle may be assigned to the contribution from daily maximum temperature. These two variables are highly correlated. In summary, the ozone exceedance days in 2017 are usually associated with dry, hot and calm meteorological conditions. The high solar radiation is not identified as a major contributing factor in the classification tree CART analysis as found in the regression tree CART analysis.

Table 12. Conditions for top 6 high ozone nodes of the classification tree CART analysis

Node Number	6	14	15	5	16	17
Mean O_3 (ppb)	62.7	62.9	64.2	64.5	76.2	76.9
O_3 exceedances in 2017	1	3	2	0	2	2
PM RH (%)	≥51.4	< 51.4	40.2-51.4	≥51.4	40.2-51.4	< 40.2
T_{max} (^oF)	> 87.1	< 89.1	> 89.1	> 87.1	> 89.1	> 89.1
O_3 Day-1 (category)		> 1.5[a]	> 1.5		> 1.5	> 1.5
PM wind (m/s)	< 5.5		< 5.6	> 5.5	< 5.6	
Td_{max} (^oF)				< 70		

[a] Ozone >1.5 category means ozone in category 2 and above, representing ozone ≥55 ppb.

High ozone day conditions

Both regression and classification tree CART analyses have found that high ozone days are always associated with low PM RH. Although T_{max} is only found to be critical in Classification tree CART analysis, it is also largely correlated with high daily maximum solar elevation angle. Both variables appear in the calculation of photochemical reaction rate. High previous day ozone is also found to be important in both CART analyses. Dry and hot are typical summer meteorological conditions in Atlanta due to high pressure systems. Under such conditions, local ozone formation would be largely enhanced. The large impact of the low RH and high air temperature on ozone formations has also been found in previous studies for the southeastern United States (Blanchard et al., 2014; Zhang and Wang, 2016). In addition, other factors such as PM wind and ozone concentrations on previous days may also cause elevated ozone conditions though their impact levels may vary. Strong correlation of cloud coverage (sky1 and sky2) with ozone exceedance days was found in the MLR analysis, but not found in the CART analyses. This is likely caused by the strongly correlation between the cloud coverage and RH.

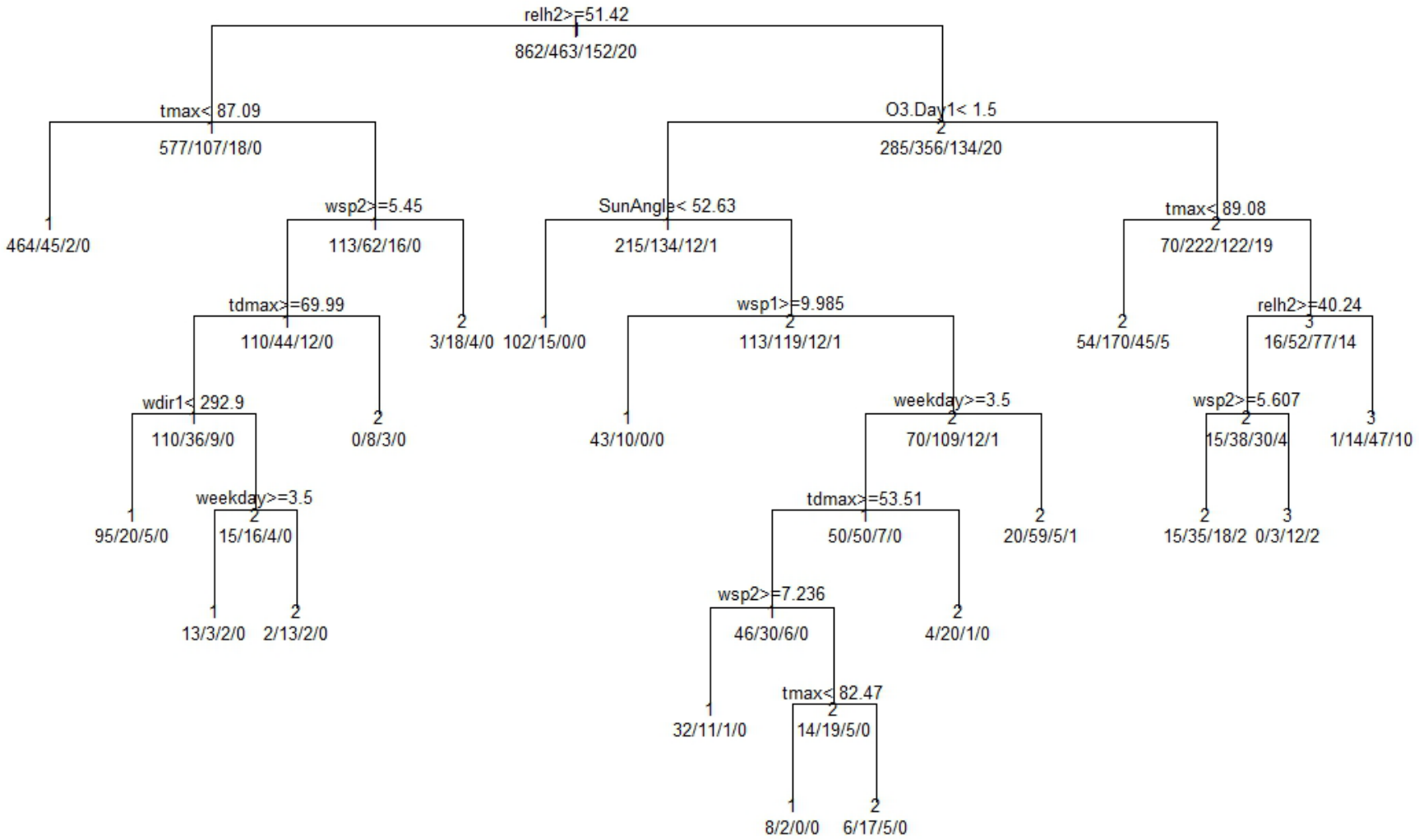

Figure 19. Best split for the classification tree CART analysis for Atlanta ozone during 2011-2017. Tree splits to the left meet the specified criteria and tree splits to the right do not meet the specified criteria.

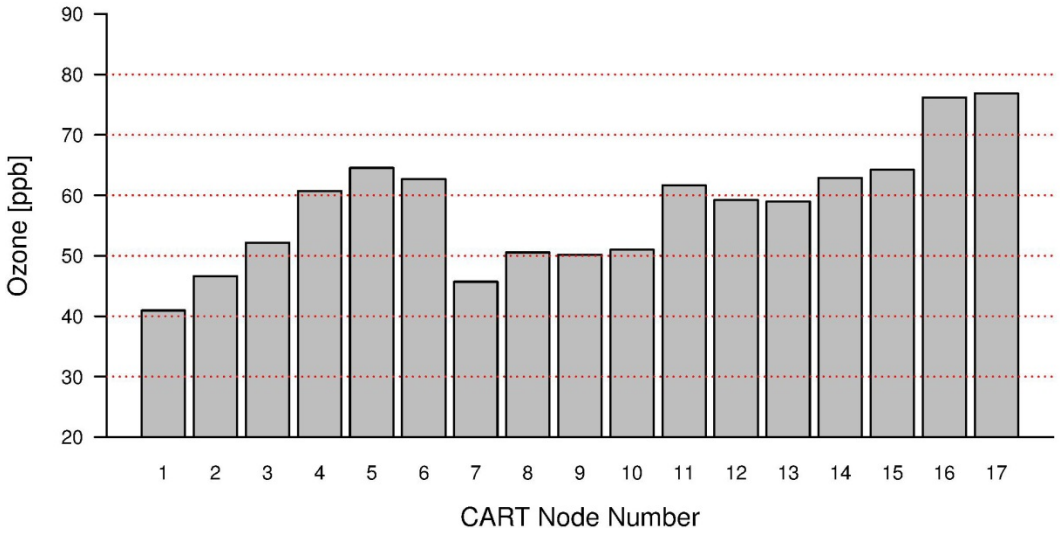

Figure 20. Mean ozone concentrations for 17 nodes found in the classification tree CART analysis.

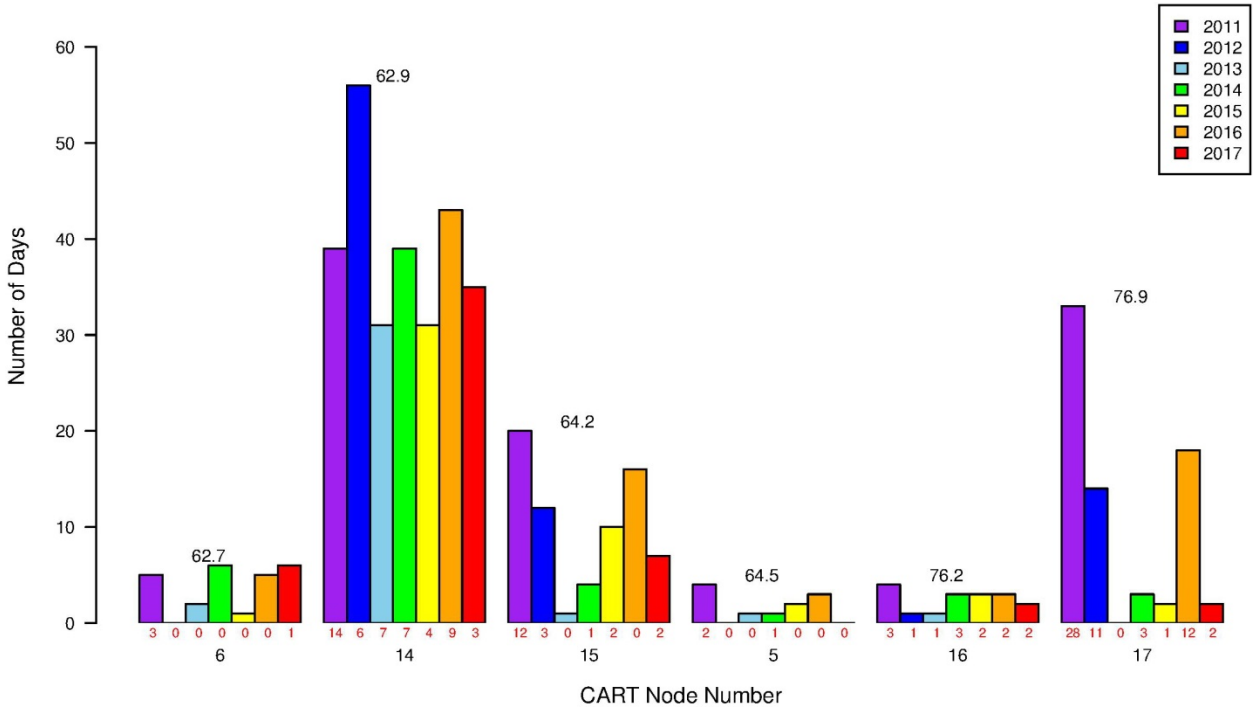

Figure 21. Number of days in 2011-2017 in the 6 high ozone nodes found in the classification tree CART analysis. Average ozone concentrations (black numbers on top) and numbers of ozone exceedance days (red numbers on bottom) are labeled for each node.

6. Ozone and Meteorological Conditions

Impacts of meteorological conditions on ozone formation and transport were investigated with ozone and meteorological condition time series plots, Hybrid Single Particle Lagrangian Integrated Trajectory (HYSPLIT, http://www.arl.noaa.gov/HYSPLIT_info.php) back trajectory modeling, animation of ozone and wind conditions, and analysis of 1-min. ozone time series data.

Ozone and meteorological condition time series analysis

Time series of hourly ozone at all exceeding monitors during each exceedance period and corresponding meteorological variables (temperature, relative humidity, and solar radiation) at the South DeKalb monitor were developed (Figure 22-Figure 29). The time series were developed for all exceedance days in the Metro Atlanta area when one or more ozone monitors exceeded the NAAQS. Each time series plot includes the data for one day before each exceedance. Ozone exceedances are associated with high temperature and low relative humidity, as well as high solar radiation as identified in the previous sections.

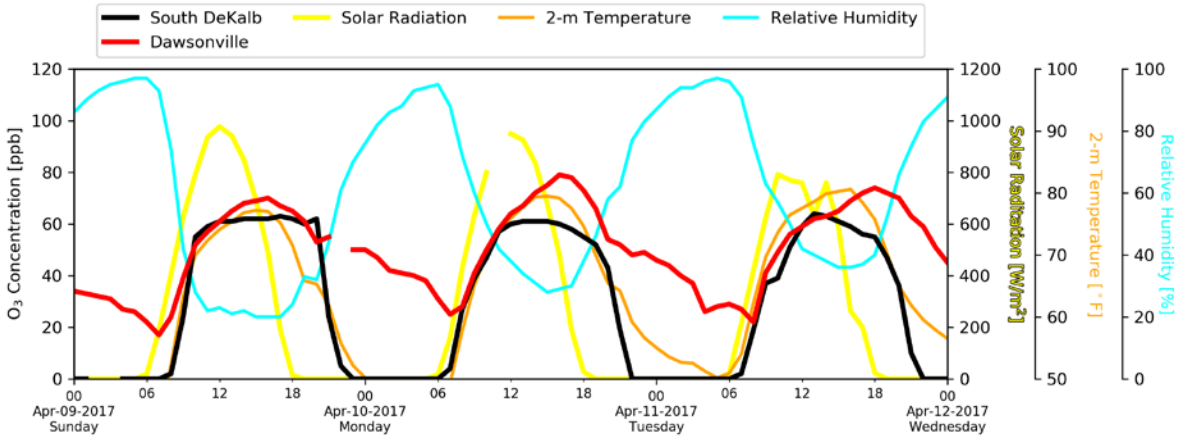

Figure 22. Time series of 1-hour ozone concentrations (left y-axis), solar radiation (the first right y-axis), 2-m temperature (the second right y-axis), and relative humidity (the rightmost y-axis) for April 9-11, 2017.

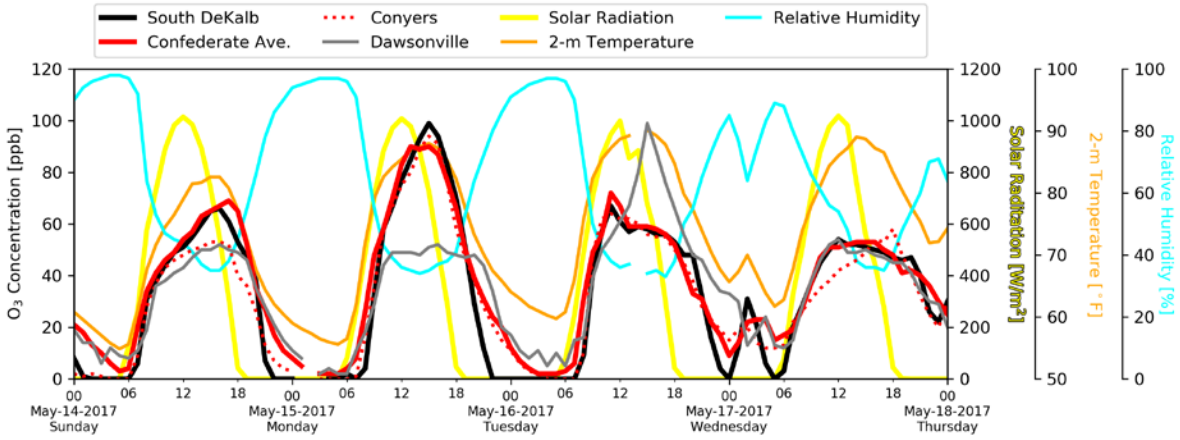

Figure 23. Time series of 1-hour ozone concentrations (left y-axis), solar radiation (the first right y-axis), 2-m temperature (the second right y-axis), and relative humidity (the rightmost y-axis) for May 14-17, 2017.

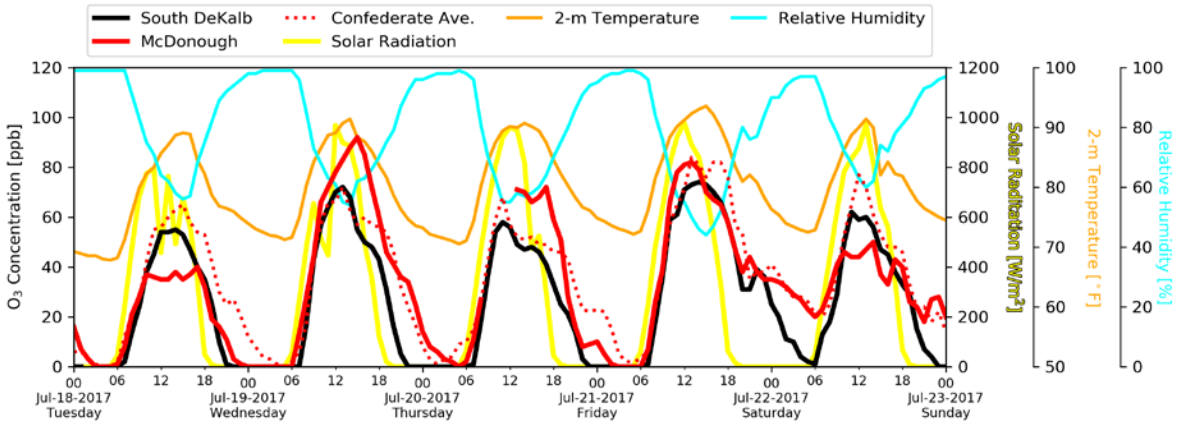

Figure 24. Time series of 1-hour ozone concentrations (left y-axis), solar radiation (the first right y-axis), 2-m temperature (the second right y-axis), and relative humidity (the rightmost y-axis) for July 18-22, 2017.

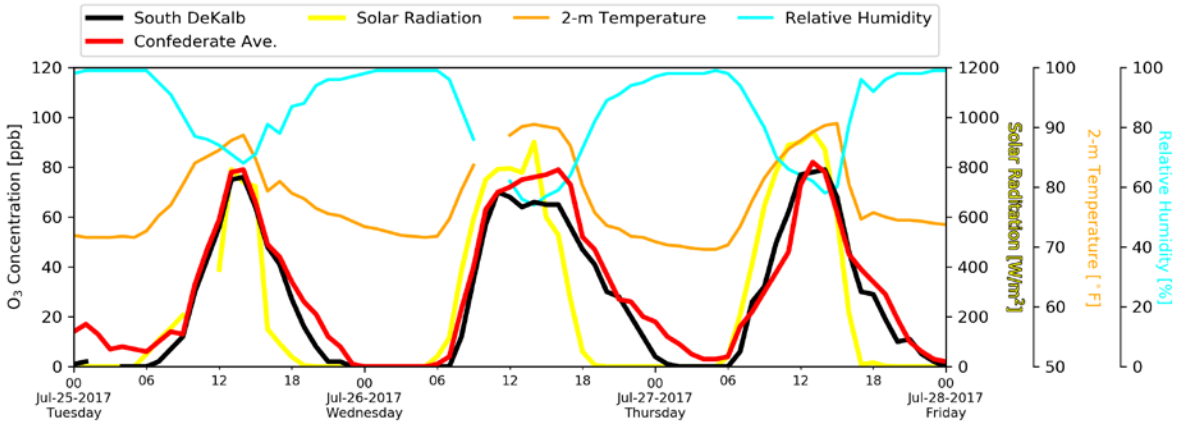

Figure 25. Time series of 1-hour ozone concentrations (left y-axis), solar radiation (the first right y-axis), 2-m temperature (the second right y-axis), and relative humidity (the rightmost y-axis) for July 25-27, 2017.

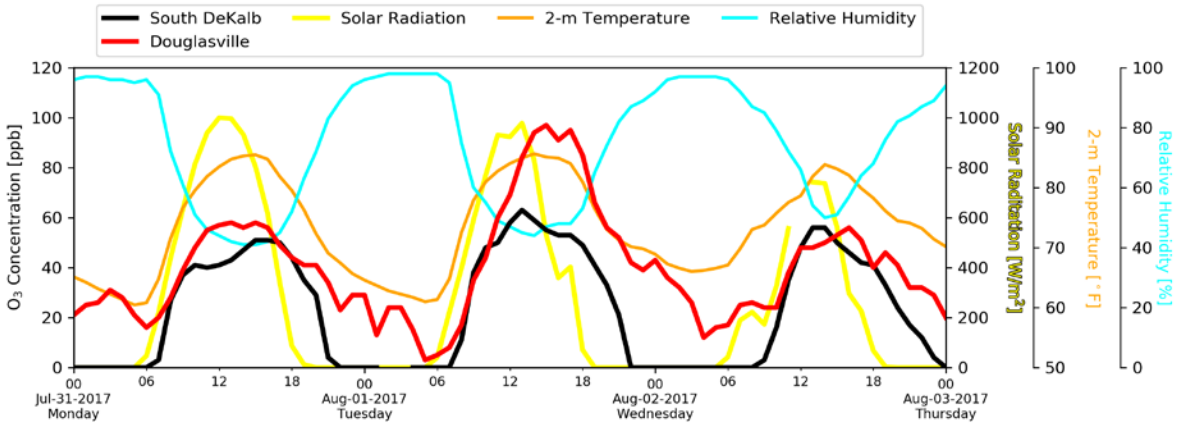

Figure 26. Time series of 1-hour ozone concentrations (left y-axis), solar radiation (the first right y-axis), 2-m temperature (the second right y-axis), and relative humidity (the rightmost y-axis) for July 31-August 2, 2017.

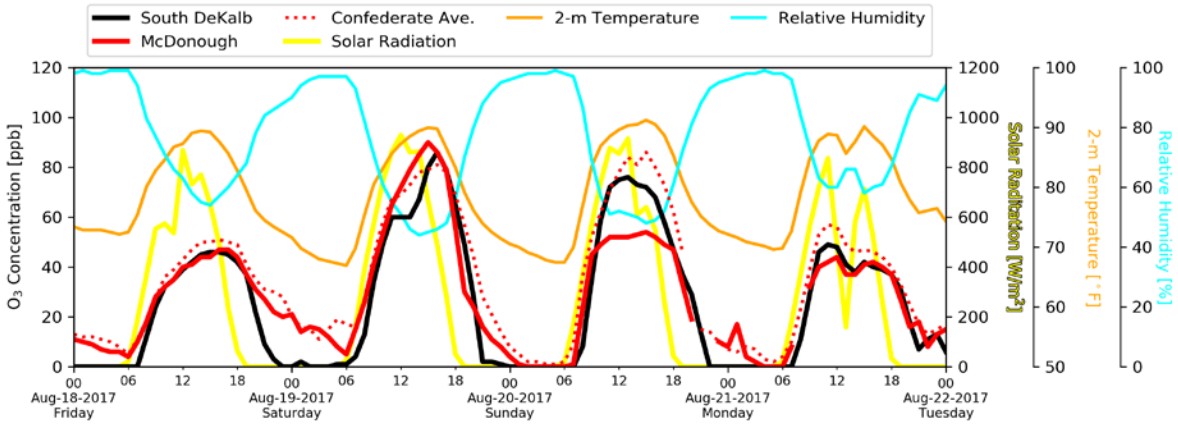

Figure 27. Time series of 1-hour ozone concentrations (left y-axis), solar radiation (the first right y-axis), 2-m temperature (the second right y-axis), and relative humidity (the rightmost y-axis) for August 18-21, 2017.

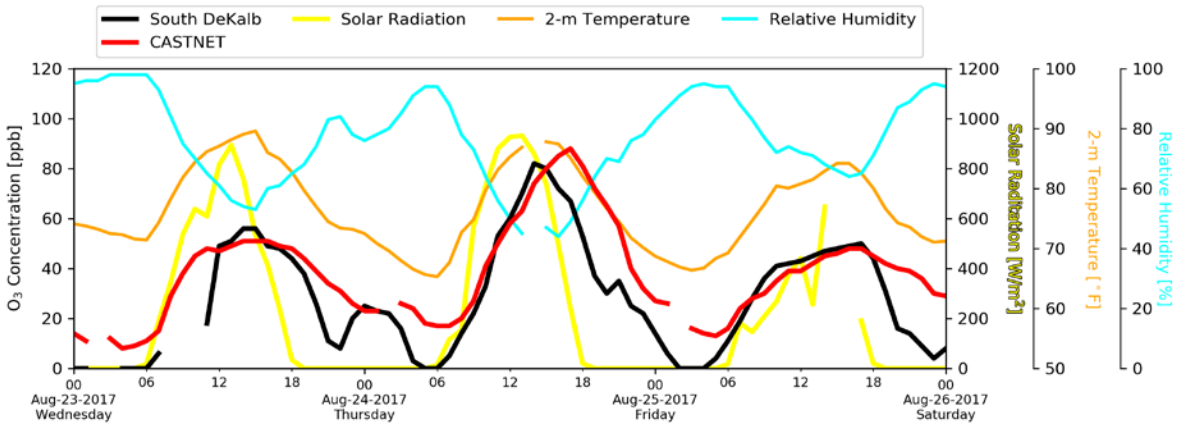

Figure 28. Time series of 1-hour ozone concentrations (left y-axis), solar radiation (the first right y-axis), 2-m temperature (the second right y-axis), and relative humidity (the rightmost y-axis) for August 23-25, 2017.

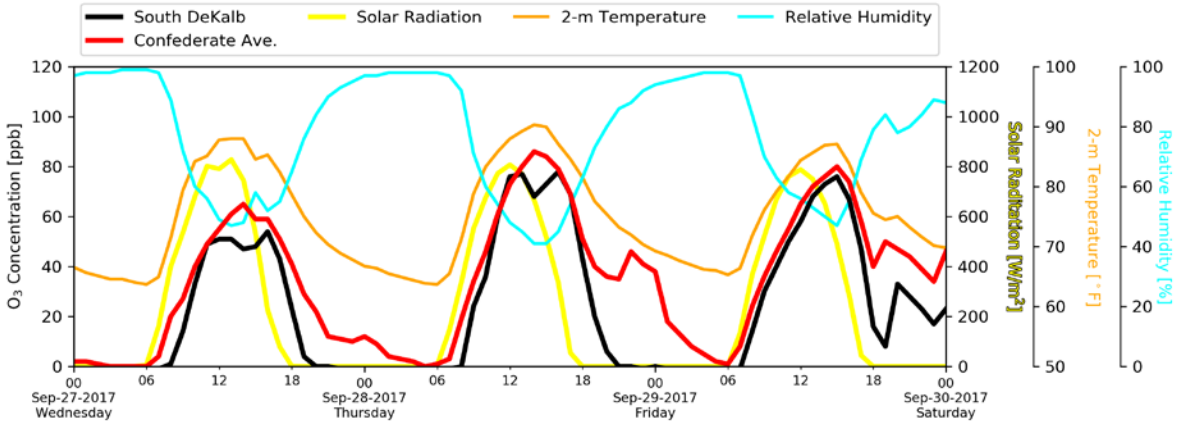

Figure 29. Time series of 1-hour ozone concentrations (left y-axis), solar radiation (the first right y-axis), 2-m temperature (the second right y-axis), and relative humidity (the rightmost y-axis) for September 27-29, 2017.

HYSPLIT back trajectory analysis

The Hybrid Single Particle Lagrangian Integrated Trajectory (HYSPLIT, http://www.arl.noaa.gov/HYSPLIT_info.php) back trajectory analysis was conducted to determine the origin of air masses and establish source-receptor relationships on ozone exceedance days. The HYSPLIT model is one of the most extensively used atmospheric transport and dispersion models in the atmospheric sciences community. In this analysis, HYSPLIT 24-hour back-trajectories were computed for each ozone exceedance in 2017 at each violating ozone monitor in Atlanta using North American Mesoscale (NAM) archive dataset[3] available at a 12-km resolution from National Oceanic and Atmospheric Administration (NOAA). For each 2017 ozone exceedance at a monitor, three back-trajectories were computed for air parcels ending at heights of 100 meters, 500 meters, and 1,000 meters at the time of the 1-hour peak ozone concentrations.

Figure 30-Figure 36 contain HYSPLIT trajectories for all exceeding monitors in 2017. The long trajectories are associated with higher wind speed and indicate more opportunities for transport impacts, while short or circular trajectories are associated with lower wind speeds and indicate stagnant or recirculation conditions and more opportunities for local impacts.

The trajectories for the height of 100 meters at these three monitors show mixed effects of a strong local impact and a long-range transport. On May 15, the trajectories at the Confederate Ave. (Figure 31), Conyers (Figure 32) and South DeKalb (Figure 36) monitors show similar urban-scale recirculation. The trajectories at the Confederate Ave. and McDonough (Figure 35) on July 21 and the trajectory at the Confederate Ave. on July 26 are short from the southeast, indicating strong local impacts. All other relatively longer trajectories for the Confederate Ave. monitor located inside of the Atlanta urban core mainly come from north, and from the Atlanta urban core for the CASTNET (Figure 30), Dawsonville (Figure 33), Douglasville (Figure 34) and McDonough monitors (Figure 35).

[3] ftp://arlftp.arlhq.noaa.gov/archives/nam12/

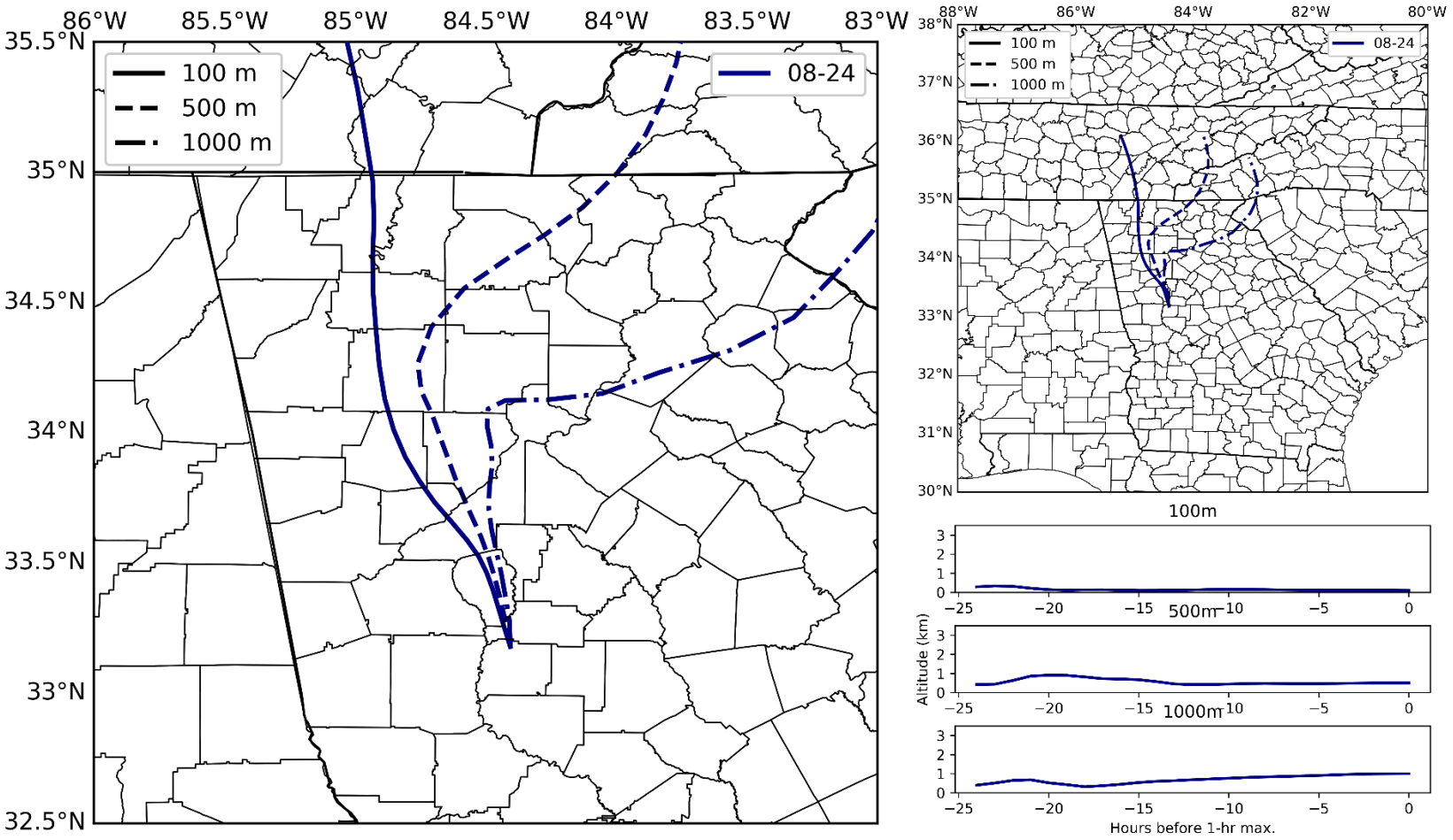

Figure 30. HYSPLIT 24 hour back-trajectories for exceedances at the CASTNET monitor and trajectory path heights.

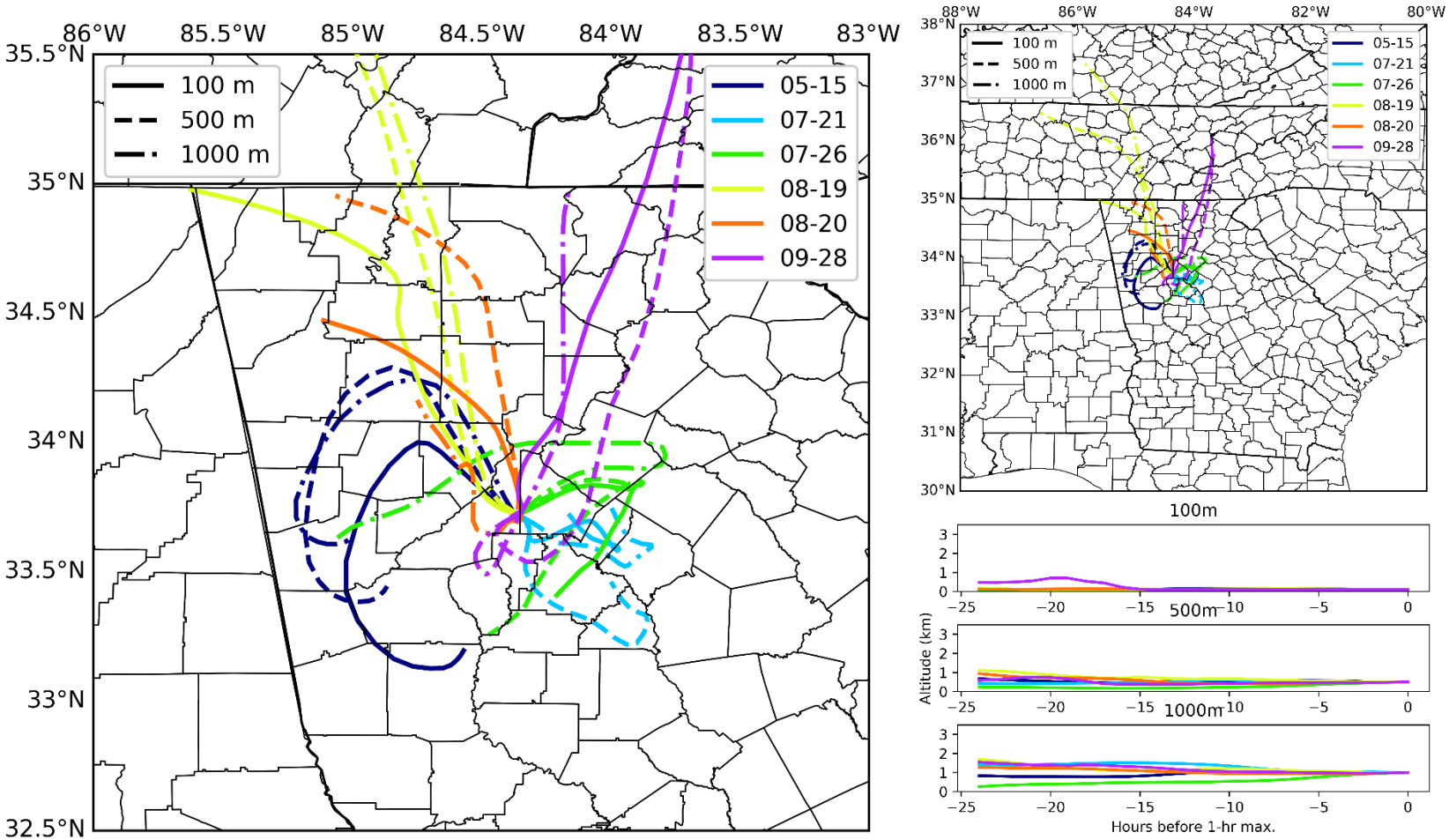

Figure 31. HYSPLIT 24 hour back-trajectories for exceedances at the Confederate Ave. monitor and trajectory path heights.

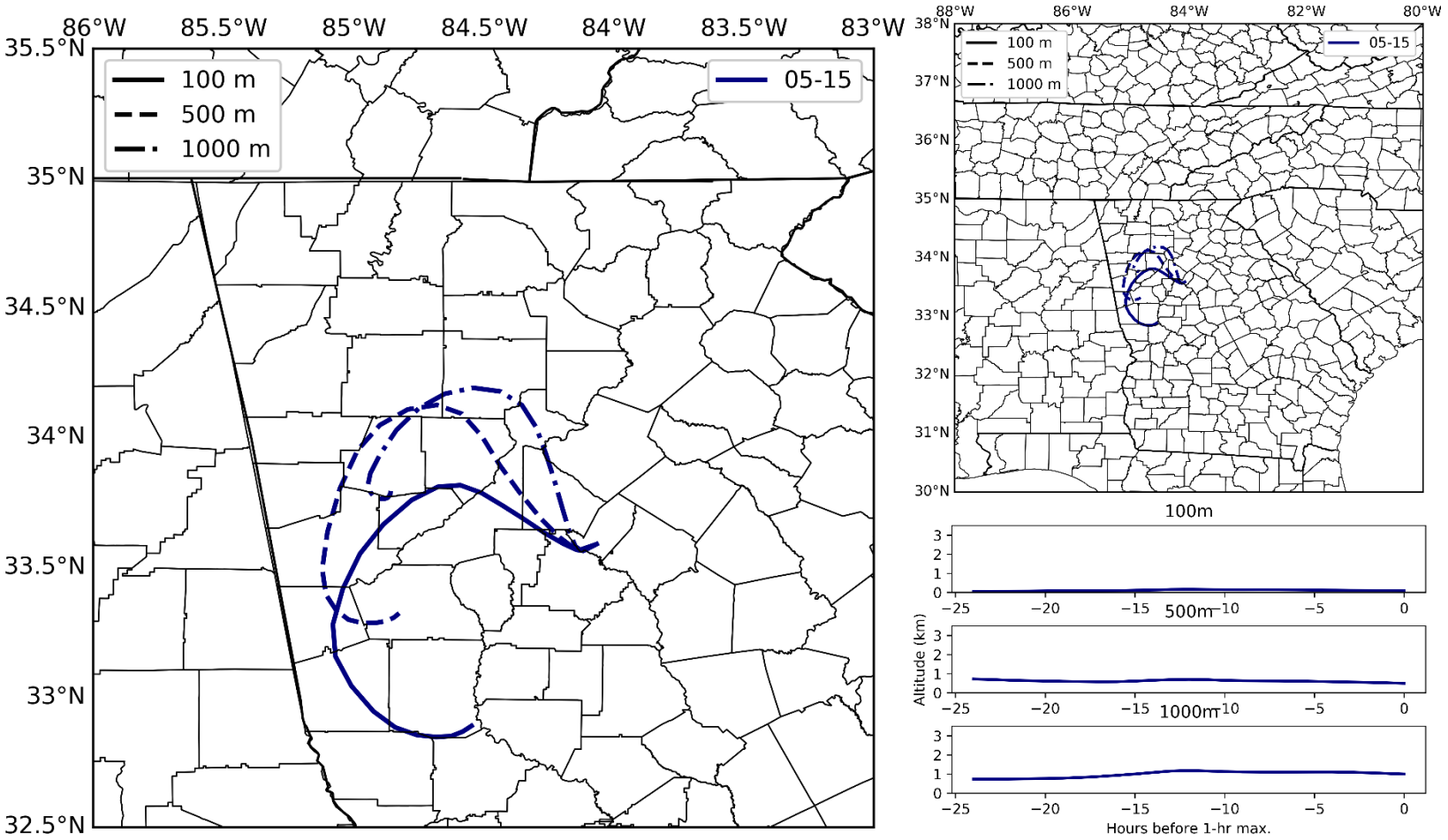

Figure 32. HYSPLIT 24 hour back-trajectories for exceedances at the Conyers monitor and trajectory path heights.

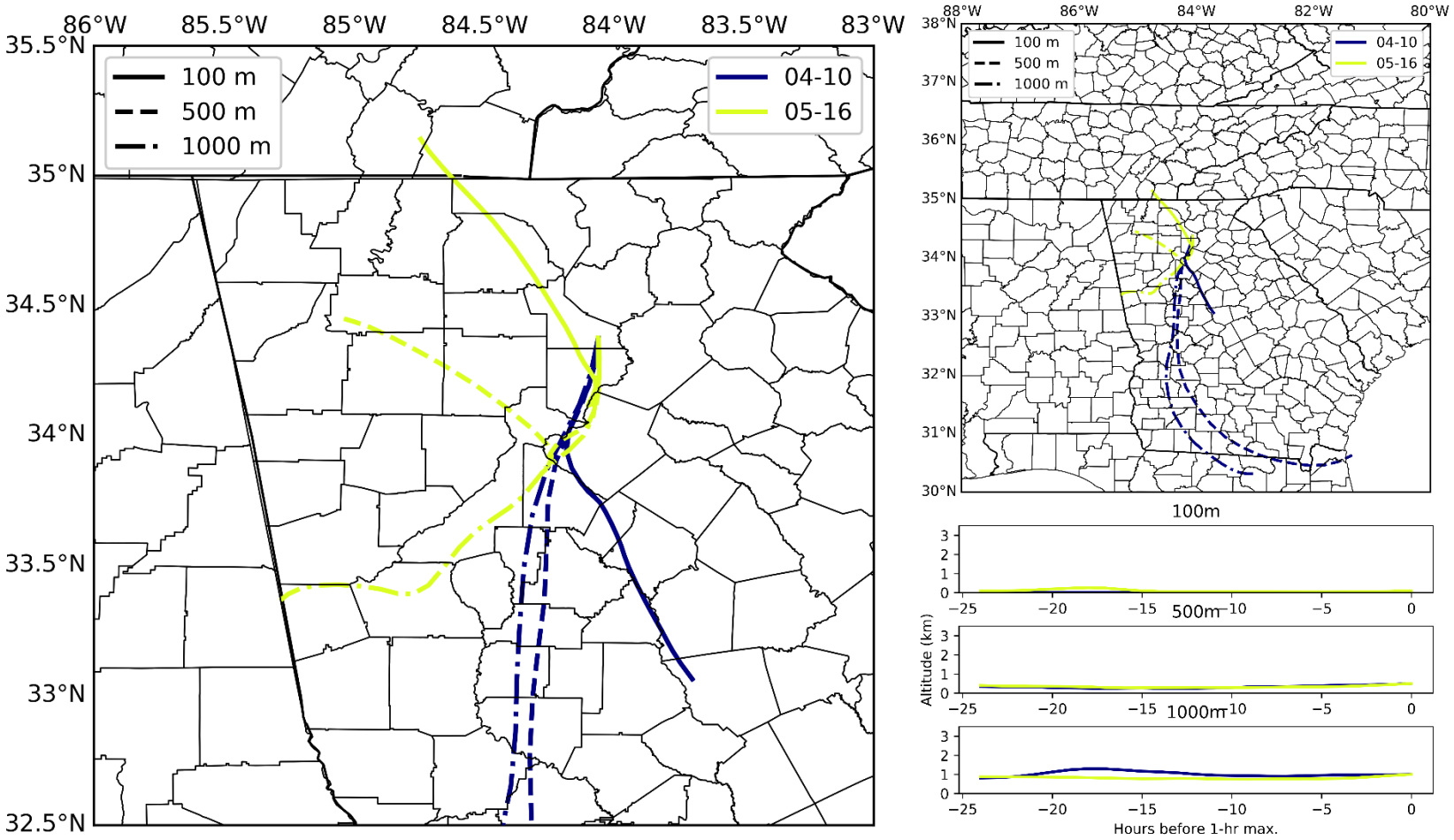

Figure 33. HYSPLIT 24 hour back-trajectories for exceedances at the Dawsonville monitor and trajectory path heights.

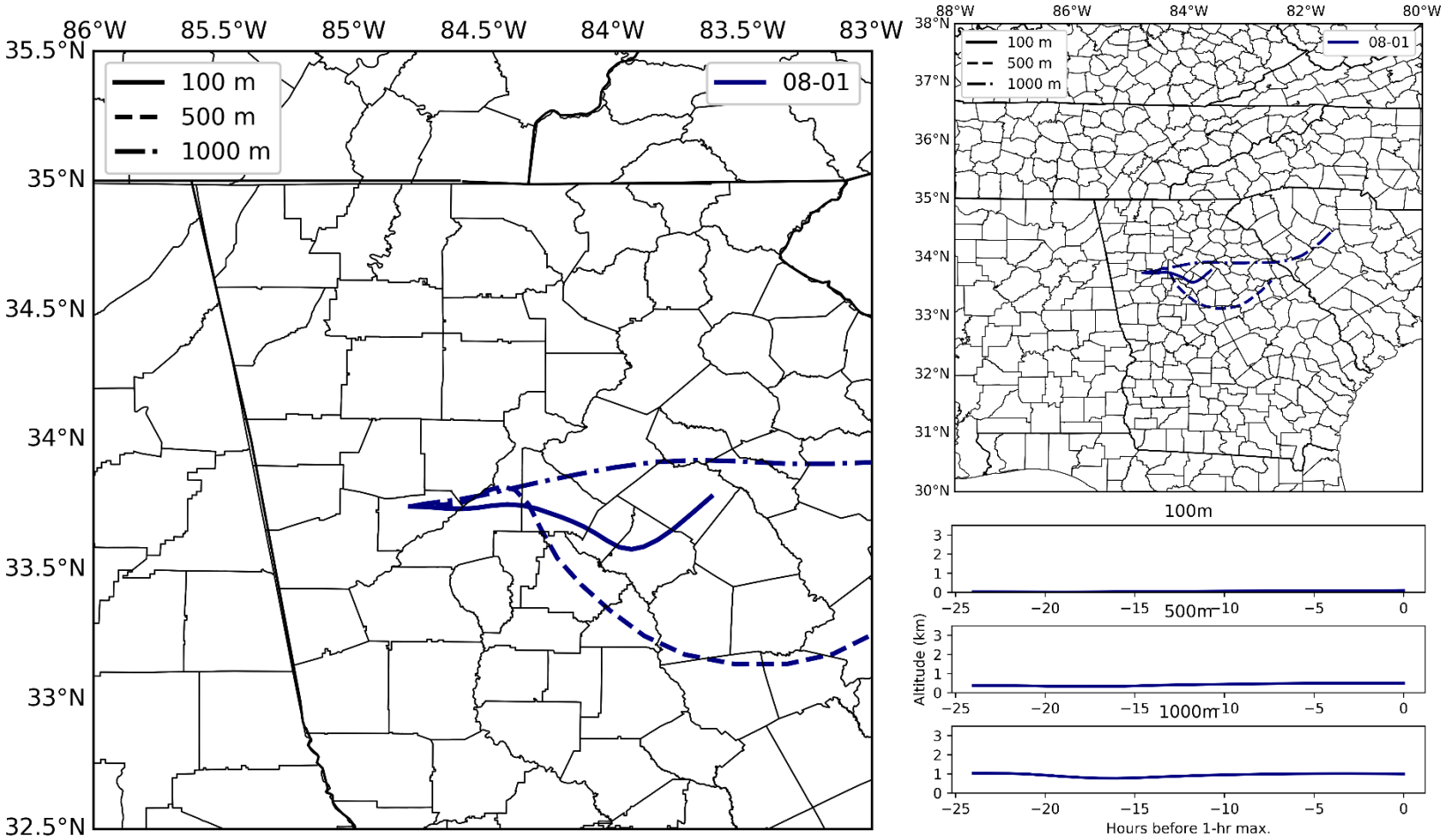

Figure 34. HYSPLIT 24 hour back-trajectories for exceedances at the Douglasville monitor and trajectory path heights.

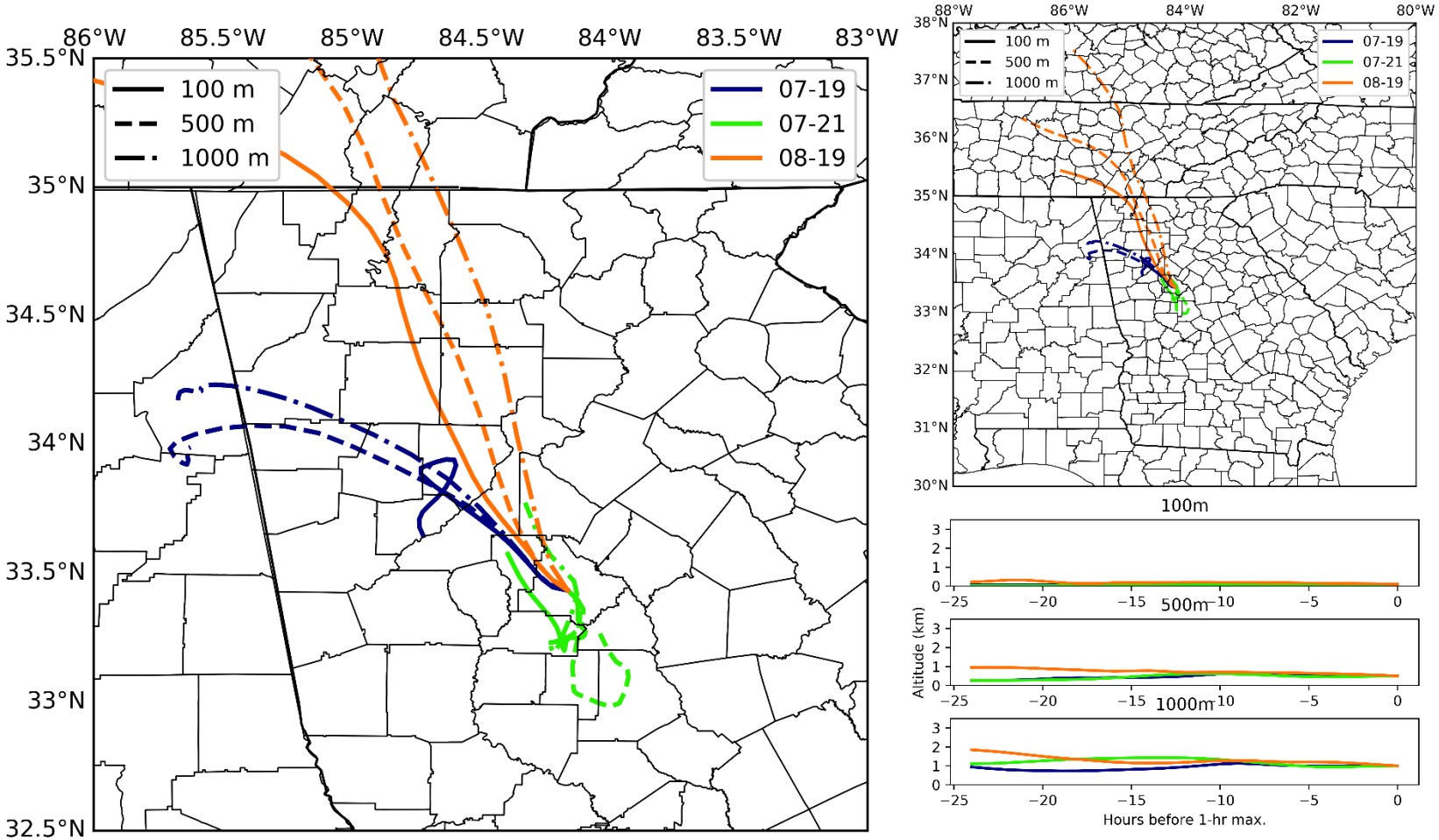

Figure 35. HYSPLIT 24 hour back-trajectories for exceedances at the McDonough monitor and trajectory path heights.

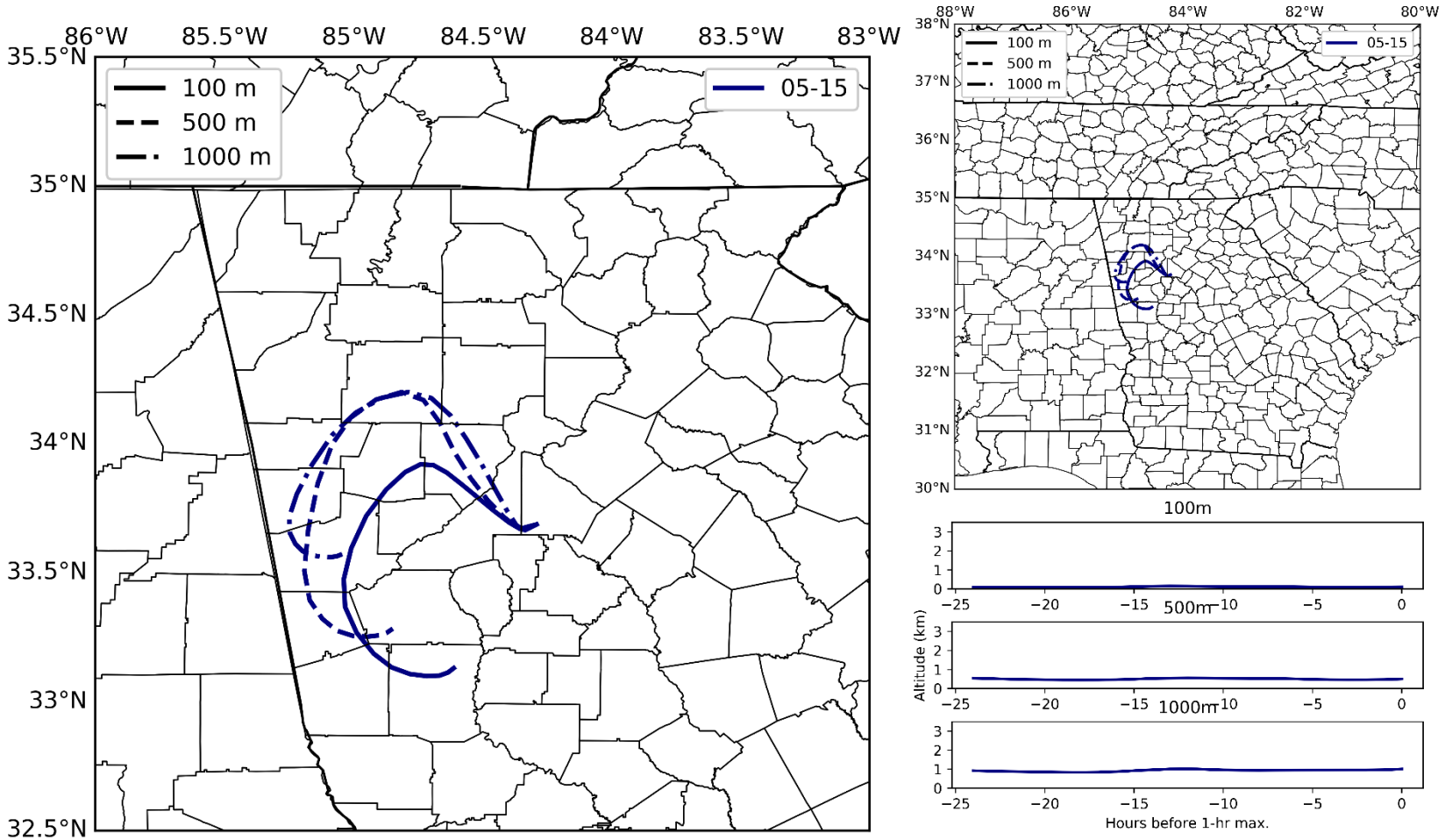

Figure 36. HYSPLIT 24 hour back-trajectories for exceedances at the South DeKalb monitor and trajectory path heights.

Animation of ozone and wind conditions

Animation of 5-minute ozone concentrations and wind conditions were developed for the 11 ozone exceedance days in 2017 over 4-km grids covering the Metro Atlanta in order to further understand the formation and transport of ozone. The 5-minute ozone concentrations were calculated using 1-minute observations at ozone monitors collected by the Ambient Monitoring Program. The 5-minute surface wind conditions were simulated using the latest version of Weather Research and Forecasting (WRF) model (v3.9.1.1). WRF was first run for the 12-km domain over the eastern United States (69×68 grids) and then run for the 4-km nested domain over Georgia (148×145 grids) (Figure 37) with NAM analysis meteorological data downloaded from NOAA FTP server (ftp://nomads.ncdc.noaa.gov/NAM/analysis_only/). The WRF configuration for physics and dynamics was the same as EPA's 2016 WRF modeling setup. Thirty five (35) vertical layers extending up to 50 mb were used. The simulation episode was 36 hours for each exceedance day with 6 spin-up hours. The 5-minute ozone data at monitors were further processed to 4-km WRF grids using Kriging 2D interpolation method with IDL[4] and plotted together with 5-minute WRF simulated wind data to generate 288 figures in postscript format for each exceedance day. These postscript format figures were then processed to a GIF animation using Linux scripts.

For each exceedance day, twelve hourly ozone and wind condition plots (7:00 AM to 6:00 PM) were shown below (Figure 38-Figure 48). For ozone exceedances that occurred outside of the Atlanta urban core, the general pattern is that wind blew from the urban core to the exceedance monitor (e.g., Figure 38). For ozone exceedances inside the Atlanta urban core, wind speeds were generally low (e.g. Figure 39). The animations dynamically demonstrate the Atlanta urban core as the origin of most high ozone events.

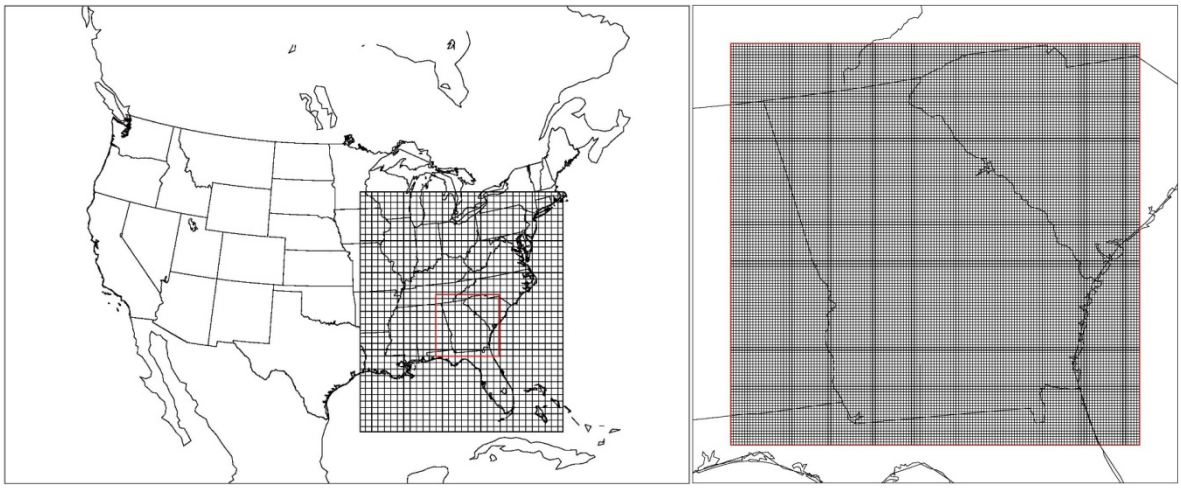

Figure 37. WRF 12-km domain over the eastern United States (left) and 4-km nested domain over Georgia (right).

[4] https://www.harrisgeospatial.com/SoftwareTechnology/IDL.aspx

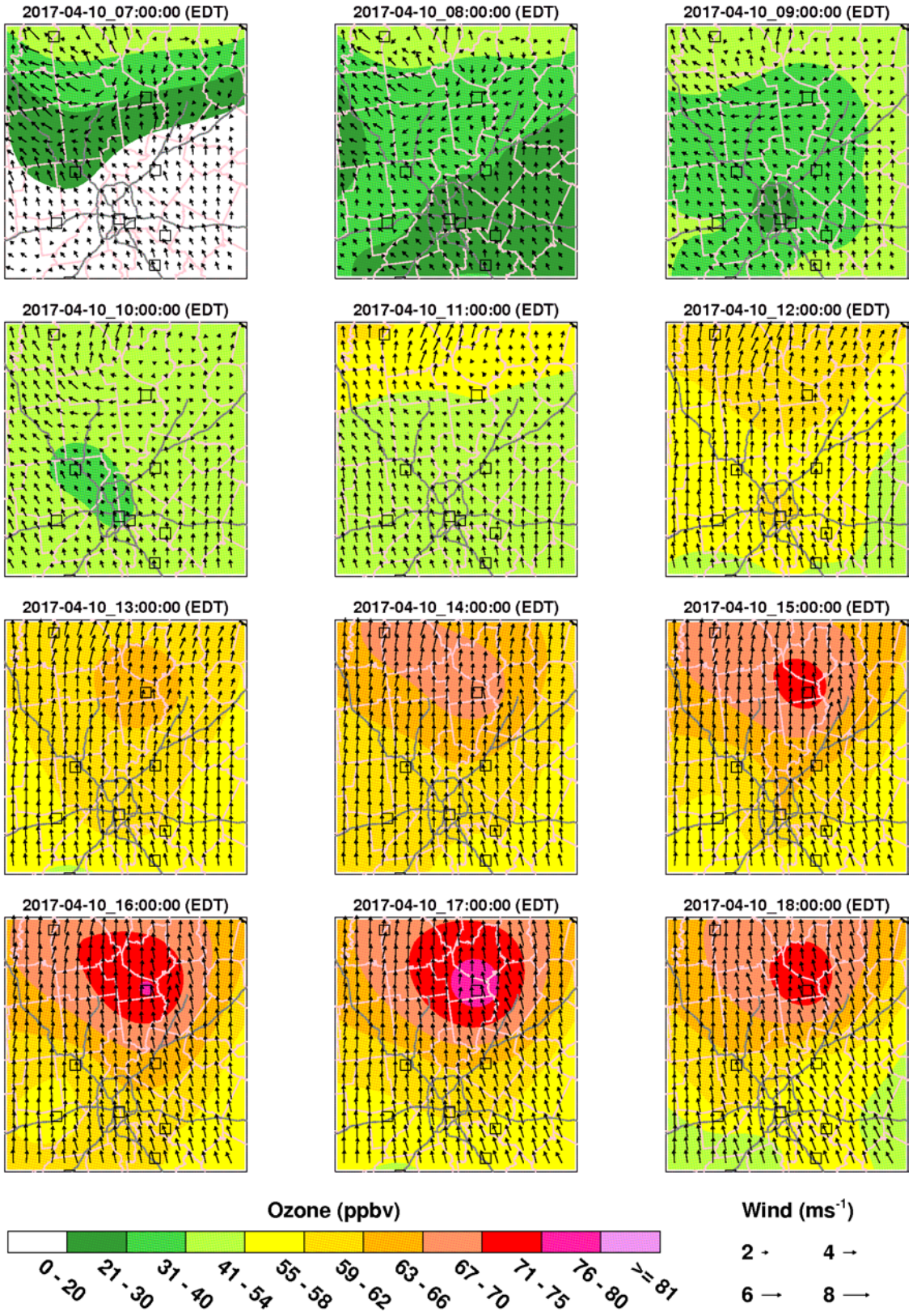

Figure 38. WRF simulated wind barbs and ozone observations (ppb) over Metro Atlanta from 7 AM to 6 PM on April 10, 2017. Ozone monitors are in black squares. The ozone exceedance occurred at the Dawsonville monitor.

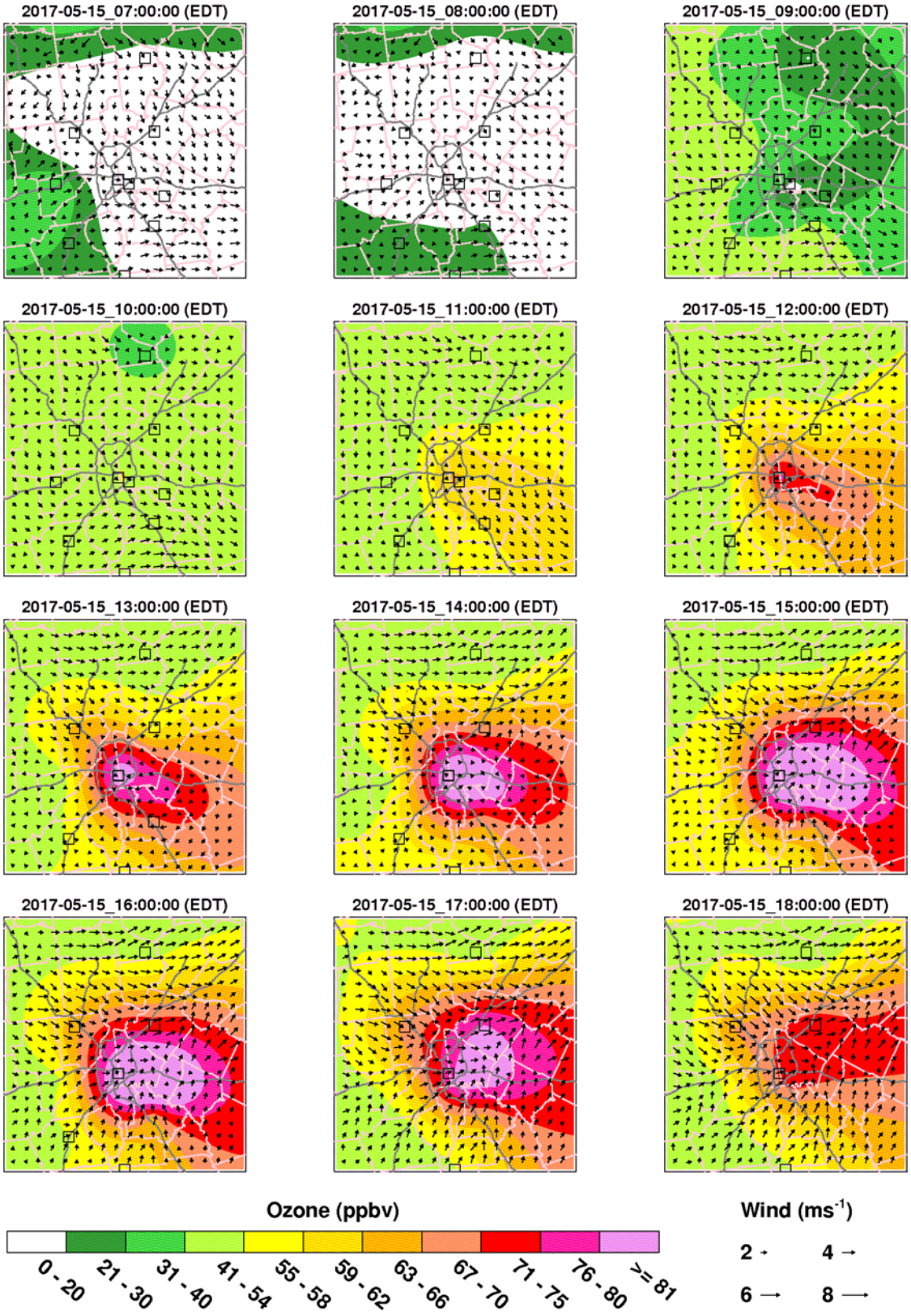

Figure 39. WRF simulated wind barbs and ozone observations (ppb) over Metro Atlanta from 7 AM to 6 PM on May 15, 2017. Ozone monitors are in black squares. The ozone exceedances occurred at the Confederate Ave., South DeKalb, and Conyers monitors.

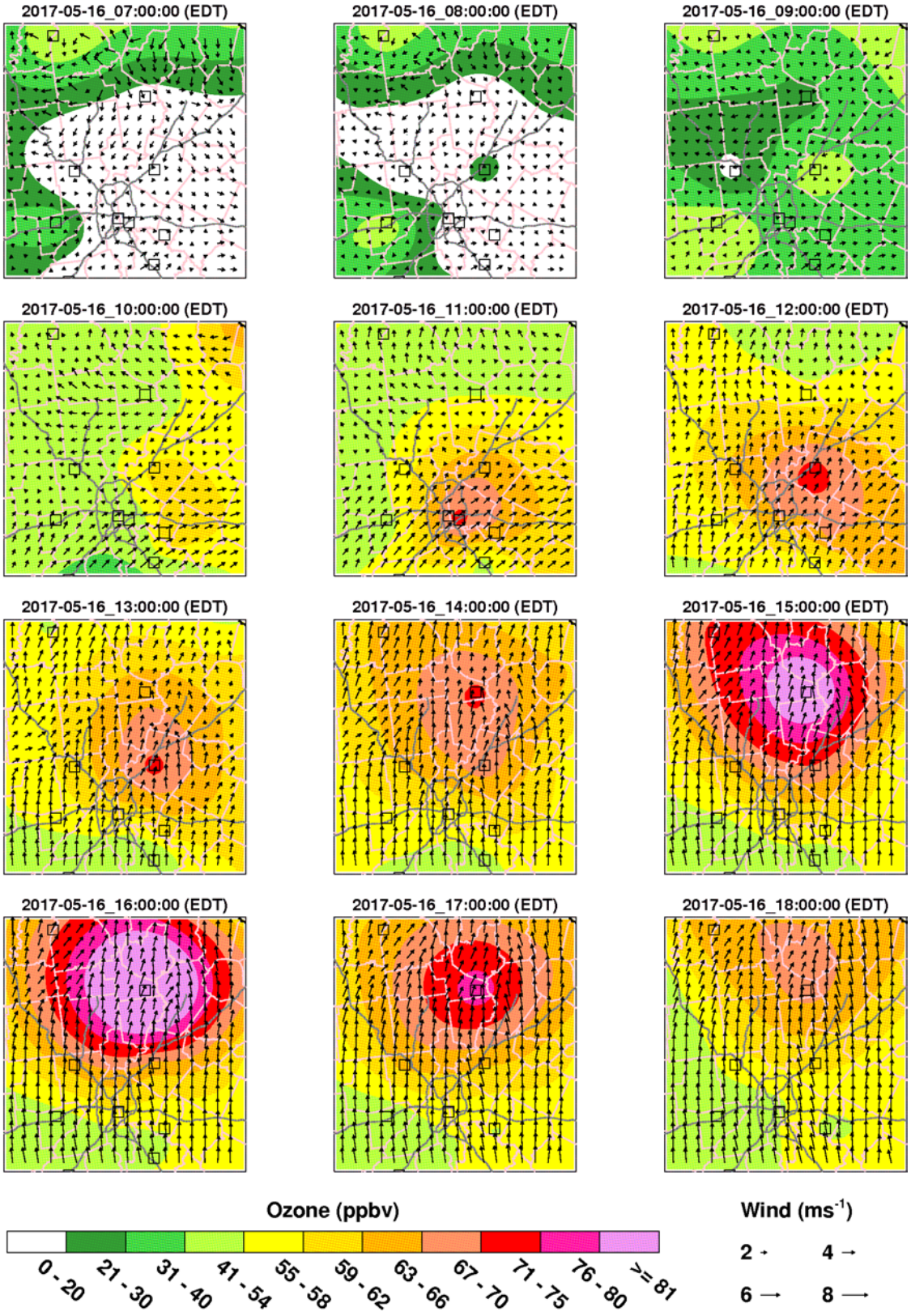

Figure 40. WRF simulated wind barbs and ozone observations (ppb) over Metro Atlanta from 7 AM to 6 PM on May 16, 2017. Ozone monitors are in black squares. The ozone exceedance occurred at the Dawsonville monitor.

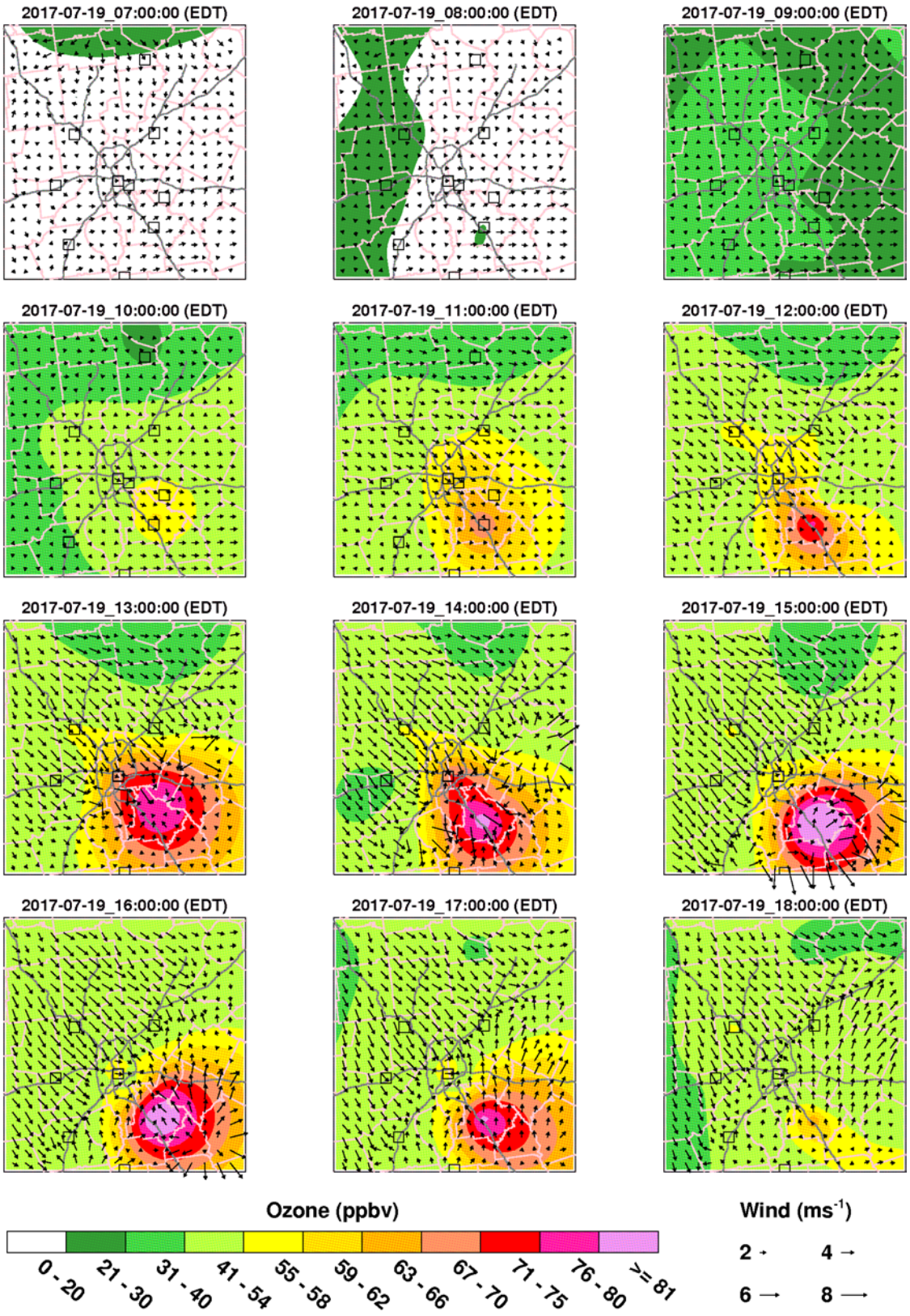

Figure 41. WRF simulated wind barbs and ozone observations (ppb) over Metro Atlanta from 7 AM to 6 PM on July 19, 2017. Ozone monitors are in black squares. The ozone exceedance occurred at the McDonough monitor.

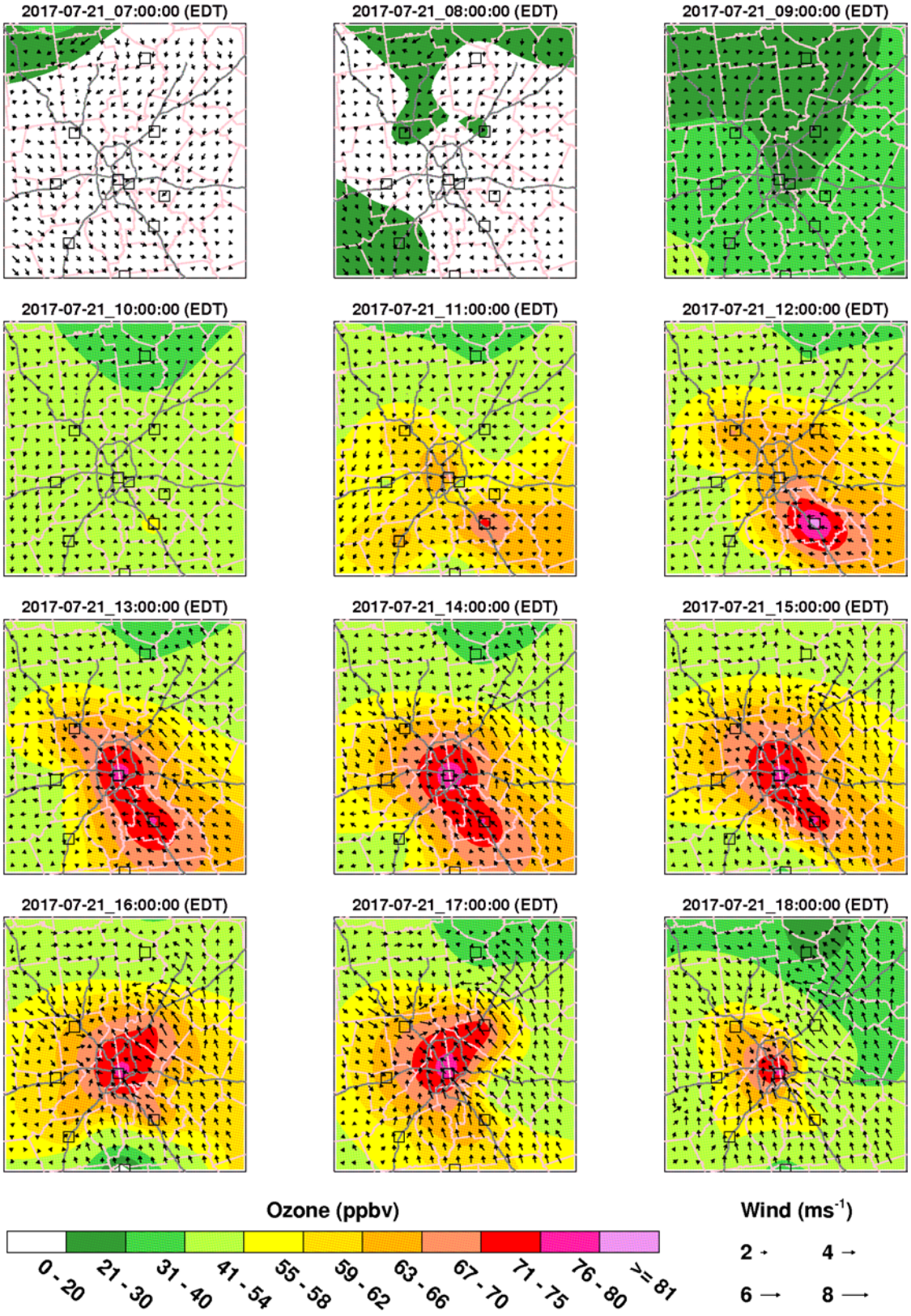

Figure 42. WRF simulated wind barbs and ozone observations (ppb) over Metro Atlanta from 7 AM to 6 PM on July 21, 2017. Ozone monitors are in black squares. The ozone exceedances occurred at the Confederate Ave. and McDonough monitors.

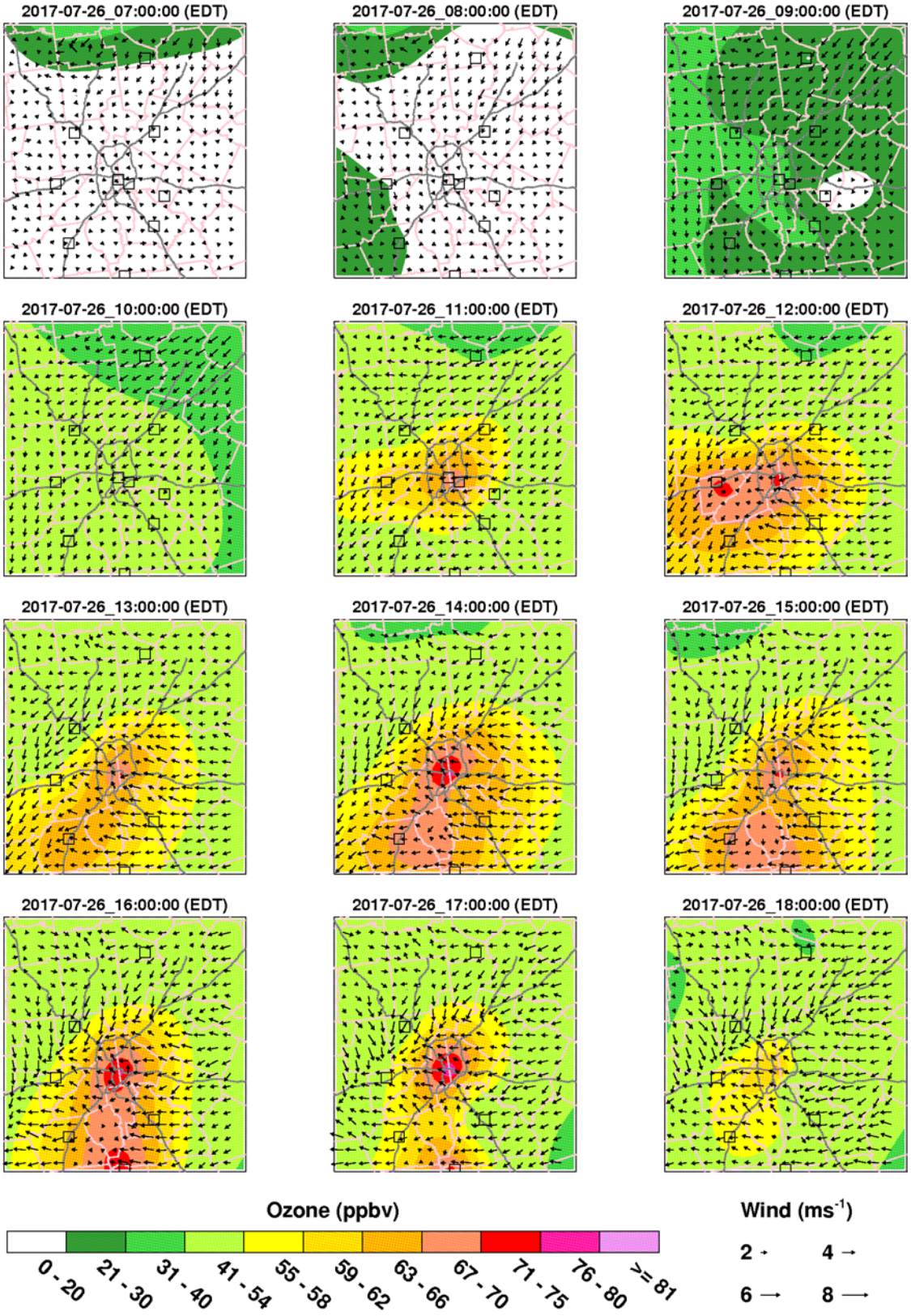

Figure 43. WRF simulated wind barbs and ozone observations (ppb) over Metro Atlanta from 7 AM to 6 PM on July 26, 2017. Ozone monitors are in black squares. The ozone exceedance occurred at the Confederate Ave monitor.

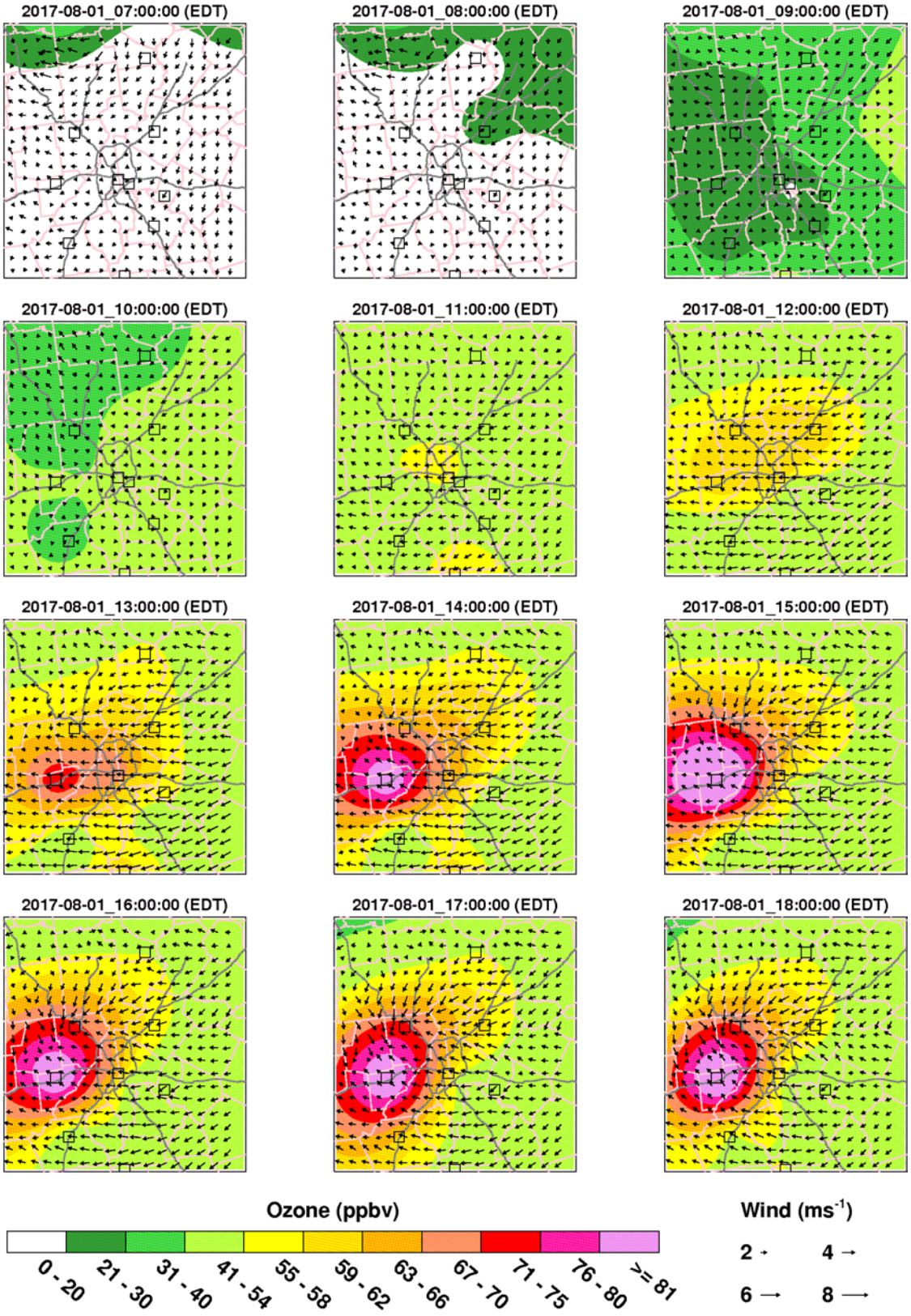

Figure 44. WRF simulated wind barbs and ozone observations (ppb) over Metro Atlanta from 7 AM to 6 PM m on August 1, 2017. Ozone monitors are in black squares. The ozone exceedance occurred at the Douglasville monitor.

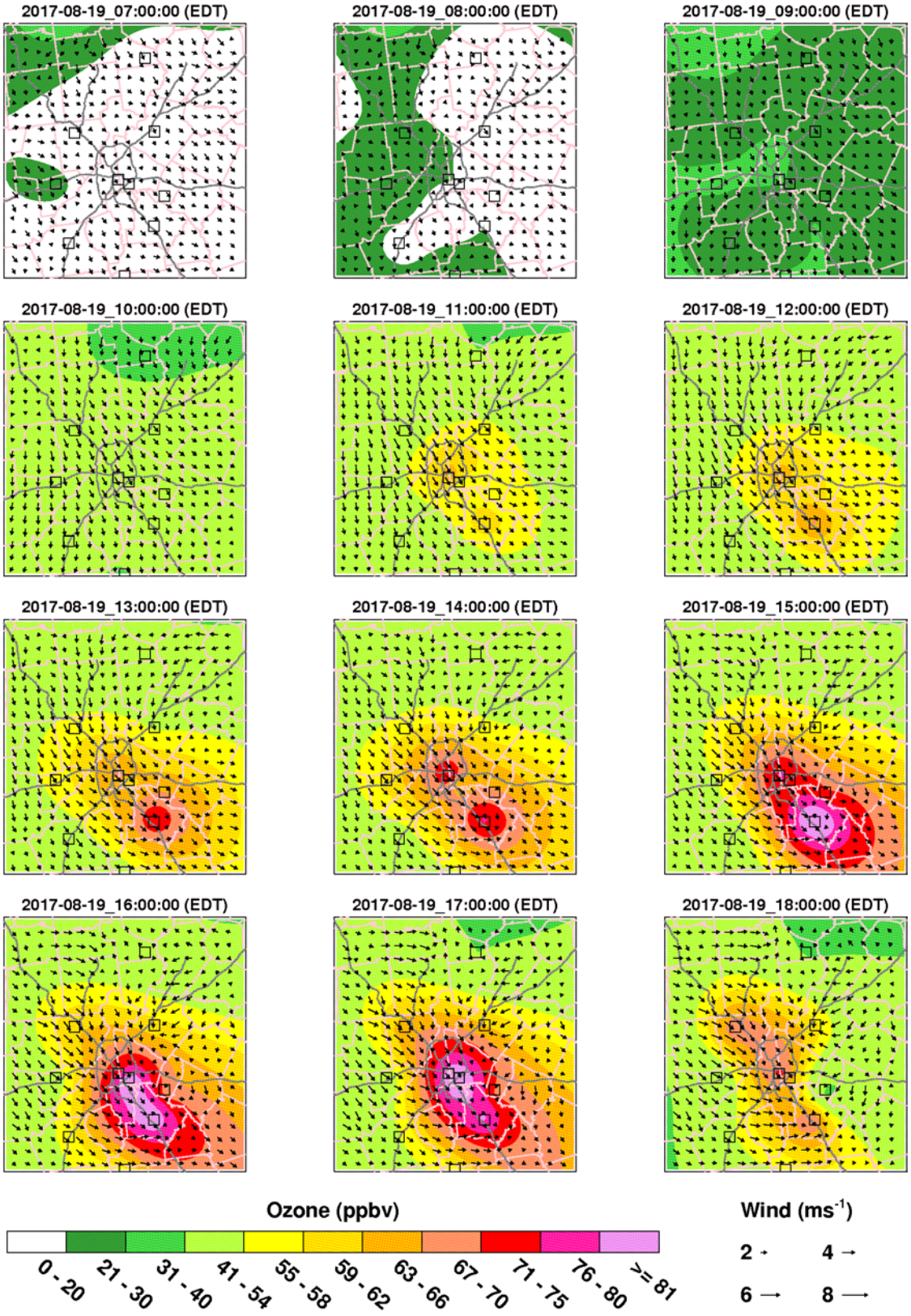

Figure 45. WRF simulated wind barbs and ozone observations (ppb) over Metro Atlanta from 7 AM to 6 PM on August 19, 2017. Ozone monitors are in black squares. The ozone exceedances occurred at the Confederate Ave. and McDonough monitors.

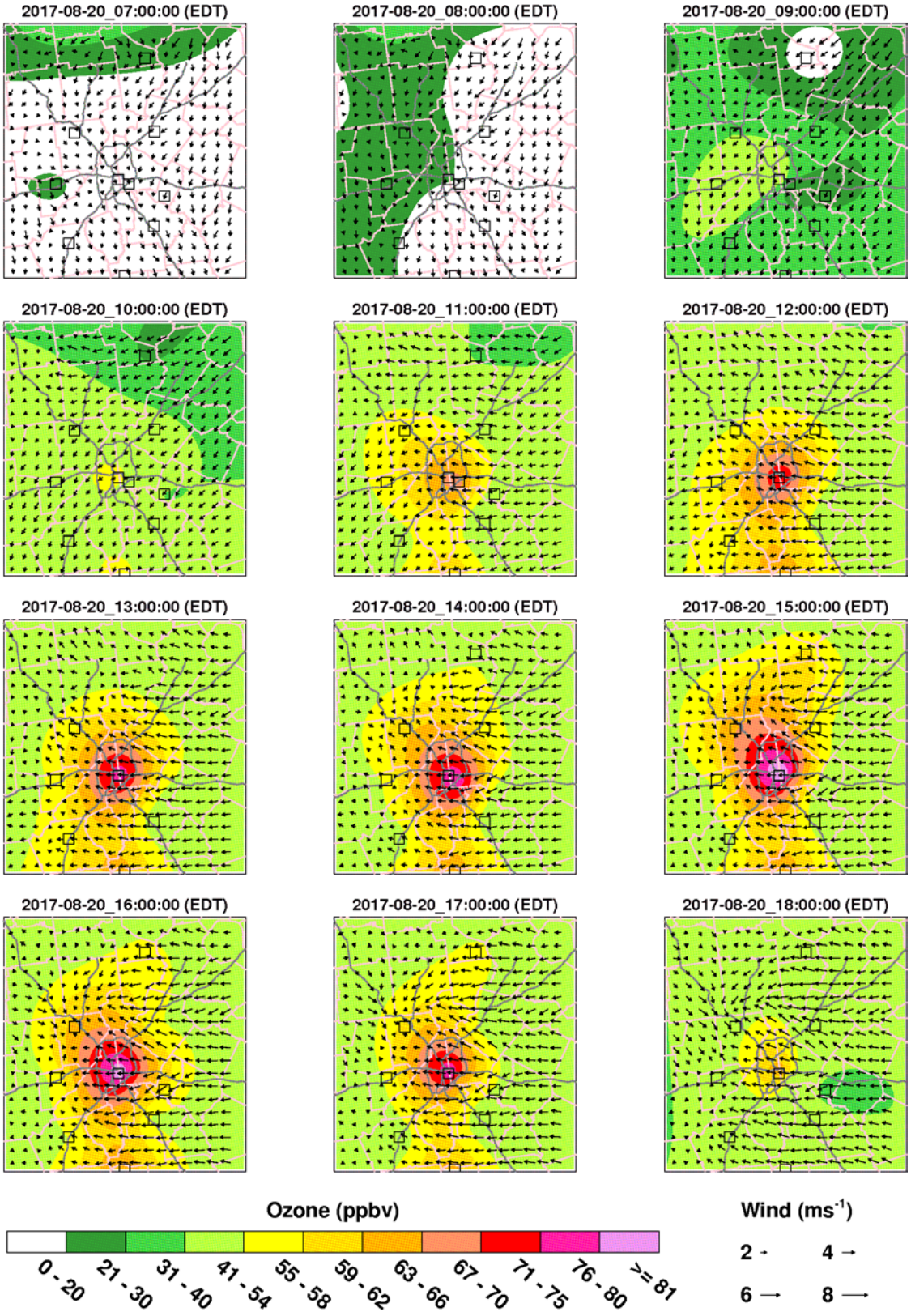

Figure 46. WRF simulated wind barbs and ozone observations (ppb) over Metro Atlanta from 7 AM to 6 PM on August 20, 2017. Ozone monitors are in black squares. The ozone exceedance occurred at the Confederate Ave. monitor.

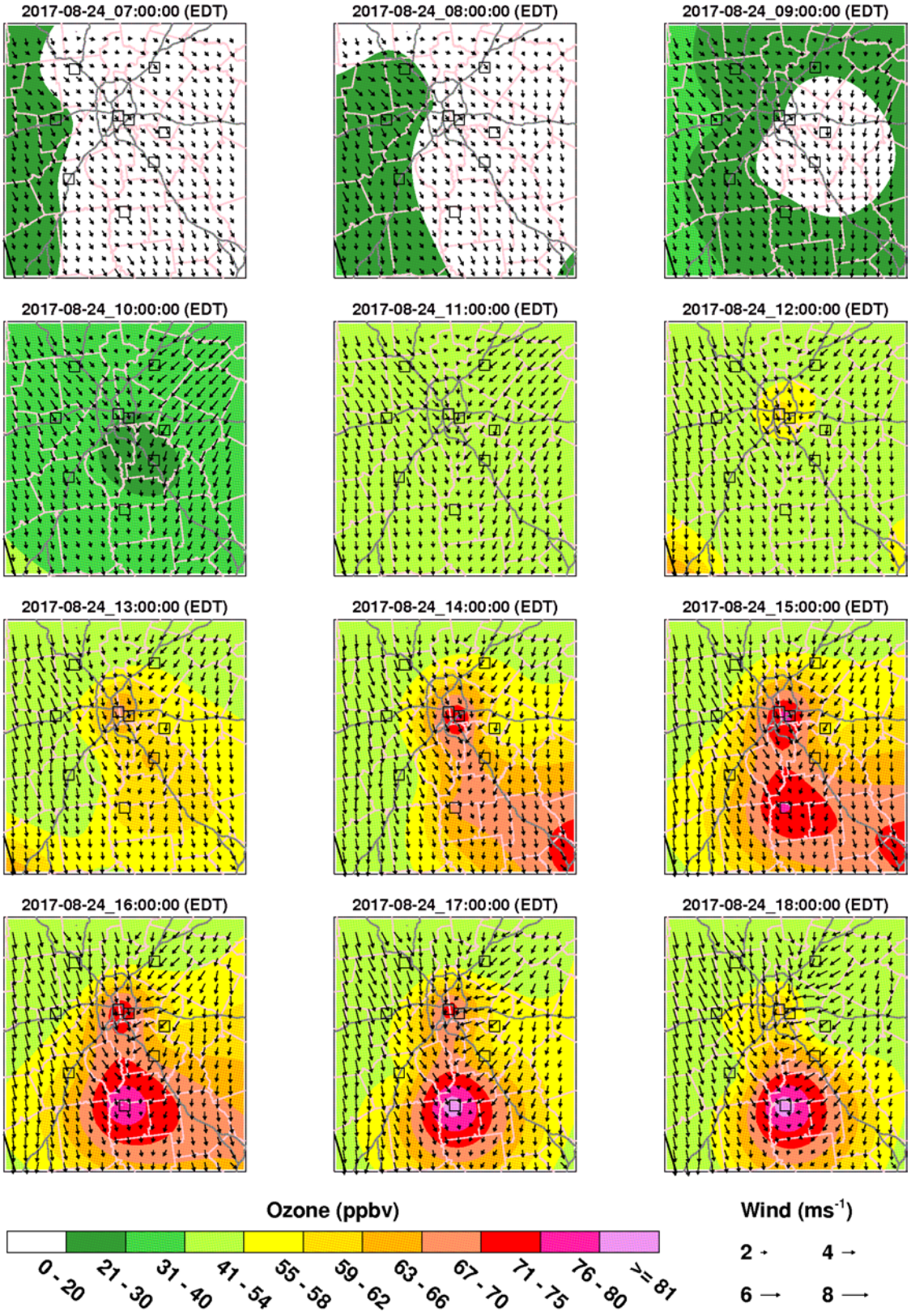

Figure 47. WRF simulated wind barbs and ozone observations (ppb) over Metro Atlanta from 7 AM to 6 PM on August 24, 2017. Ozone monitors are in black squares. The ozone exceedance occurred at the CASTNET monitor.

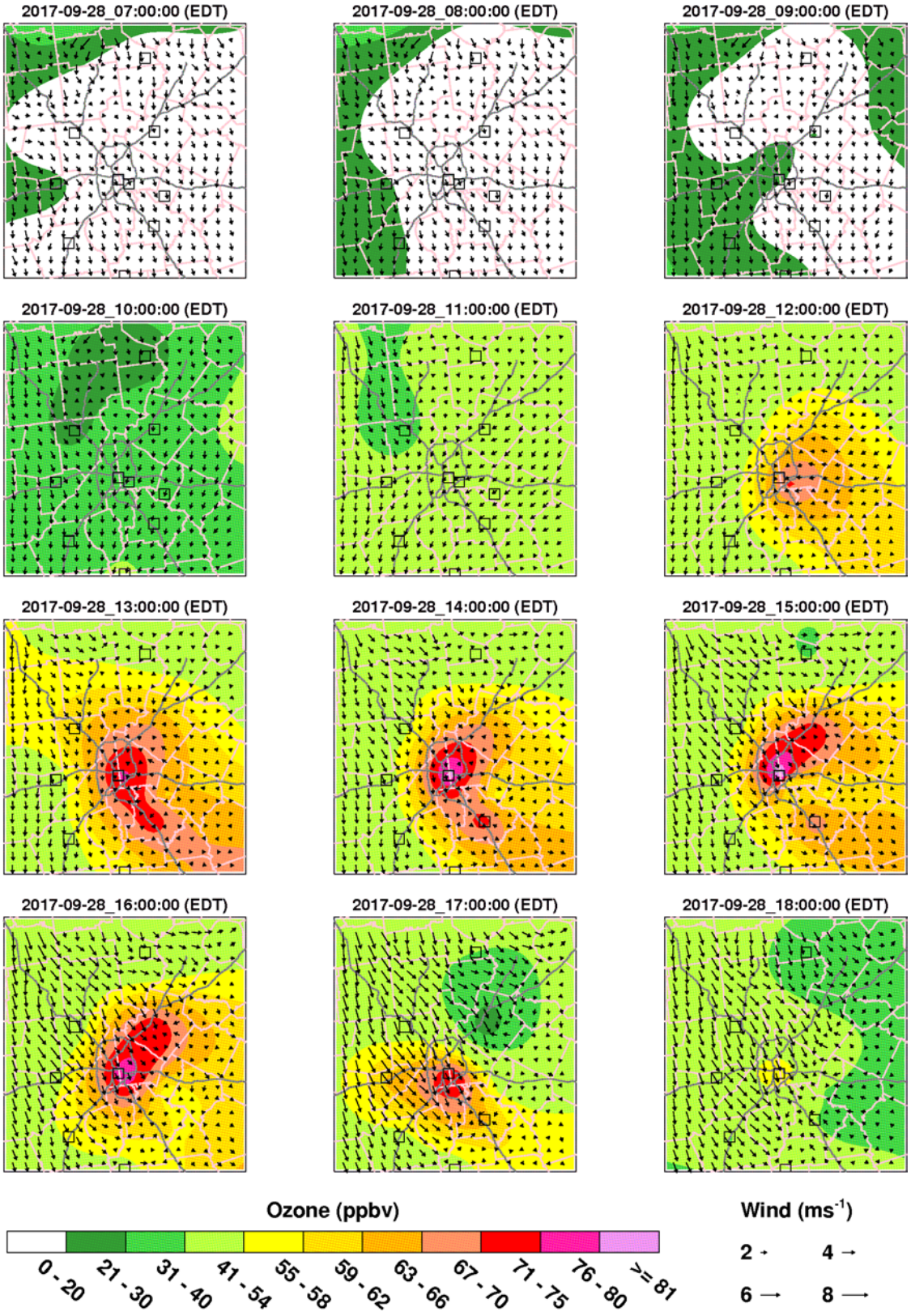

Figure 48. WRF simulated wind barbs and ozone observations (ppb) over Metro Atlanta from 7 AM to 6 PM on September 28, 2017. Ozone monitors are in black squares. The ozone exceedance occurred at the Confederate Ave. monitor.

1-minute ozone concentrations on exceedance days

The 1-minute ozone concentrations on exceedance day at exceeding monitors were further examined to study the timing of elevated ozone formation. For ozone exceedances at the monitors outside the Atlanta urban core, ozone concentrations (Figure 49) usually started to elevate around 1:00 or 2:00 PM (e.g. Dawsonville on April 10 and May 16, Douglasville on August 1, and CASTNET on August 24). For ozone exceedances at monitors inside the Atlanta urban core, ozone concentrations usually started to elevate before noon. The late occurrence time of the elevated ozone at the monitors outside the Atlanta urban core implies that either ozone formed in the Atlanta urban core is transported to the exceedance monitor or ozone precursor emissions from the Atlanta urban core are transported to the exceedance monitors where ozone is formed. In addition, the quick increase or decrease of 1-minute ozone concentrations indicates that an ozone plume hits or leaves the monitor. For example, the quick rise of 1-minute ozone concentrations at the Dawsonville monitor on May 16 (30 ppb in 1-hour) indicates that an ozone plume hit this monitor. Similarly, it appears that an ozone plume hit the McDonough monitor on July 19 and 21 and the Douglasville monitor on August 1. This is consistent with the findings from the “Animation of ozone and wind conditions” section.

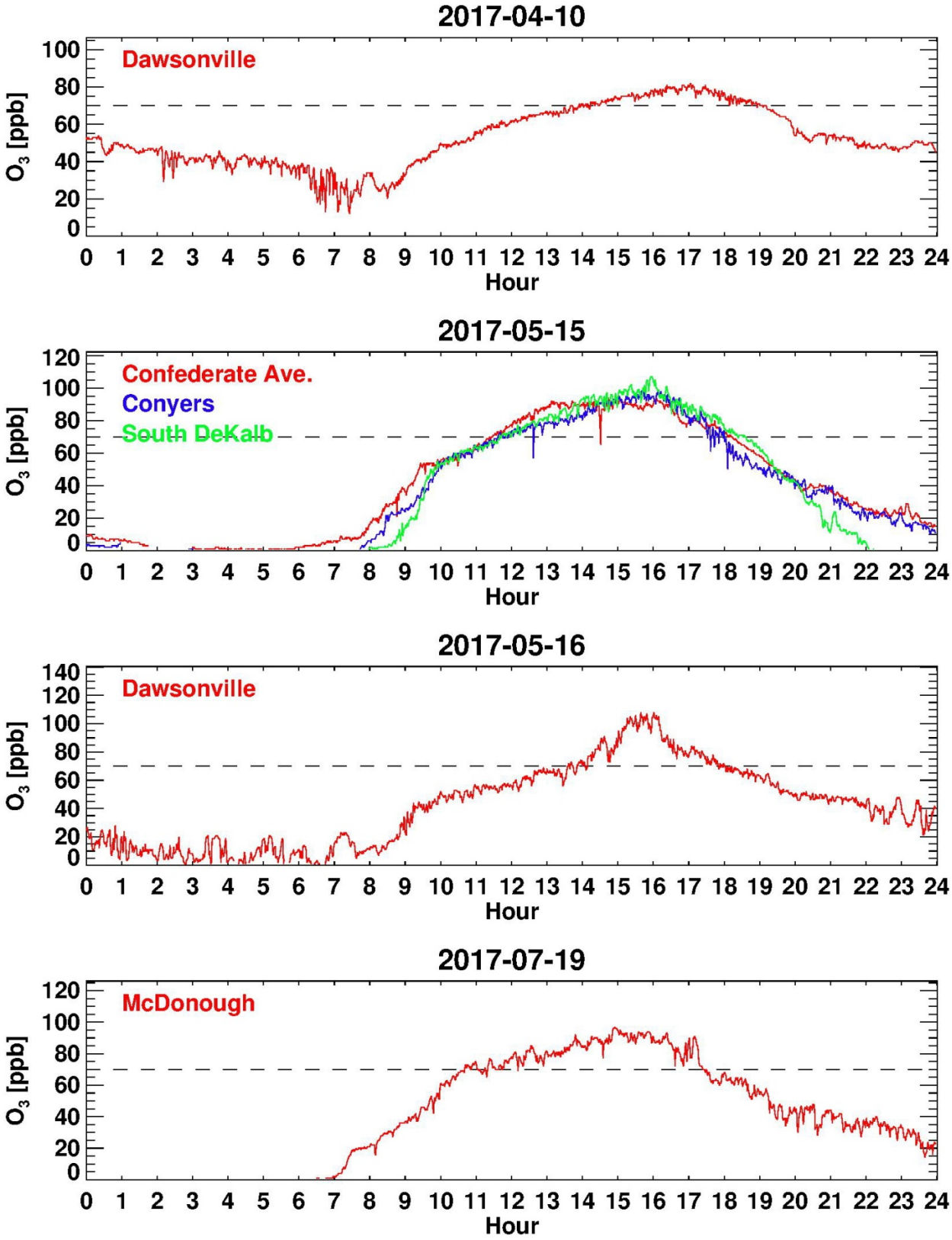

Figure 49. 1-minute ozone concentrations on exceedance days.

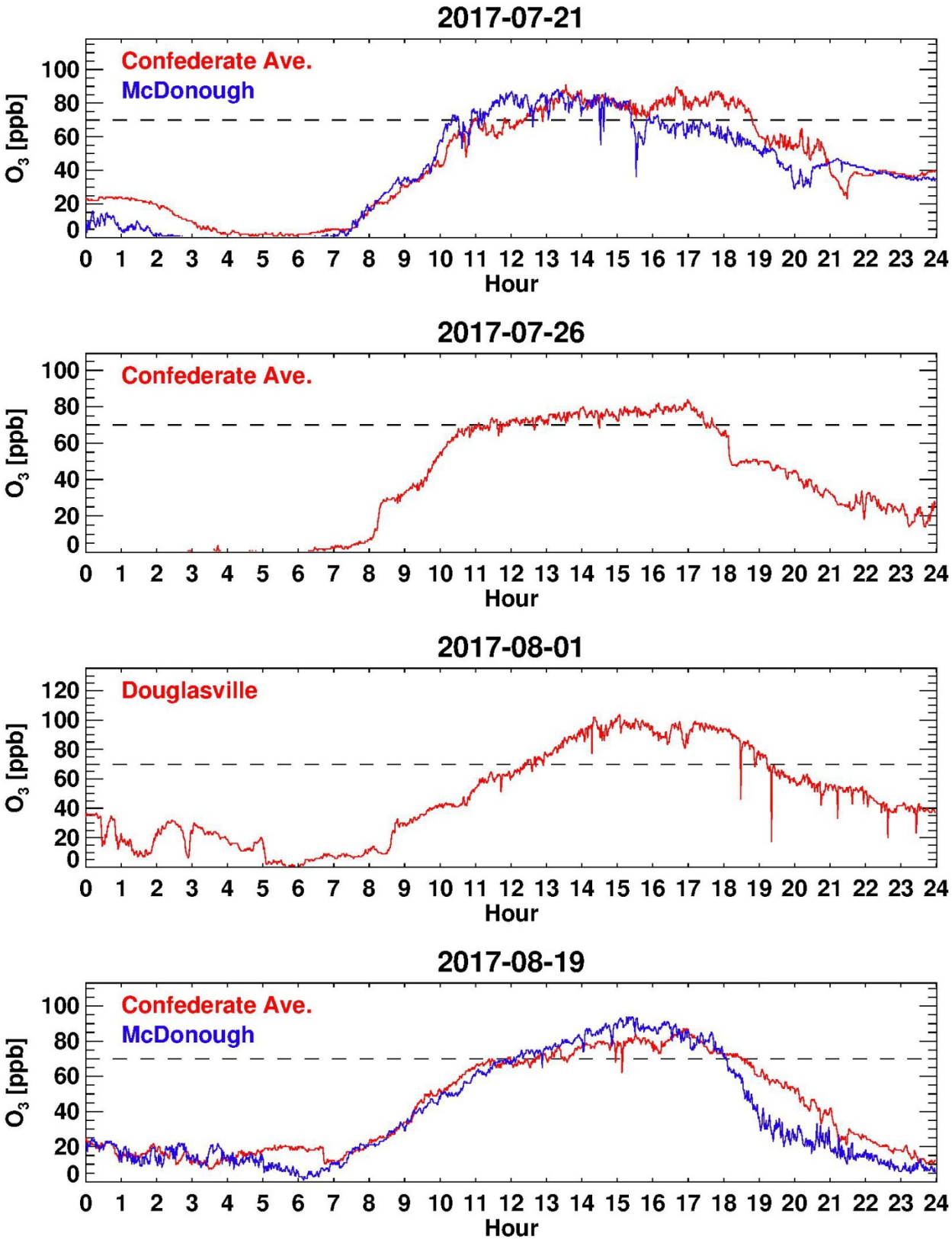

Figure 49. (Continued) 1-minute ozone concentrations on exceedance days.

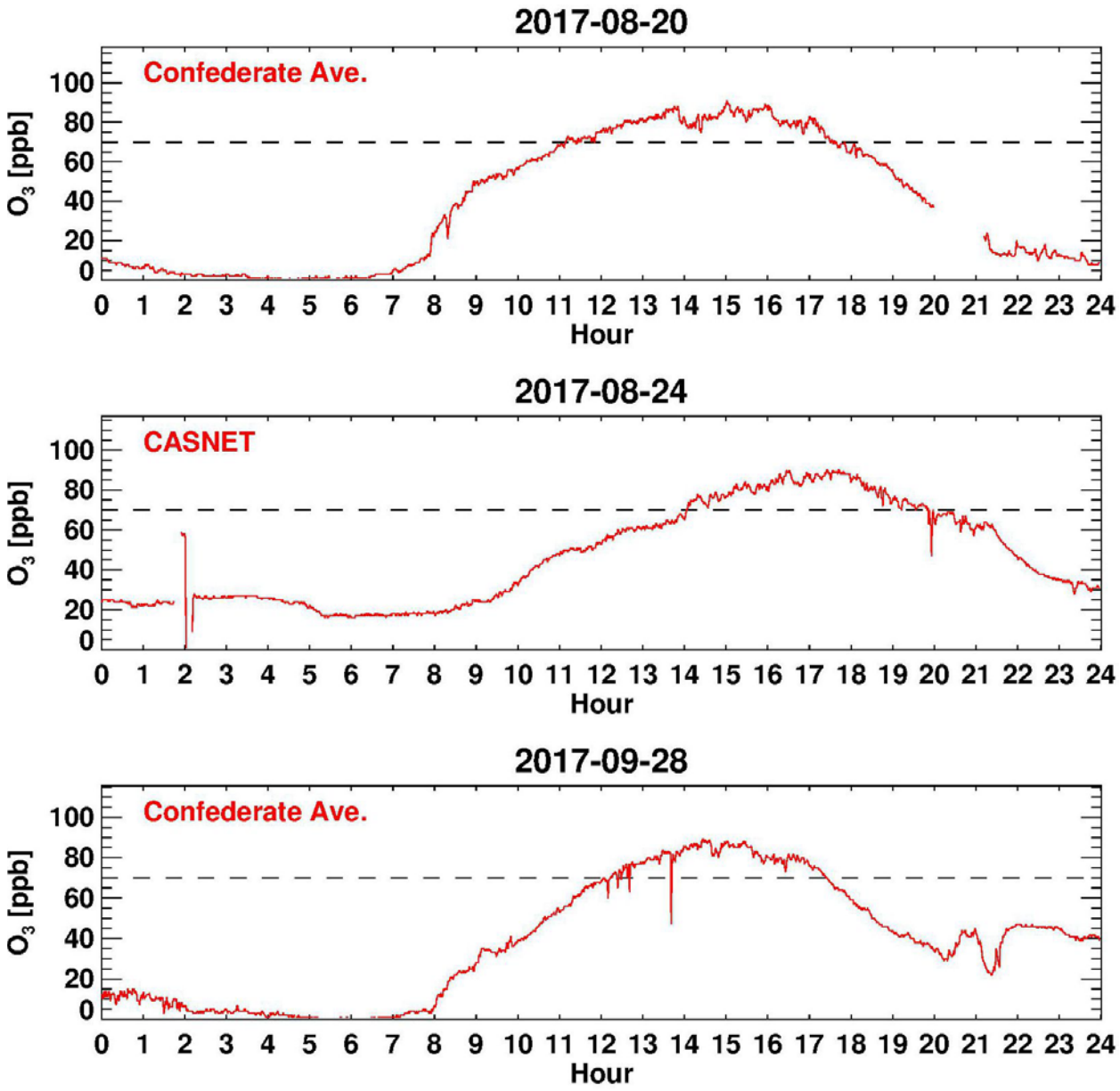

Figure 49. (Continued) 1-minute ozone concentrations on exceedance days.

7. Ozone and NOx precursor

Ozone is not emitted directly into the air but is formed by the reaction of volatile organic compounds (VOCs) and nitrogen oxides (NOx) in the presence of heat and sunlight. The relationship of ozone and NOx precursor is very nonlinear since NOx can not only help ozone formation, but also deplete ozone through NOx titration[5]. NOx can be emitted from passenger cars, trucks, and various non-road vehicles (e.g., construction equipment, boats, etc.) as well as stationary combustion sources such as power plants, industrial boilers, cement kilns, and turbines. In the Metro Atlanta area during 2014, 58% of NOx emissions were from on-road mobile sources and 20% from non-road mobile sources (Figure 50). In this study, the impacts of local NOx on ozone exceedances are investigated by analyzing NOx observations at the South DeKalb monitor and two roadside monitors (NR-285 and NR-GA Tech) located adjacent to major interstates (Figure 51) during multiple ozone seasons (April - October). The two roadside monitors are investigated to identify impacts from on-road mobile NOx emissions. Scatter plots of MDA8O3 and NOx measurements at 8 AM and 4 PM (Figure 52) imply that high ozone concentrations generally occur when NOx concentrations are within a specific window. When NOx concentrations are low, ozone concentrations are also low since not enough radicals are propagated. However, when NOx concentrations are too high (>150 ppb at 8:00 AM or >11 ppb at 4:00 PM), the excess NOx removes ozone via NOx titration. Figure 52 shows that high ozone concentrations in Atlanta are highly correlated with low relative humidity (dry condition).

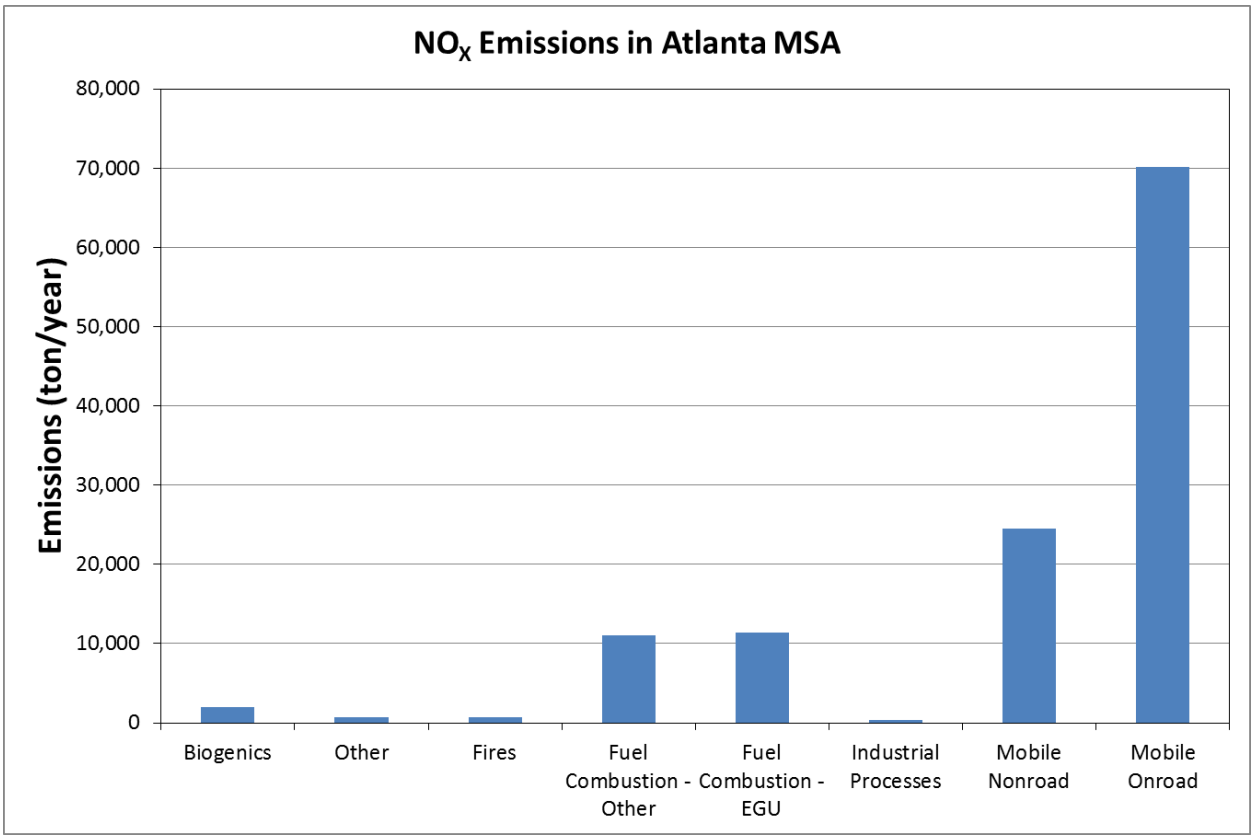

Figure 50. 2014 NOx emissions (tons/year) by source sectors in the Metro Atlanta area.

[5] The removal of ozone through the reaction of $O_3 + NO \rightarrow O_2 + NO_2$.

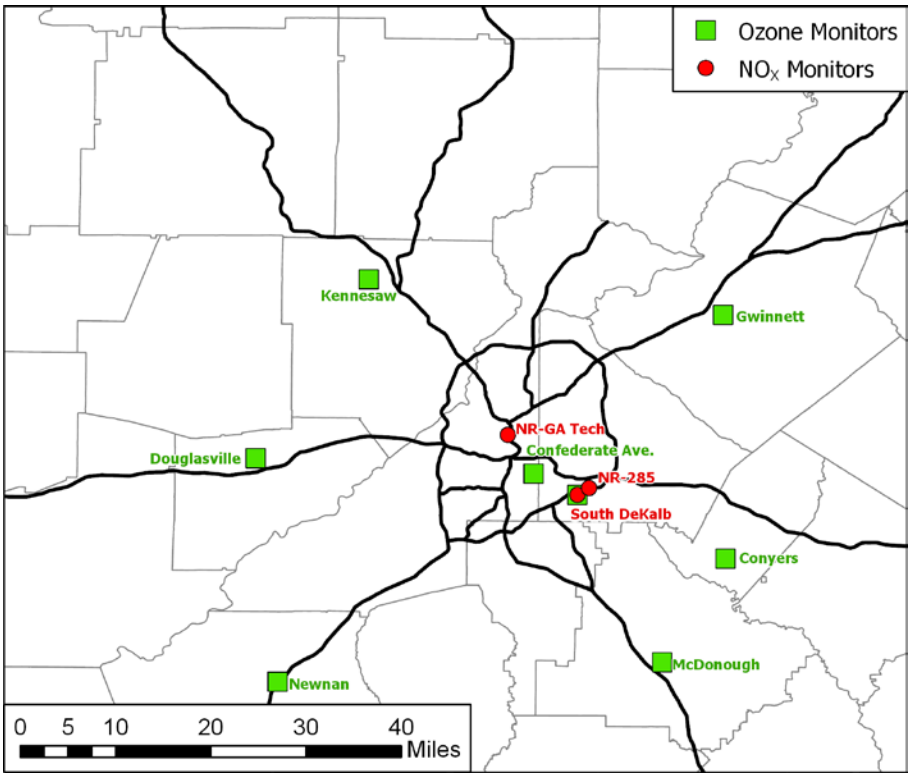

Figure 51. Locations of ozone and NOx monitors in the Metro Atlanta area

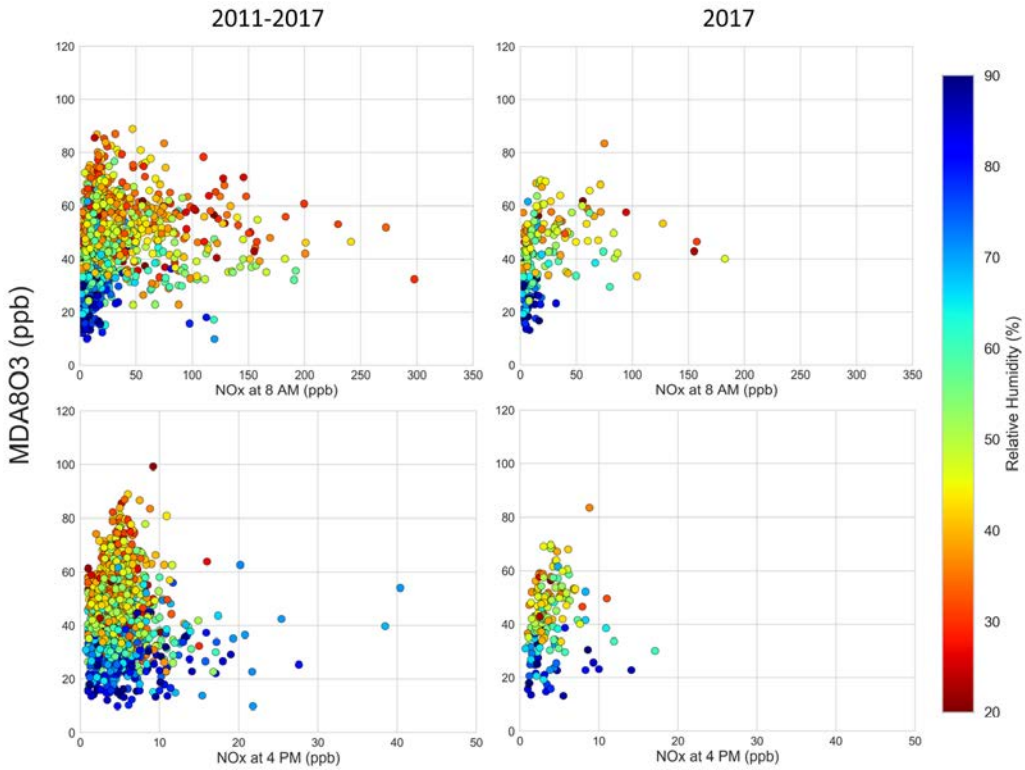

Figure 52. Scatter plots of MDA8O3 and NOx at 8 AM (top row) and 4 PM (bottom row) at the South DeKalb monitor. The color of dots reflects afternoon (noon-6 PM) relative humidity levels.

Diurnal patterns of NOx observations on ozone exceedance days

The boxplots showing the statistics (mean, 10^{th}, 25^{th}, 75^{th}, and 90^{th} percentiles) are developed by hour of day for NOx observations during the 2017 ozone season at the three NOx monitors. These boxplots are overlaid with NOx observations on ozone exceedance days at the Confederate Ave. (Figure 53), South DeKalb (Figure 54), and McDonough (Figure 55) monitors. NOx observations at the two roadside monitors are higher than those at the South DeKalb monitor, indicating large impacts from mobile sources. There is also a clear diurnal variation in NOx observation, peaking in the morning when NOx emissions are high due to commuter traffic and NOx emissions are trapped at low altitudes as the planetary boundary layer (PBL) is still quite low. NOx observations then rapidly decrease when the PBL expands and photochemistry becomes stronger during the day, and increase again at night when the PBL collapses. On ozone exceedance days, morning time NOx observations tend to be higher than the average NOx observations, especially from 6 AM to 8 AM when traffic volumes are highest, though the pattern is not clear for NOx observations during evening/nighttime compared with morning time. However, morning time NOx concentrations on ozone exceedance days of August 19, 2017 and August 20, 2017 are low compared to average values at Confederate Ave. and McDonough. Both days are weekend days and thus there are no increased NOx emissions from morning commuter traffic.

Day-of-Week patterns of NOx observations on ozone exceedance days

Variation of NOx observations by day of week is analyzed by developing similar boxplots for NOx observations at 8 AM at the three NOx monitors (Figure 56). The NOx observations at 8 AM are chosen since they are likely correlated with high ozone levels as identified in the diurnal pattern analysis for the NOx observations. The NOx observations are higher on weekdays than the weekends, corresponding to similar traffic patterns (i.e. heavier commuter traffic during weekdays than weekend). Sunday morning NOx observations are typically lower than Saturday morning. Mean Friday morning NOx observations also tend to be slightly lower than mean Wednesday or Thursday NOx observations at the NR-GA Tech and NR-285 roadside monitors. The boxplots are overlaid with NOx observations on ozone exceedance days labeled as red circles. The size of the circle indicates the number of exceeding ozone monitors. At the South DeKalb and NR-285 monitors, NOx observations on ozone exceedance days are mostly higher than average conditions. However, NOx observations on ozone exceedance days at the NR-GA Tech monitor are not consistently higher than the average conditions.

Monthly patterns of NOx observations on ozone exceedance days

Variation of NOx observation by month is then analyzed by developing similar boxplots for NOx observations at 8 AM at the three NOx monitors (Figure 57). The mean morning time NOx observations at the two roadside monitors are between 20 and 70 ppb, usually higher than NOx observations at the South DeKalb monitor. The mean morning time NOx observations at the South DeKalb monitor tend to be less than 20 ppb throughout most of the ozone season except in April, September and October. NOx begins to increase through the winter because there is less photochemistry to remove atmospheric NOx. NOx observations at the NR-285 and NR-GA Tech monitors also start to increase in September. The boxplots are overlaid with NOx observations on ozone exceedance days (labeled as red circles). The size of the circle indicates the number of exceeding ozone monitors. Most exceedances took place in May, July, and August. One exceedance occurred in April and September, respectively. There was no

exceedance in June. Usually, morning time NOx observations on an ozone exceedance day are higher than the mean NOx observations in a month when the exceedance took place except for the NOx observations at the NR-GA Tech monitor.

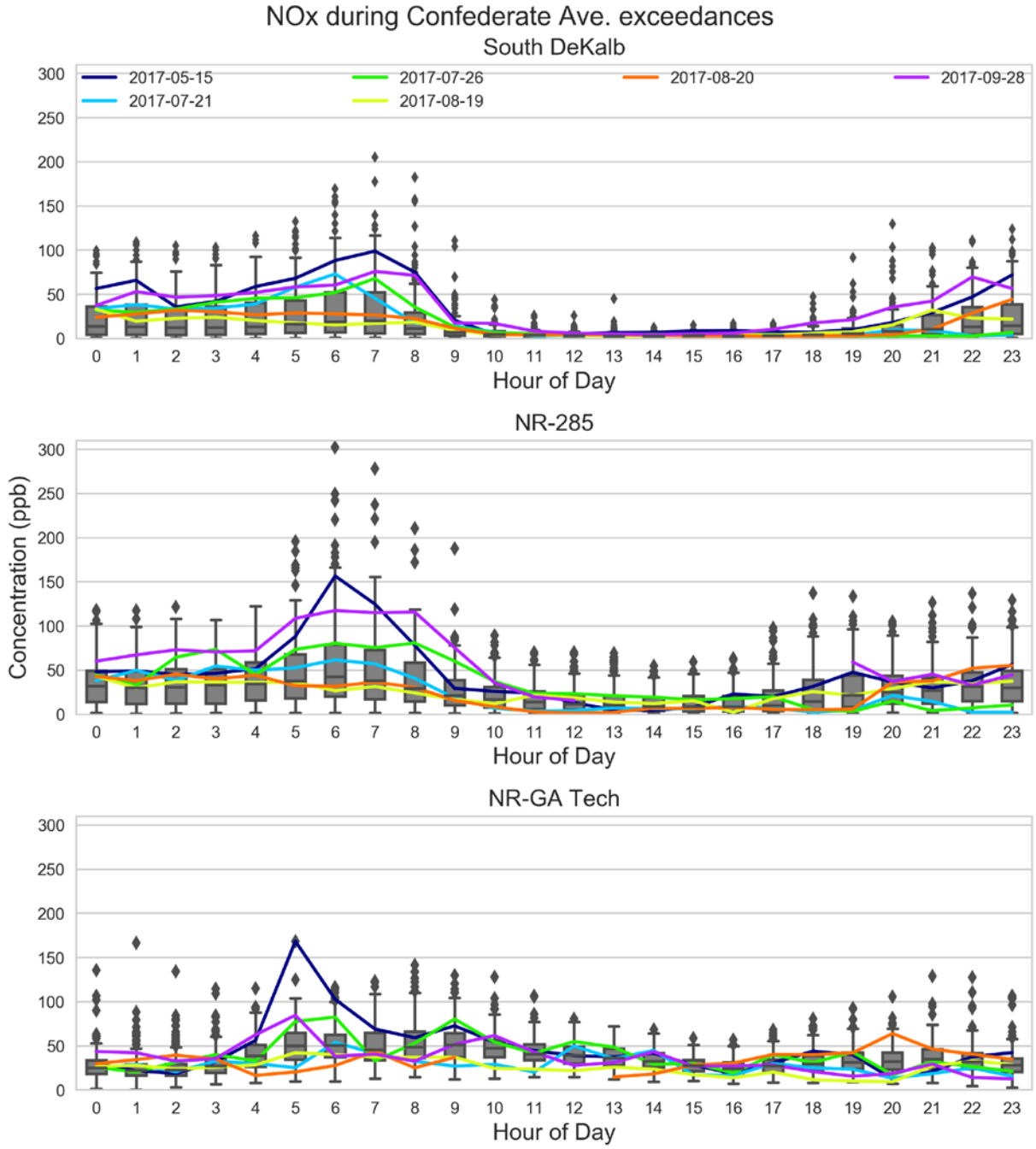

Figure 53. Boxplots by hour of day for NOx observations during 2017 ozone seasons at three NOx monitors. Colored lines are NOx observations on ozone exceedance at Confederate Ave.

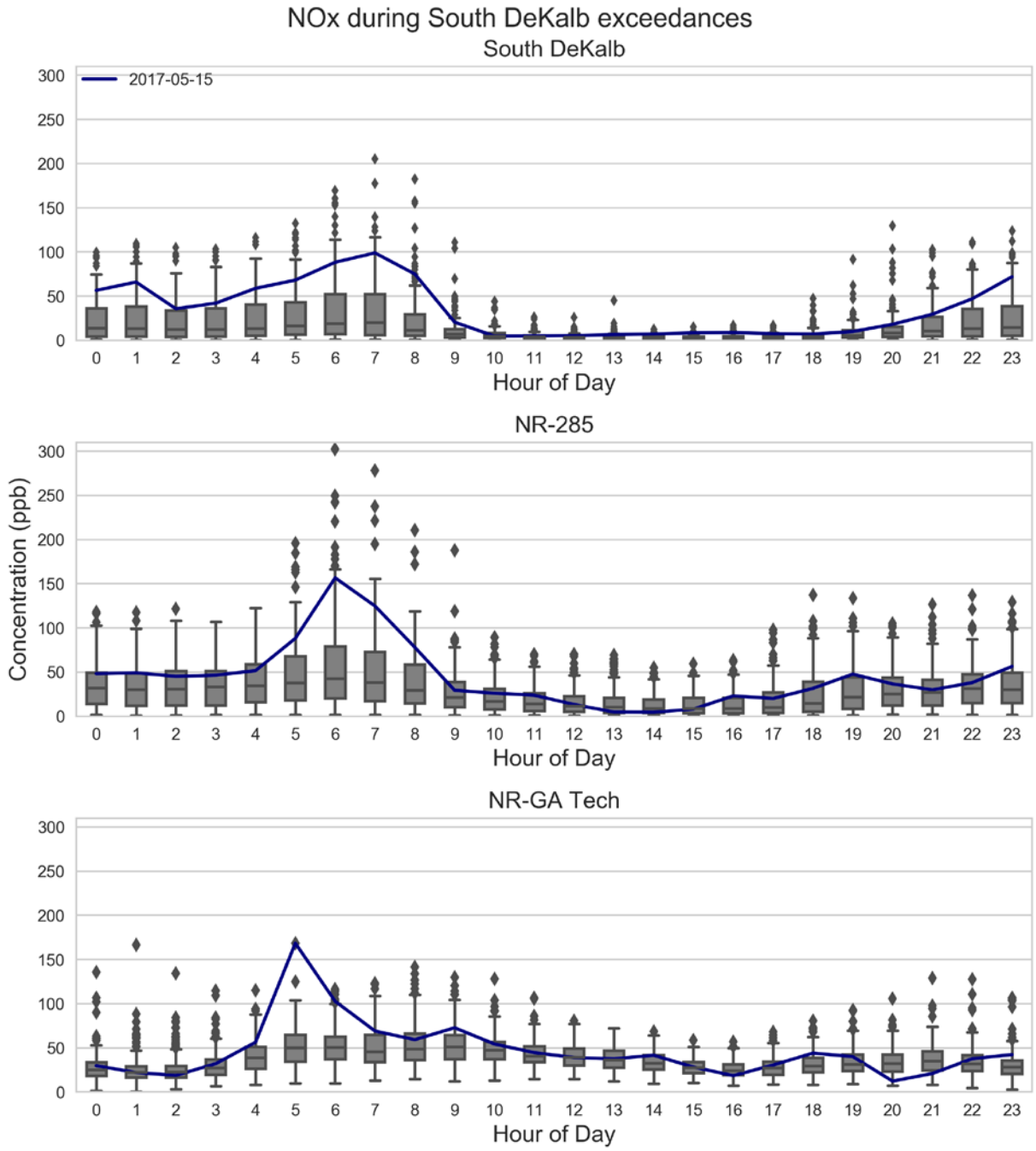

Figure 54. Boxplots by hour of day for NOx observations during 2017 ozone seasons at three NOx monitors. Colored lines are NOx observations on ozone exceedance at South DeKalb.

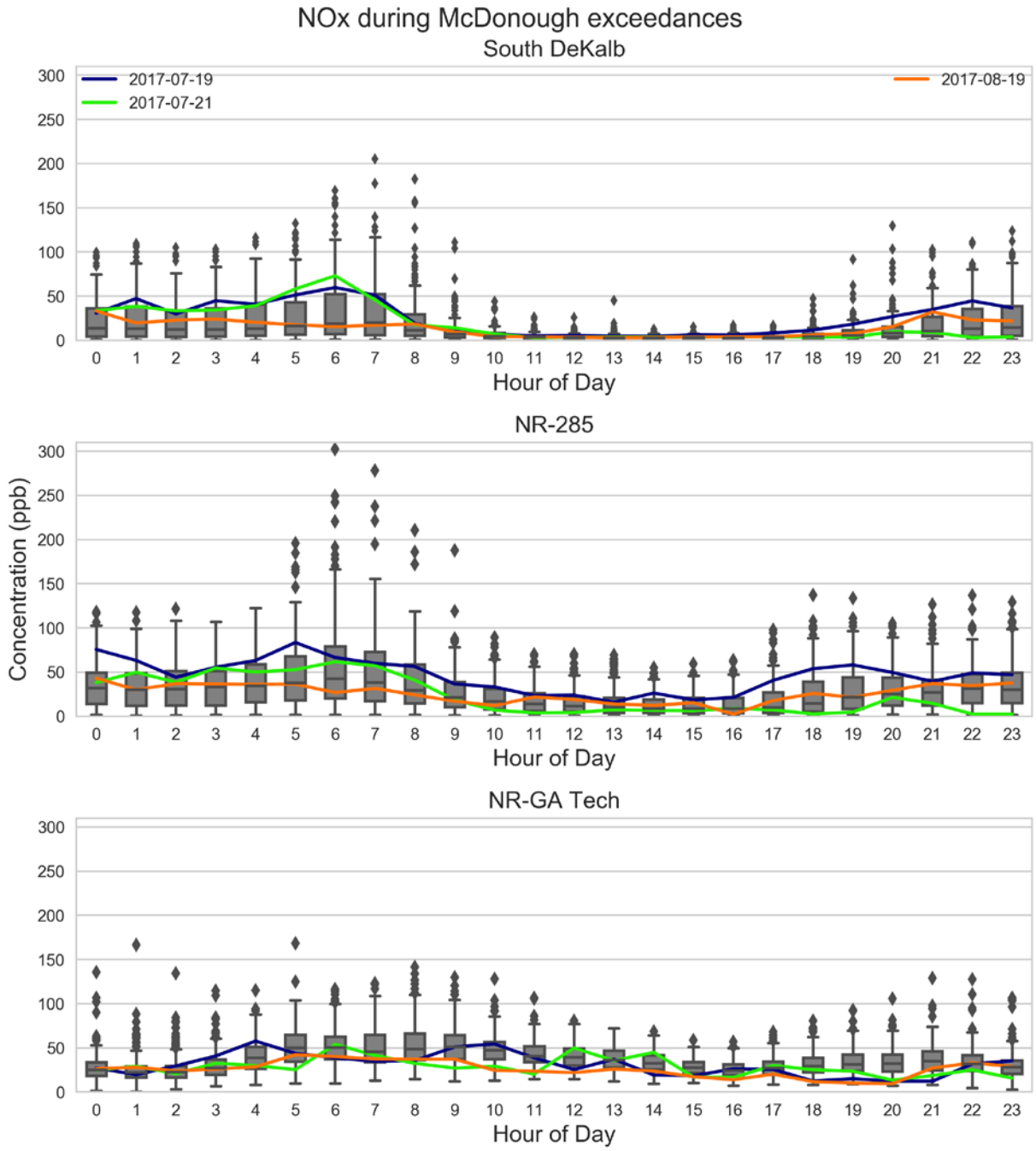

Figure 55. Boxplots by hour of day for NOx observations during 2017 ozone seasons at three NOx monitors. Colored lines are NOx observations on ozone exceedance at McDonough.

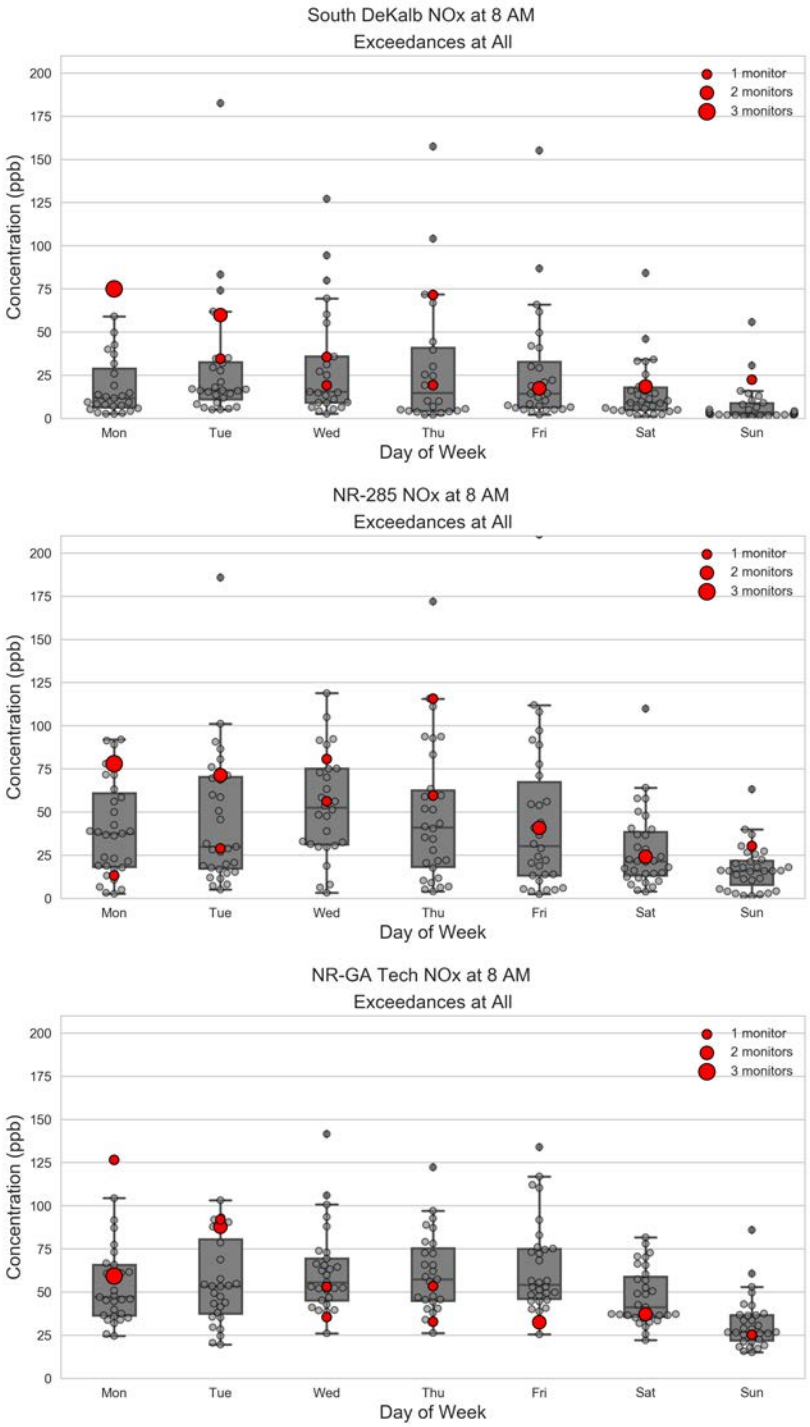

Figure 56. Boxplots by day of week for NOx observations at 8 AM during the 2017 ozone seasons at three NOx monitors. Red dots are average NOx observations on ozone exceedance days in Georgia. The size of red dots refers to the number of monitors exceeding the 2015 ozone NAAQS. Note that NOx observation at 8 AM on April 10 (Monday) is not available at the South DeKalb monitor when the Dawsonville monitor exceeded.

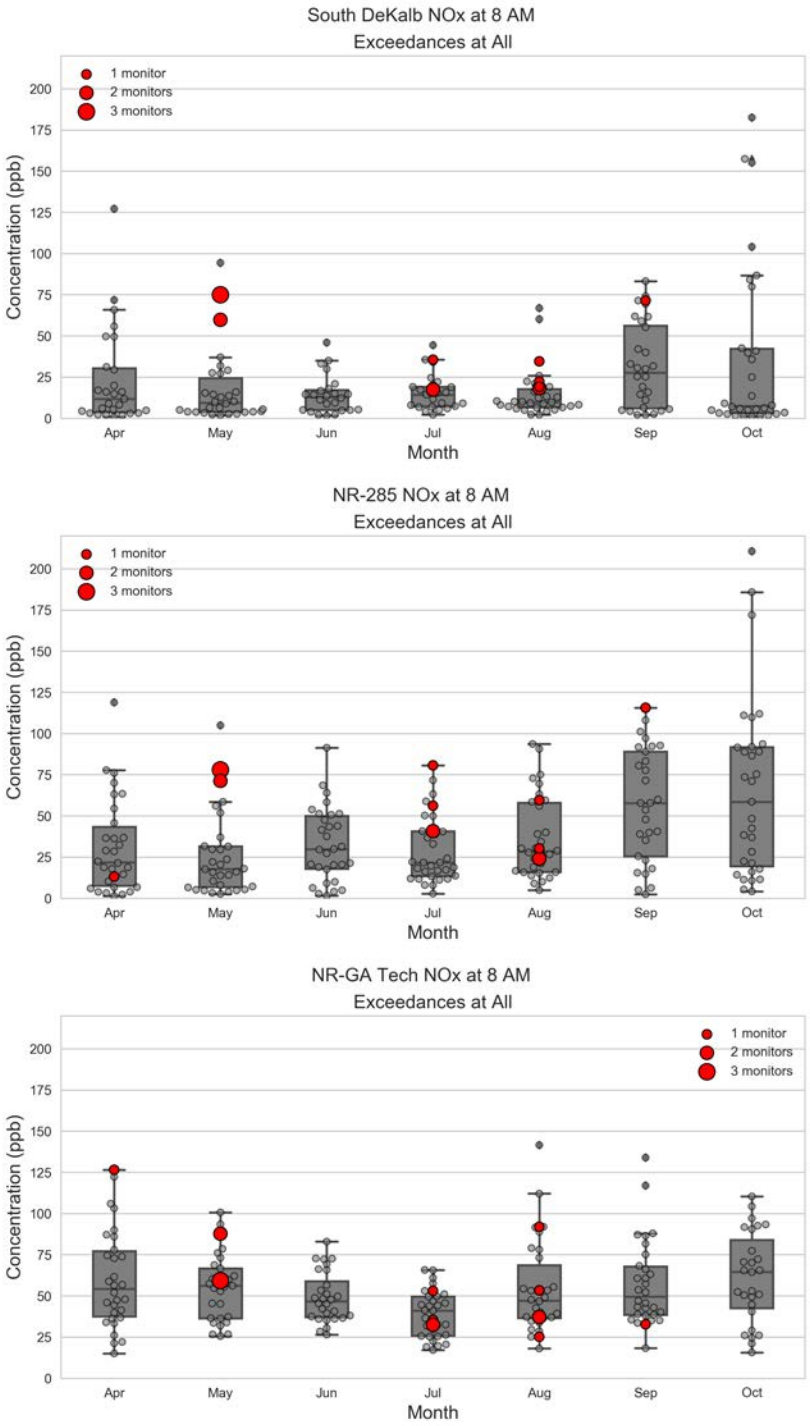

Figure 57. Boxplots by month for NOx observations at 8 AM during the 2017 ozone seasons at three NOx monitors. Red dots are average NOx observations on ozone exceedance days in Georgia. The size of red dots refers to the number of monitors exceeding the 2015 ozone NAAQS. Note that NO_X observation at 8 AM on April 10 (Monday) is not available at the South DeKalb monitor when the Dawsonville monitor exceeded.

Indicator analysis

The ratio of ozone to NOx is calculated for 2011-2017 data at the South DeKalb monitor in this study as an indicator of local ozone production efficiency (Tonnesen et al., 2000). When the ratio of ozone to NOx is high, radical propagation is reduced and thus ozone is not produced efficiently; while when the ratio of ozone to NOx is low, NO can remove ozone through titration. In the 2010 Tonnesen study, ozone is produced most efficiently with the ratio of ozone to NOx being ~8 during a morning period (9 AM to 10 AM), the ratio being ~15 around noon (12 PM to 1 PM), and the ratio being 16 to 20 during an afternoon period (4 PM to 5 PM). The analysis for 2017 ozone exceedance days may not representative since May 15 was the only exceedance day at the South DeKalb monitor in 2017 and it was not in a month with peak ozone production.

Diurnal profiles of median ozone and NOx for each ozone season and exceedance days during 2011-2017 (Figure 58 and Figure 59) have shown that NOx concentration decreases when ozone increases, and vice versa. In general, NOx concentrations during low-ozone hours are much higher on ozone exceedance days. The ratios of ozone to NOx calculated here are compared with the ratios suggested in the 2010 Tonnesen study (Figure 60). In the morning period (9 AM to 10 AM), the ratios of ozone to NOx for ozone exceedance days are lower than Tonnesen's ratio for peak ozone production and there is no clear difference between the ozone exceedance days and the average conditions during the ozone season, except for the ratio of ozone to NOx for the ozone exceedance day in 2017 which is higher and comparable with Tonnesen's ratio for peak ozone production. In the noon period (12:00 PM to 1:00 PM), the ratios of ozone to NOx for ozone exceedance days are mostly higher than those for the average conditions during ozone season. Such ratios are lower than Tonnesen's ratio for peak ozone production (~15), except for the ratios corresponding to exceedance days in 2011 and 2014. In the afternoon period (4 PM to 5 PM), the ratios of ozone to NOx for ozone exceedance days are mostly higher than those for the average conditions during the ozone season. The ratios for exceedance days during 2011, 2014, and 2016 are close to Tonnesen's ratio for peak ozone production (16-20). The ratios of ozone to NOx for the ozone exceedance day in 2017 are much lower, reflecting a potential different atmospheric chemistry conditions. However, due to limited data for 2017 ozone exceedances at the south DeKalb monitor, further investigation is needed.

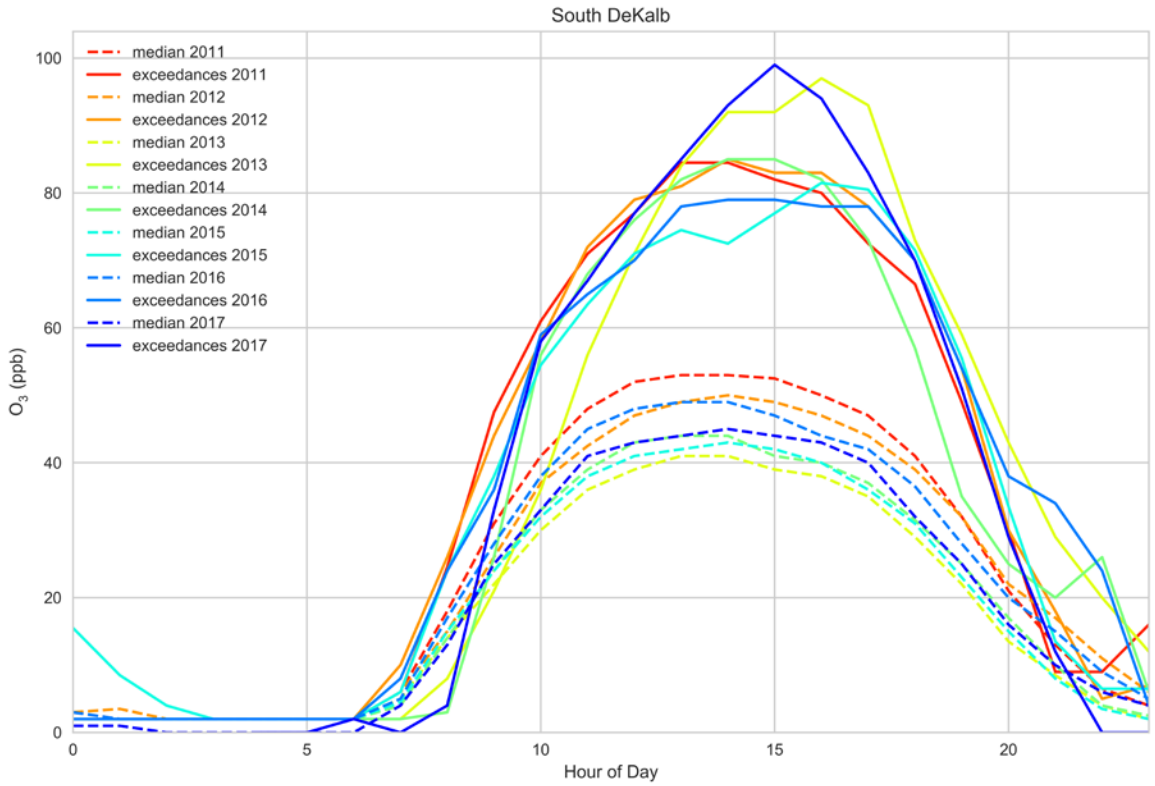

Figure 58. Diurnal profile of median ozone for each ozone season (dashes) and exceedance days (solid lines) during 2011-2017.

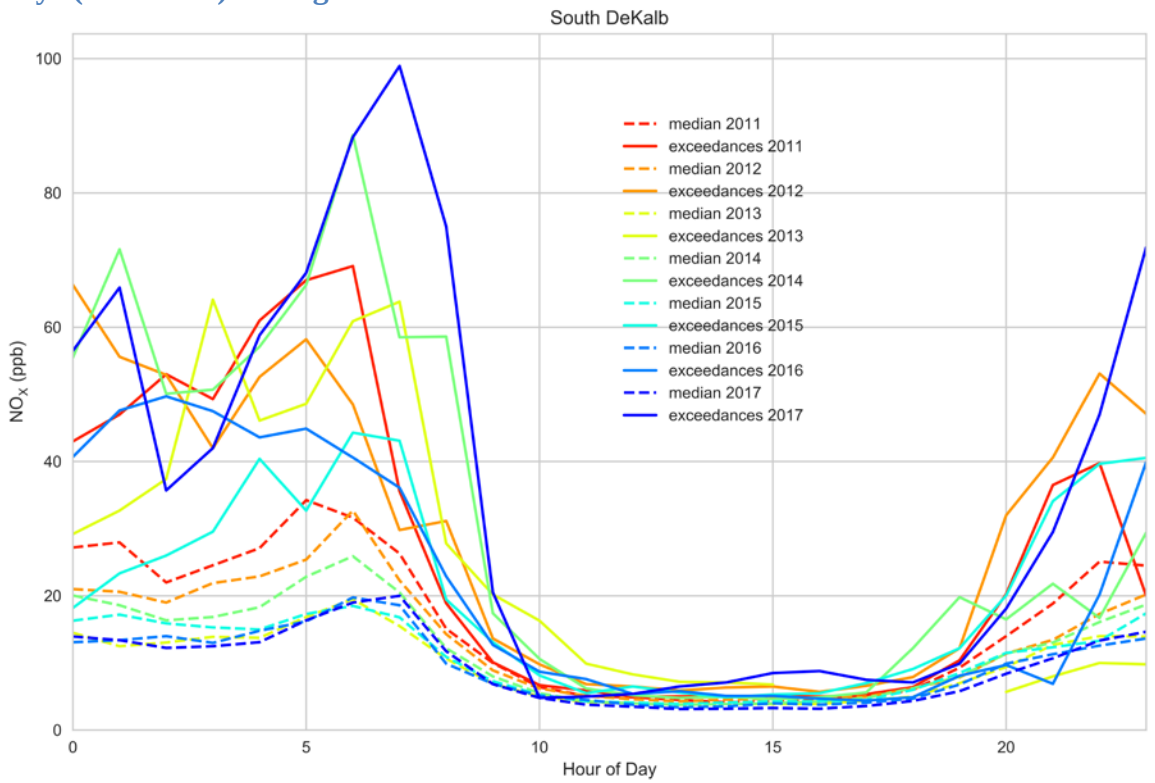

Figure 59. Diurnal profile of median NOx for each ozone season (dashes) and exceedance days (solid lines) during 2011-2017.

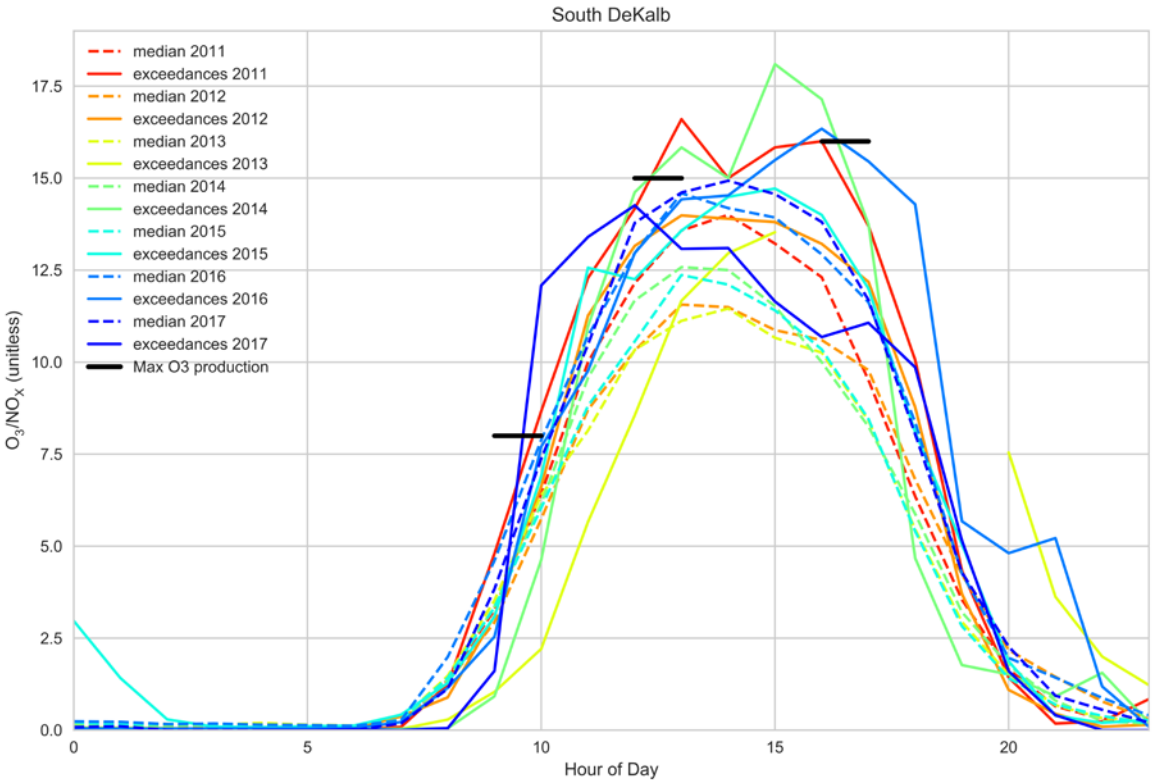

Figure 60. Diurnal profile of median ozone to NOx ratio for each ozone season (dashes) and exceedance days (solid lines) during 2011-2017. The black bars at 9 AM to 10 AM, noon to 1 PM, and 4 PM to 5 PM represent the ratios where peak ozone production occurs according to Tonnesen's 2010 study.

NOx Trends Based on OMI Satellite Data

NOx trends in Atlanta during 2005-2017 ozone seasons are evaluated using the daily tropospheric NO_2 columns by Ozone Monitoring Instrument (OMI) onboard NASA's Aura satellite. The polar orbit satellite has a 1:45 PM ±15 minute equator crossing time, which means OMI provides NO_2 information in early afternoon when local ozone production is near its daily peaks. Since there are large fractions of tropospheric NO_2 columns at the ground level as shown from in situ and aircraft measurements (e.g. Steinbacher et al., 2007; Heland et al., 2002; Martin et al., 2004), the tropospheric NO_2 columns can generally represent the surface NOx conditions, especially at hot spots over urban areas. The standard tropospheric OMI NO_2 column product has a ground pixel size of 13×24 km^2 (Bucsela et al., 2013), and was processed onto 0.1×0.1 $degree^2$ global grid (Lamsal et al., 2014). The Metro Atlanta area is defined in this study as 9×9 grids centering at Five Points and covering 4 grids (=0.4^o) in all 4 directions.

Spatial distribution of the 13-year average OMI NO_2 columns during 2005-2017 over the Metro Atlanta area (Figure 61) shows higher NO_2 concentrations in the urban core extending slightly to the suburban areas in the southeast. The hot spot of NO_2 columns clearly shows strong local NOx emissions in the Metro Atlanta area.

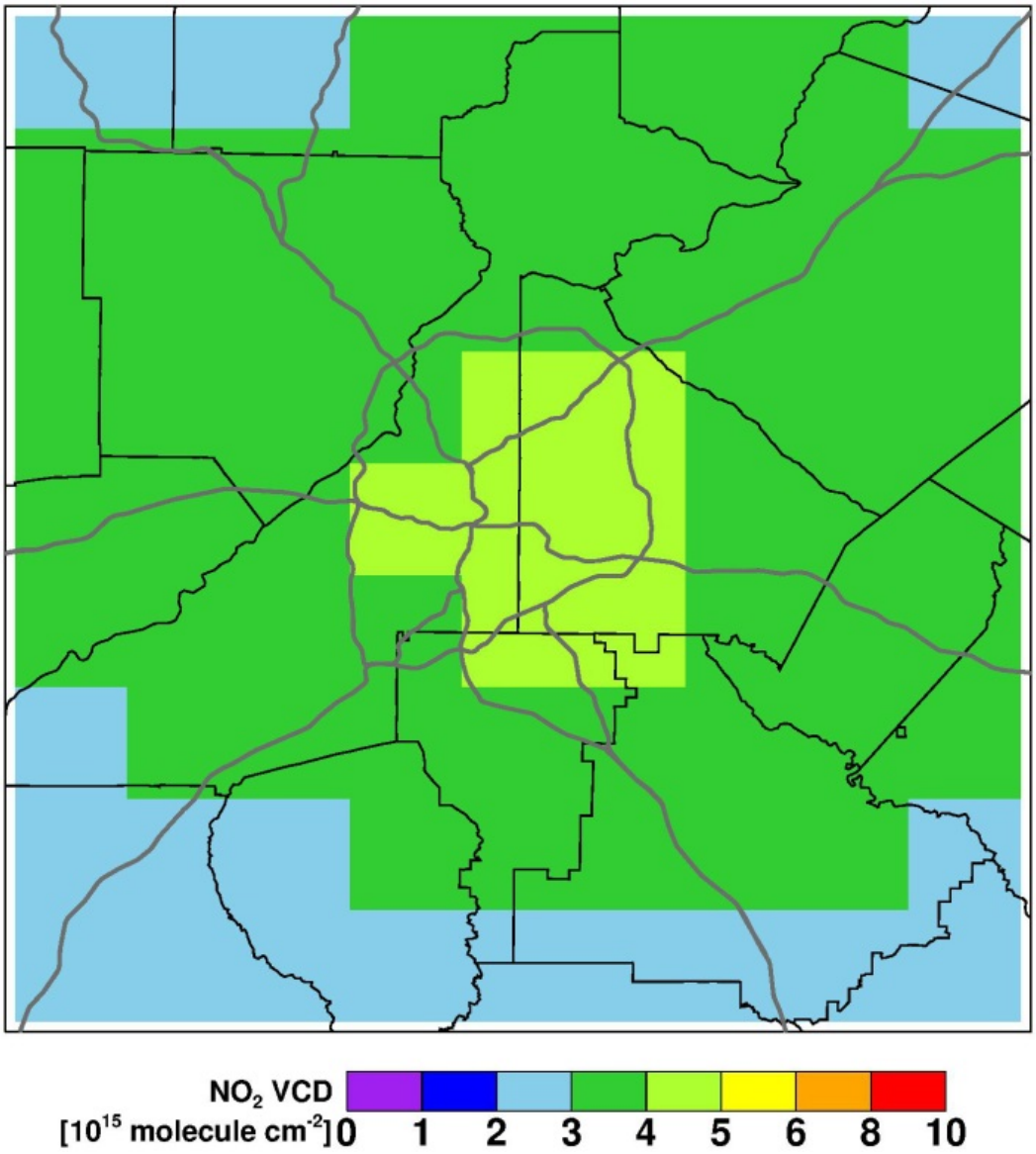

Figure 61. Mean OMI Tropospheric NO_2 columns over the Metro Atlanta area during 2005-2017.

The inter-annual comparison of NO_2 columns in ozone season shows significant decrease in NO_2 concentrations since 2005 (Figure 62 and Figure 63). NO_2 columns in warm months are much lower than in cold months (Figure 64) due to additional photochemistry during the warmer months. Therefore, only OMI NO_2 columns during the ozone season (April to October) were used to develop the inter-annual trend (Figure 63). The inter-annual NO_2 variation based on OMI data matches well with the large ozone decreasing trends in recent years. Day-of-week patterns of OMI NO_2 columns (Figure 65) show higher values during weekdays than weekends, consistent with findings based on NO_2 ground-based observations and temporal patterns of onroad mobile sources. In summary, OMI NO_2 columns and ground-based NOx observations have shown similar inter-annual and day-of-week patterns, which are also consistent with the trend for the ozone concentrations, indicating that NOx plays an important role in tropospheric ozone formation.

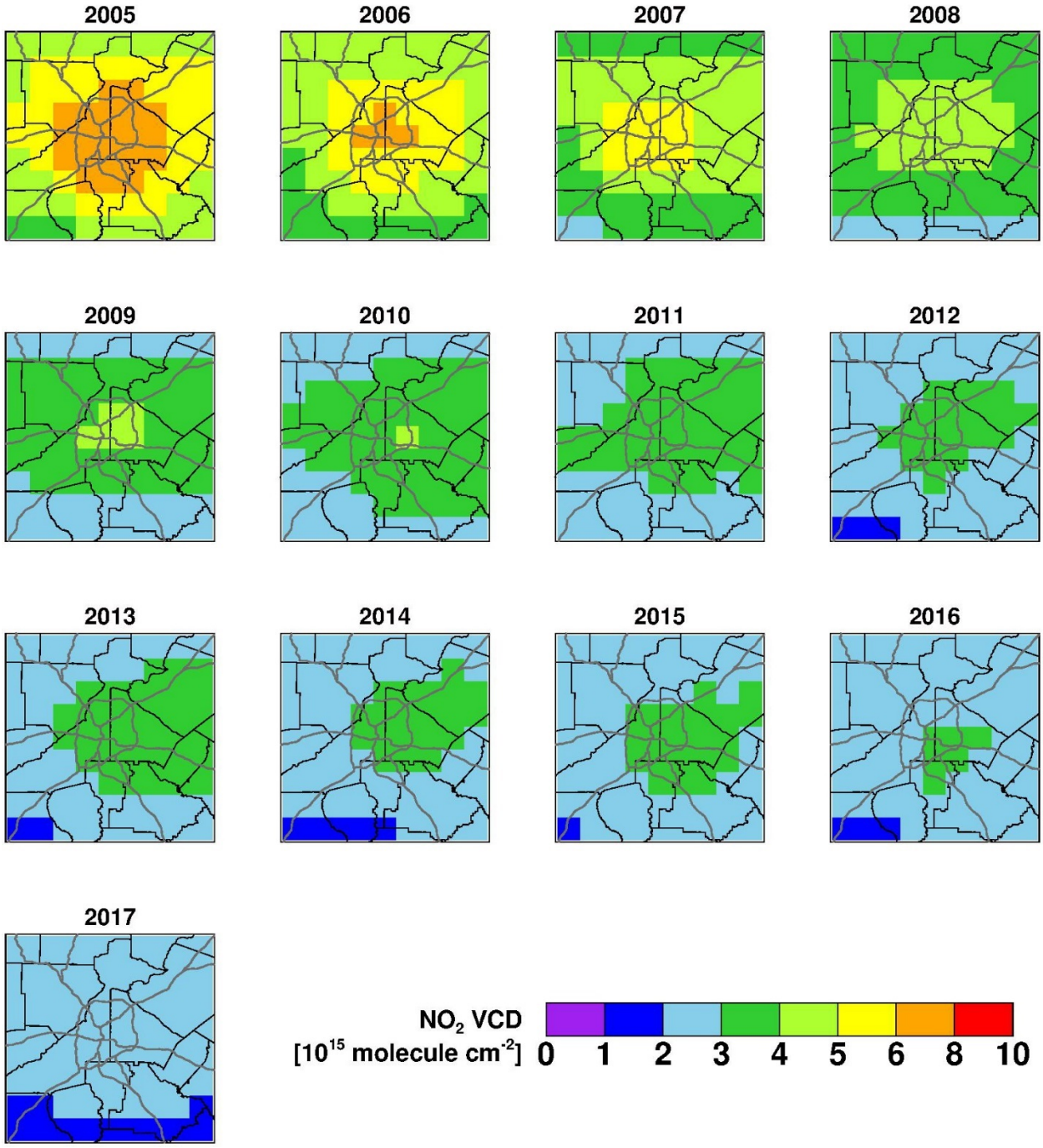

Figure 62. Annual mean OMI NO_2 tropospheric columns over the Metro Atlanta area during 2005-2017.

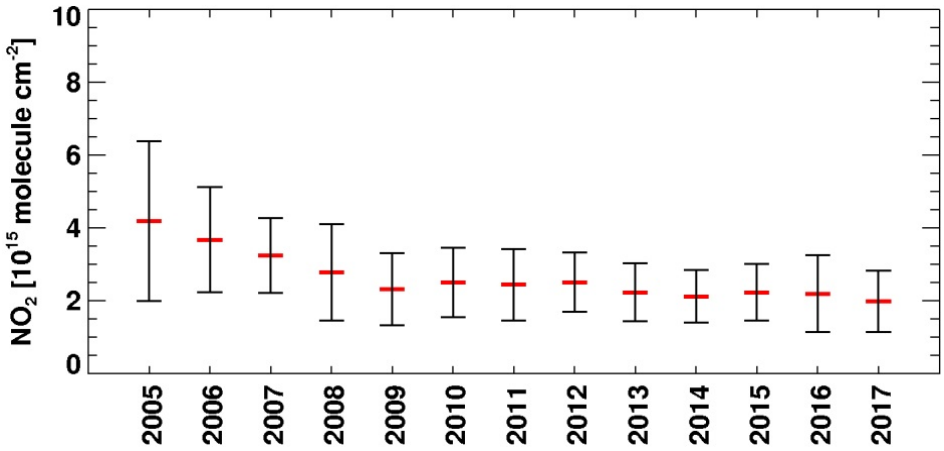

Figure 63. Annual spatial mean OMI NO_2 tropospheric columns over the Metro Atlanta area during April-October of 2005-2017. The means (red bar) and its standard deviations (black bars) are shown.

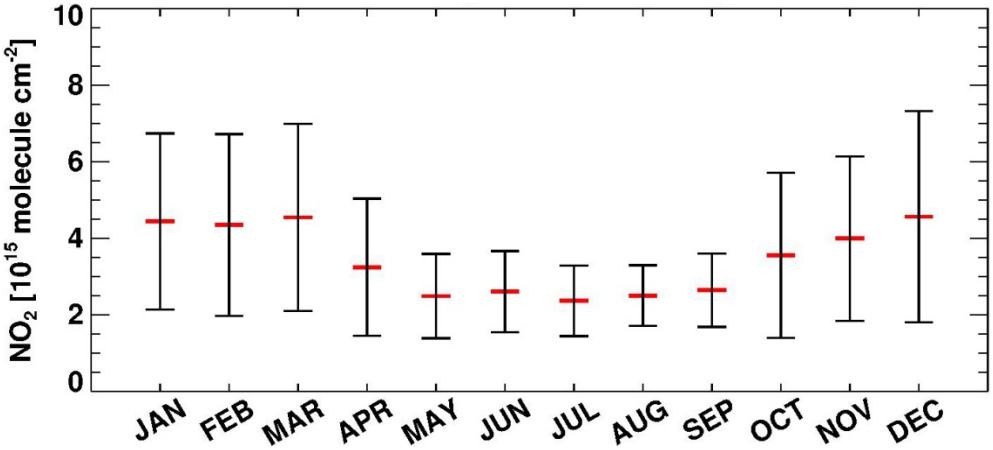

Figure 64. Monthly OMI NO_2 tropospheric columns in 2005-2017 over the Metro Atlanta area. The means (red bar) and its standard deviations (black bars) are shown.

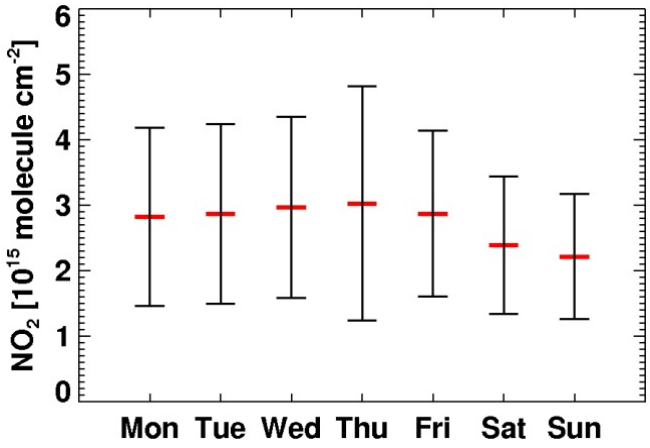

Figure 65. Mean OMI NO_2 tropospheric columns on each day of week over Metro Atlanta area in April-October, 2005-2017. The mean (red bar) and its standard deviations (black bars) are shown.

Ozone and traffic conditions

The impact of ozone exceedances from congestion in Atlanta is further investigated by analyzing hourly Google traffic condition data since NOx emissions are mainly from mobile sources in Atlanta (Figure 50) and NOx and VOC emissions rates tend to be higher in congested traffic conditions (Anderson, et al, 1996, De Vlieger, et al, 2000, Zhang et al., 2011). Traffic condition data are displayed in four colors (Dark Red, Red, Orange, and Green) in Google maps. Each color represents a different traffic condition: Green as free flow, Orange as light congestion, Red and Dark Red as severe congestions. Hourly screenshots of google map with traffic conditions over the Metro Atlanta area were captured from May 18, 2017 to October 31, 2017 using Python scripts by Georgia EPD since such detailed electronic data were not publicly available. Figure 66 is a screenshot example for June 29, 2017 at 18:00 PM which has the highest number of congestion pixels. A total of 2,992 hours of valid screenshots were collected in the 2017 ozone season.

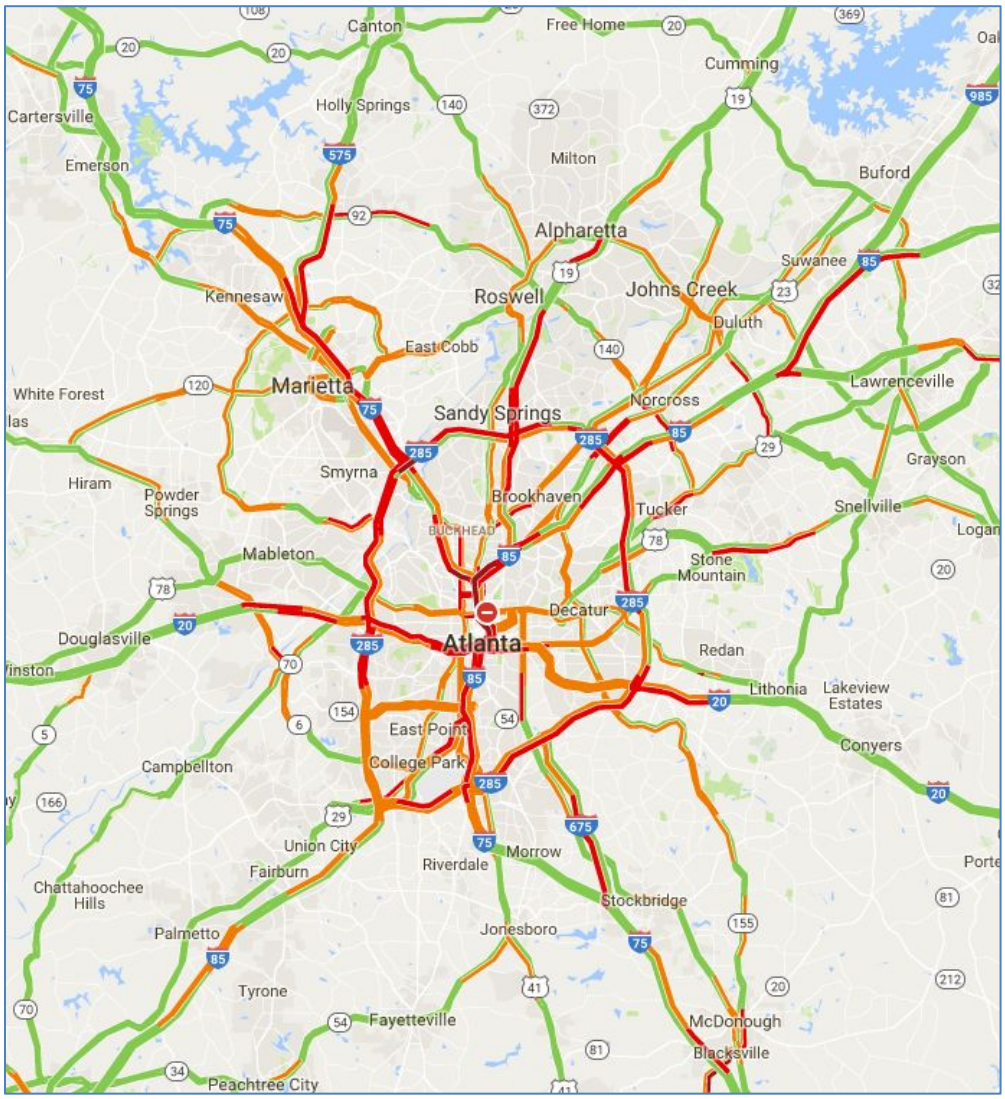

Figure 66. Google map screenshot for the Metro Atlanta area at 18:00 PM on June 29, 2017.

The hourly screenshots were then processed using Python scripts to count the number of pixels by colors, which can represent the traffic conditions. The higher number of pixels in Red and Dark Red indicates more serious congestion. Statistics of the number of pixels by colors in the hourly google traffic map over Metro Atlanta area show that the number of total pixels in a hourly google traffic map ranges from 66,618 to 32,631, with a mean of 62,962 (Table 13) and 84% above 60,000.

Table 13. Statistics of the number of pixels by colors in the hourly google traffic map over the Metro Atlanta area.

Color	Max	Min	Median	Mean	Standard Deviation
Dark Red	2,707	19	149	245	260
Red	1,790	0	32	170	294
Orange	22,537	0	1,073	2,489	3,064
Green	65,971	31,289	61,591	59,951	4,891
Hourly Total	66,618	32,631	64,543	62,962	3,663

Traffic conditions vary greatly with hours of the day (Figure 67). Most of the pixels are Green, while a lot of Dark Red, Red and Orange pixels concentrate in the Atlanta urban core. There are two peaks for the number of pixels in Dark Red, Red and Orange: one peak during the morning rush hours (7 AM – 9 AM) and the other in the evening rush hours (4 PM – 6PM). In addition to these two peaks, there is another small peak for the number of pixels in Orange around 1 PM.

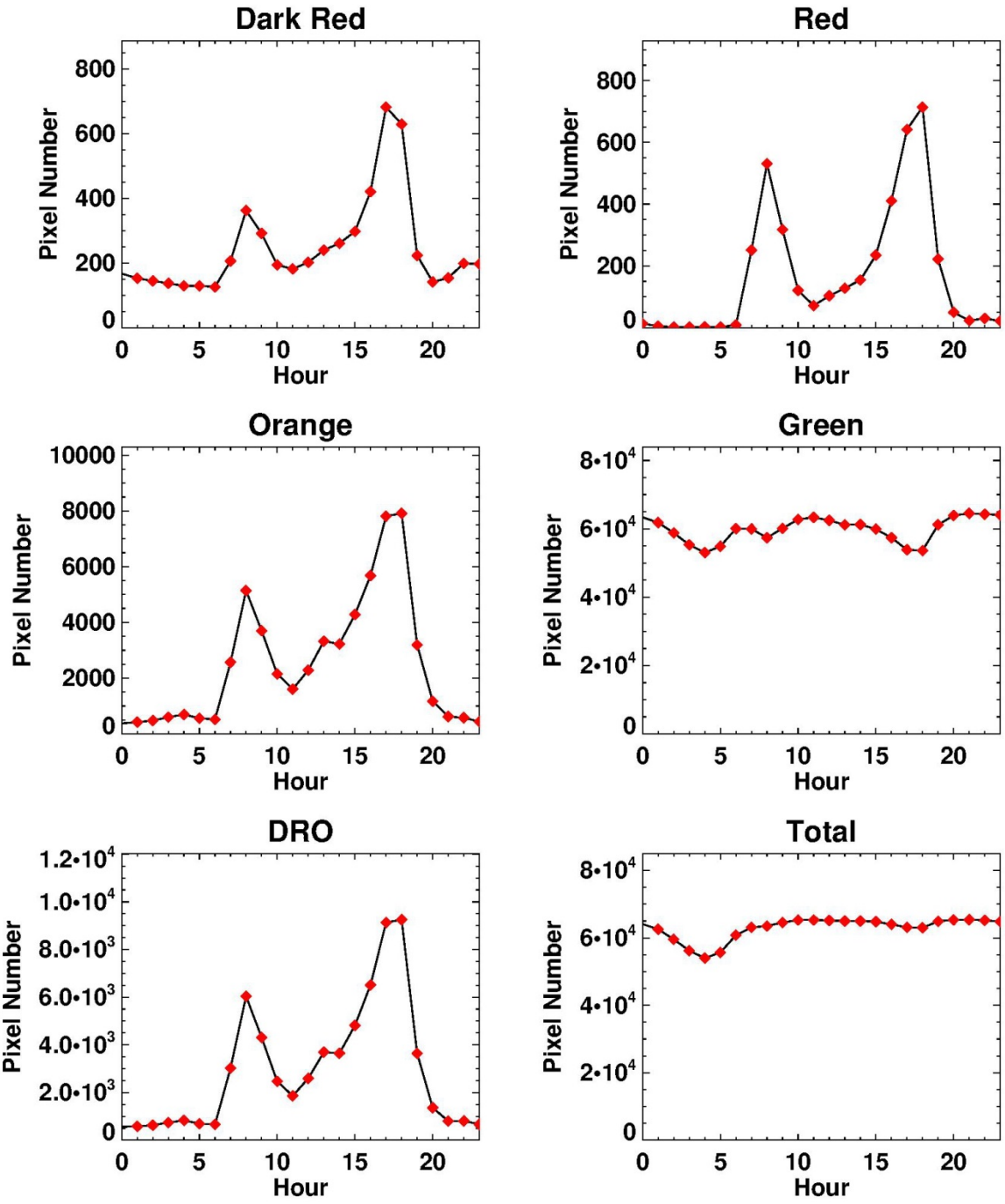

Figure 67. The average number of pixels by colors in the hourly google traffic map over the Metro Atlanta area. DRO is the sum of dark red, red, and orange pixels.

In this study, the number of pixels for Dark Red, Red, and Orange were added together and referred to as DRO pixels to represent the overall congestion levels. The mean percentage of the number of DRO pixels to total pixels is 4.5%. The percentage of the number of DRO pixels of the total pixels during morning and evening rush hours can reach 14.5% and 20% (Figure 68).

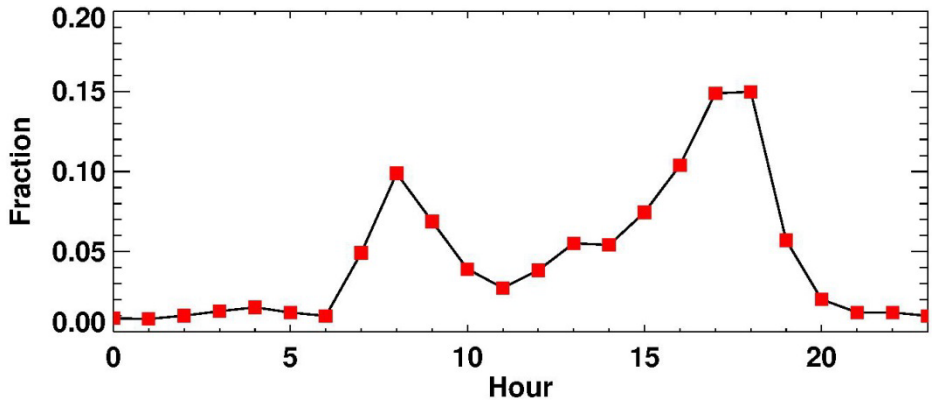

Figure 68. The average fractions of the number of DRO pixels of the total pixels in the hourly Google traffic map over the Metro Atlanta area.

The hourly traffic conditions also vary greatly with days of the week. Only days with valid 24-hour data were used in this analysis. There are more than 20 valid days in June, July and August of 2017, and the total pixel number in the 24 hours is very similar (Figure 69). The number of DRO pixels is much less on weekends than weekdays and have two peaks for weekdays and one longer peak for weekend (Figure 70). During the weekdays, the number of DRO pixels increases gradually from Monday to Friday, except that the number of DRO pixels for the morning period on Friday is less than other weekdays. For weekends, the number of DRO pixels on Saturday is higher than Sunday, and peaks earlier on Saturday than on Sunday. The number of DRO pixels during the daytime were further summarized by three 4-hour windows (6 AM – 10 AM, 10 AM – 2 PM, 2 PM – 6PM) corresponding to morning hours, mid-day hours, and evening hours, respectively (Figure 71). The DRO numbers for the evening hours are higher than those for the morning hours and mid-day hours. The DRO numbers during the mid-day hours and evening hours increase from Monday to Friday and decrease on weekends. The DRO numbers during morning hours are similar from Tuesday to Thursday, less on Monday and Friday, and least on Saturday and Sunday.

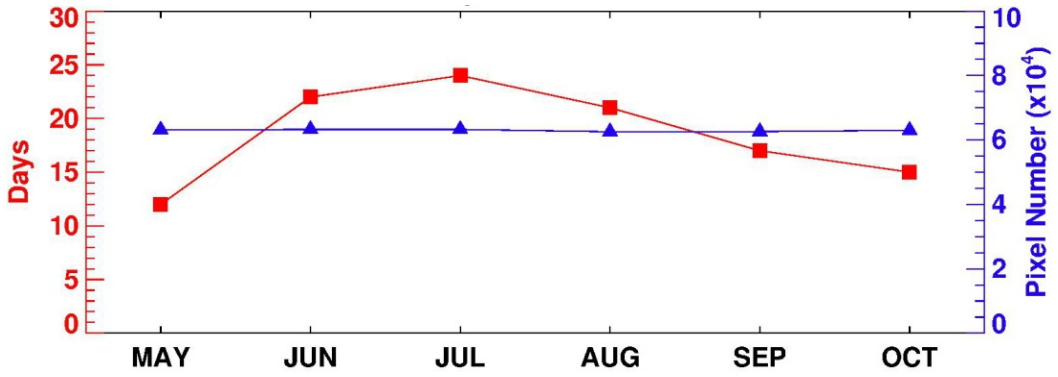

Figure 69. The number of valid days (red squares) and hourly average number of pixels (blue triangles) for the hourly Google traffic maps over the Metro Atlanta area from May to October, 2017.

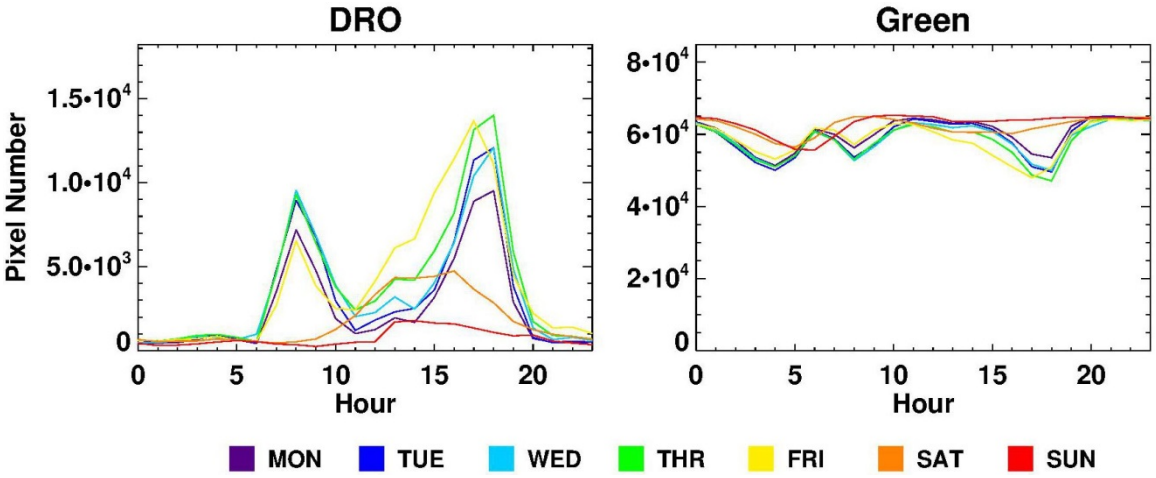

Figure 70. The number of DRO and Green pixels on each day of week over the Metro Atlanta area.

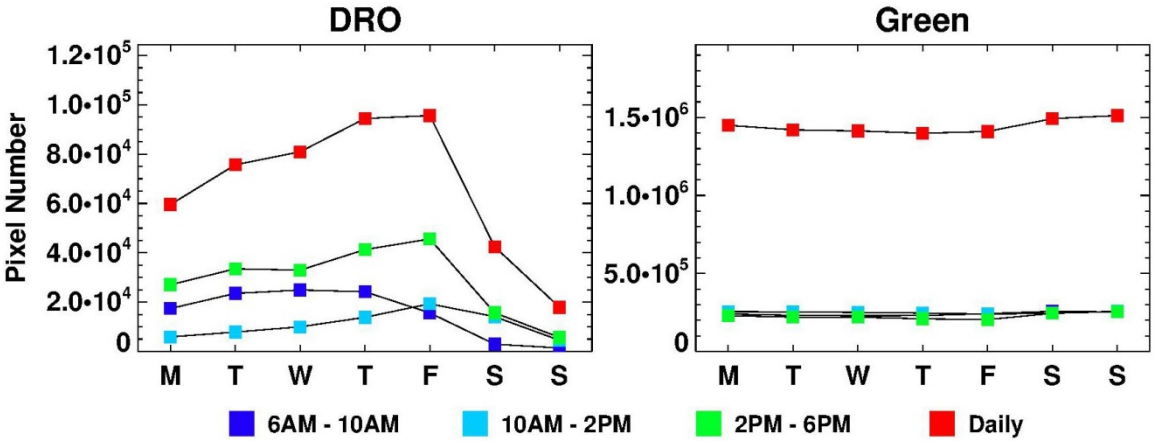

Figure 71. The number of DRO and Green pixel numbers during three periods (6 AM – 10 AM, 10 AM – 2 PM, 2 PM – 6PM) on each day of week over the Metro Atlanta area.

The number of DRO pixels on eight ozone exceedance days were compared with those on the two days before and two days after the ozone exceedance days in 2017 (Figure 72). Google traffic data on ozone exceedances days of April 10, May 15 and May 16 were not captured. The DRO numbers during the mid-day hours on exceedance days on the weekend (August 19 and 20) are similar to those on weekdays, suggesting that the mobile NOx emissions during weekend mid-day hours have higher impacts on ozone formation since the DRO numbers during the morning and evening hours are very low. The DRO numbers on weekday exceedances don't have a clear pattern.

In addition, the hourly average number of DRO pixels on each ozone exceedance days was compared with that on all days, all weekdays/weekends, and the corresponding day of week (Figure 73 - Figure 80). On ozone exceedance day on Tuesday (August 1), the number of DRO pixels is higher than the average weekday and Tuesday conditions during the morning hours. On ozone exceedance days on Wednesday (July 19 and July 26), the number of DRO pixels is higher than the average weekday and Wednesday conditions during the mid-day hours when atmospheric photochemistry is very active. On ozone exceedance days on Thursday (August 24 and September 28), the number of DRO pixels is higher than the average weekday and Thursday conditions during the morning hours. On ozone exceedance days on Friday (July 21), the number of DRO pixels is higher than the average weekday conditions during the mid-day and evening hours, but not higher than the average Friday conditions. On ozone exceedance days on Saturday, the number of DRO pixels is not higher than the average Saturday conditions. The Sunday exceedance holds the same pattern as the Saturday one.

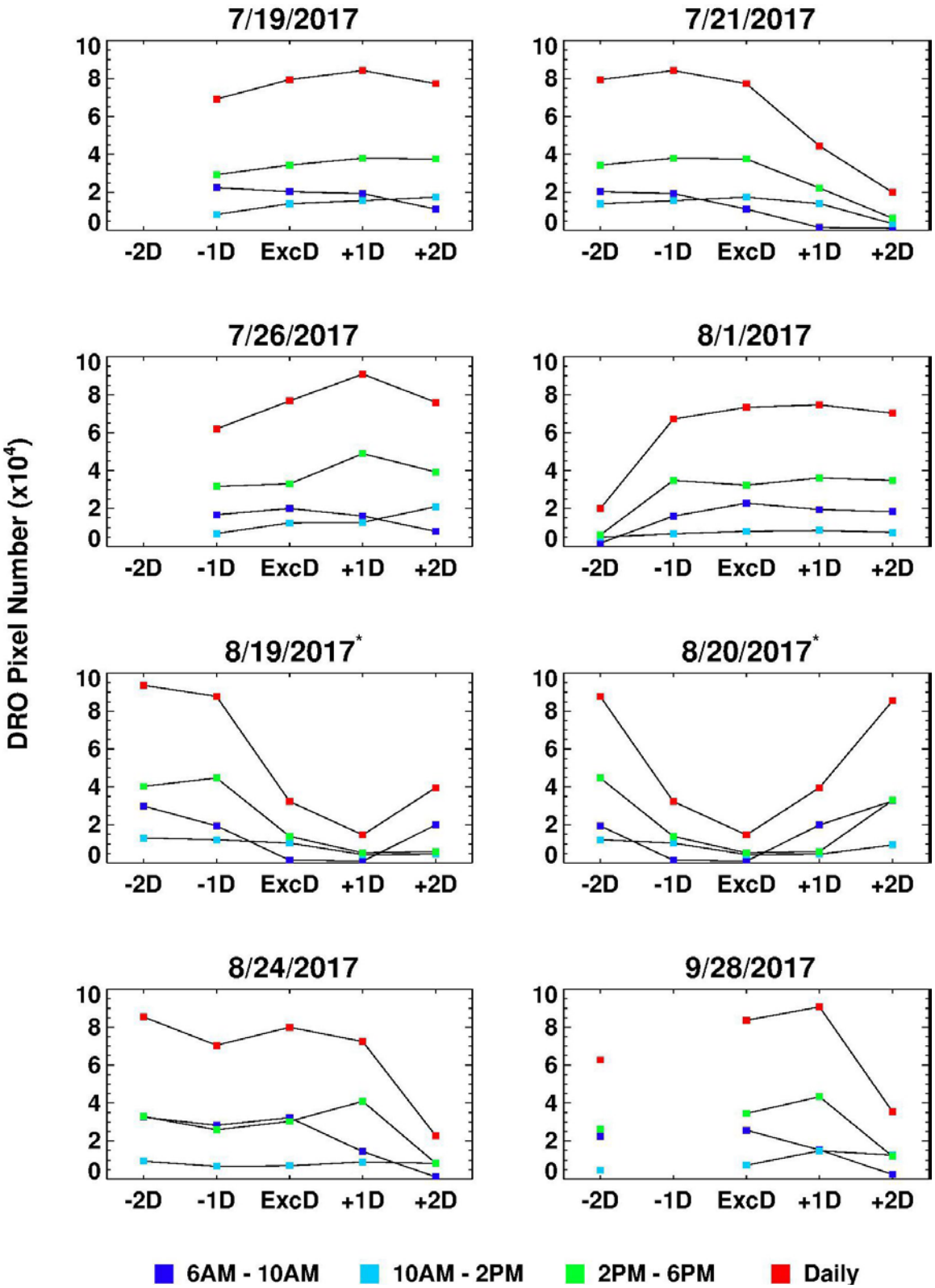

Figure 72. The number of DRO pixels by three periods on eight ozone exceedance days and 2 days before and after ozone exceedance days in 2017. '*' indicates exceedances on weekend.

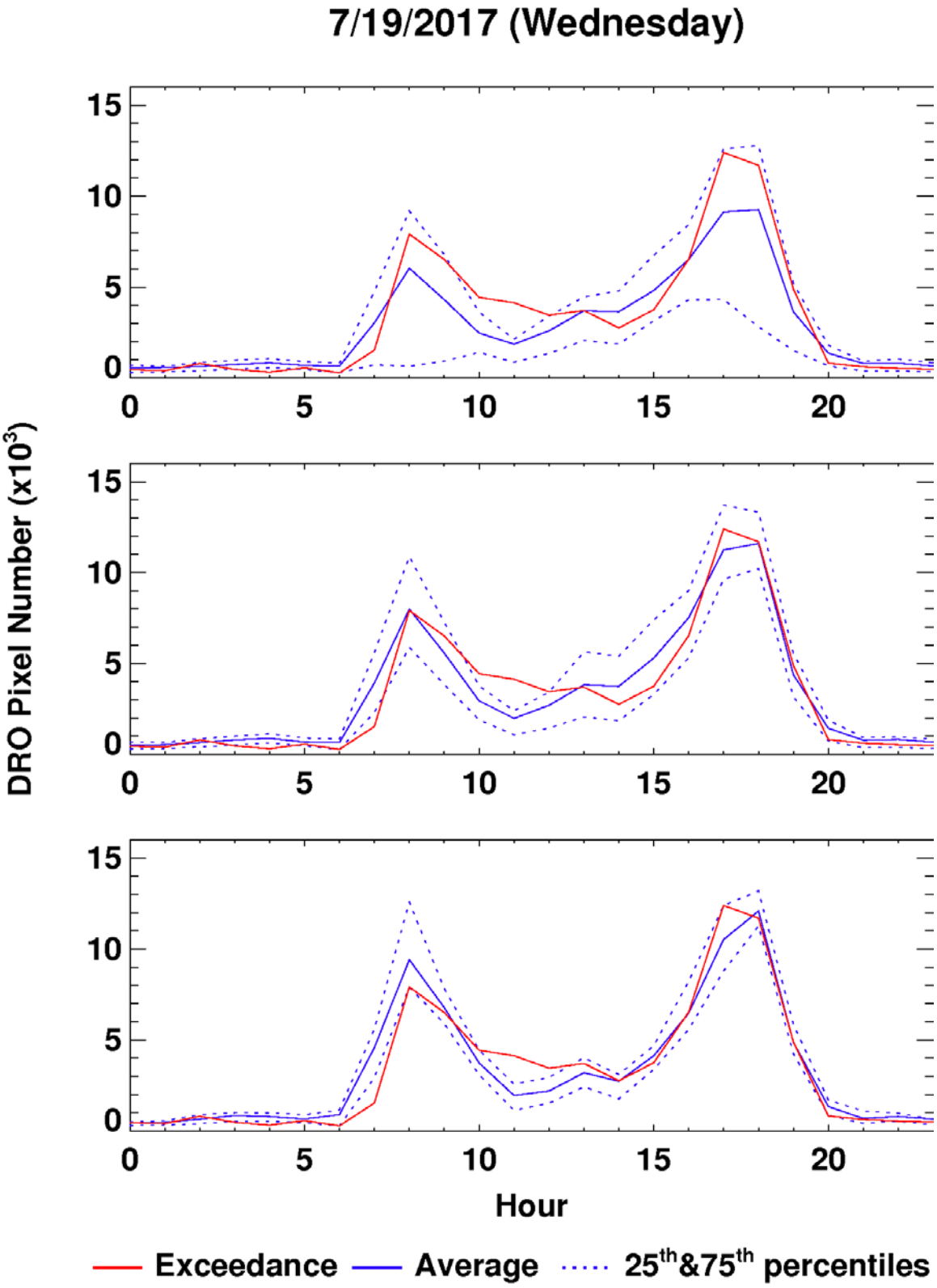

Figure 73. The hourly DRO pixel numbers on July 19, 2017, an ozone exceedance day (red line), and the hourly averages (blue solid line), 25th and 75th percentiles (blue dash lines) of DRO numbers on all days (top), weekdays (middle), and Wednesday (bottom).

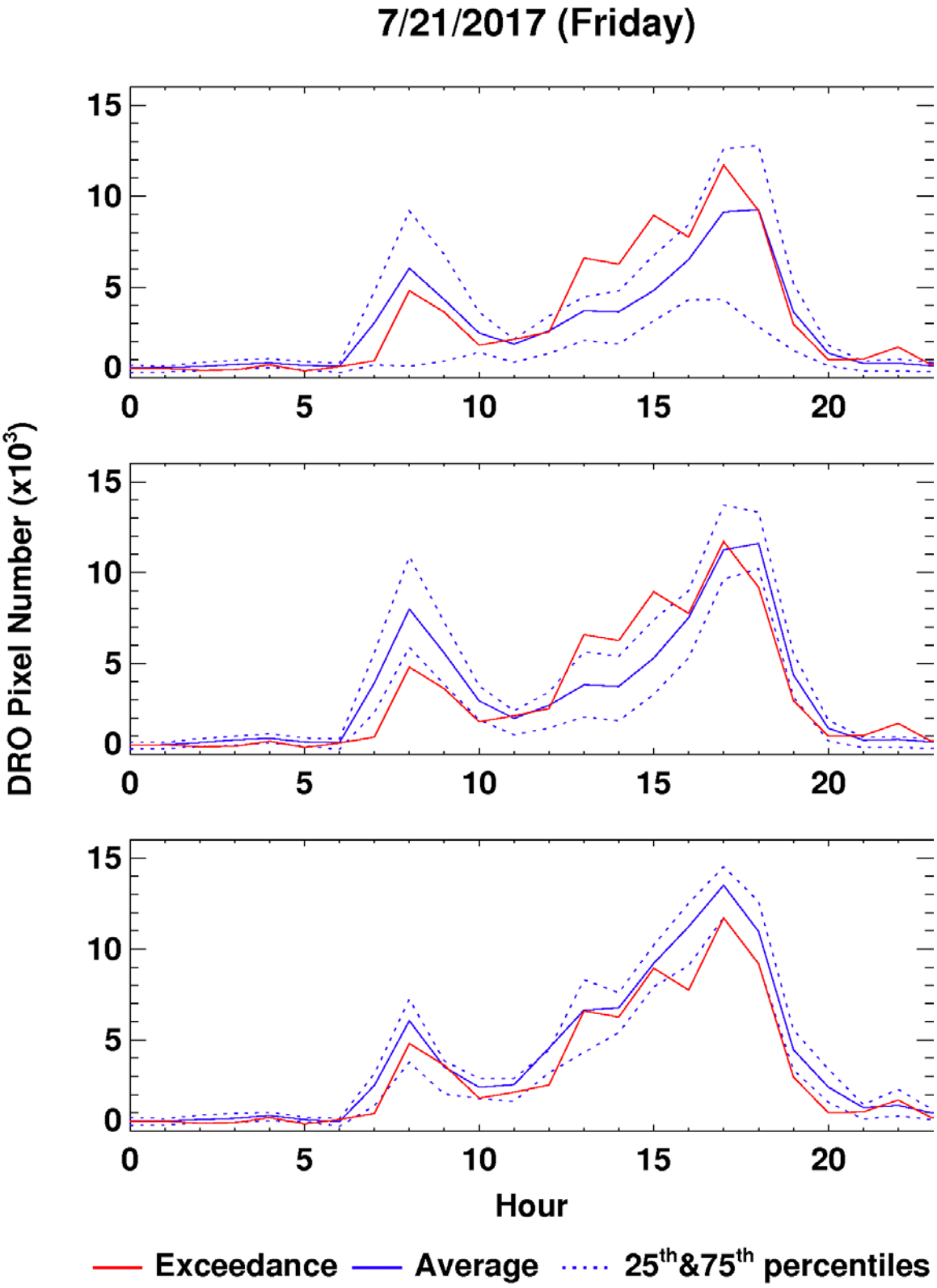

Figure 74. The hourly DRO pixel numbers on July 21, 2017, an ozone exceedance day (red line), and the hourly averages (blue solid line), 25th and 75th percentiles (blue dash lines) of DRO numbers on all days (top), weekdays (middle), and Friday (bottom).

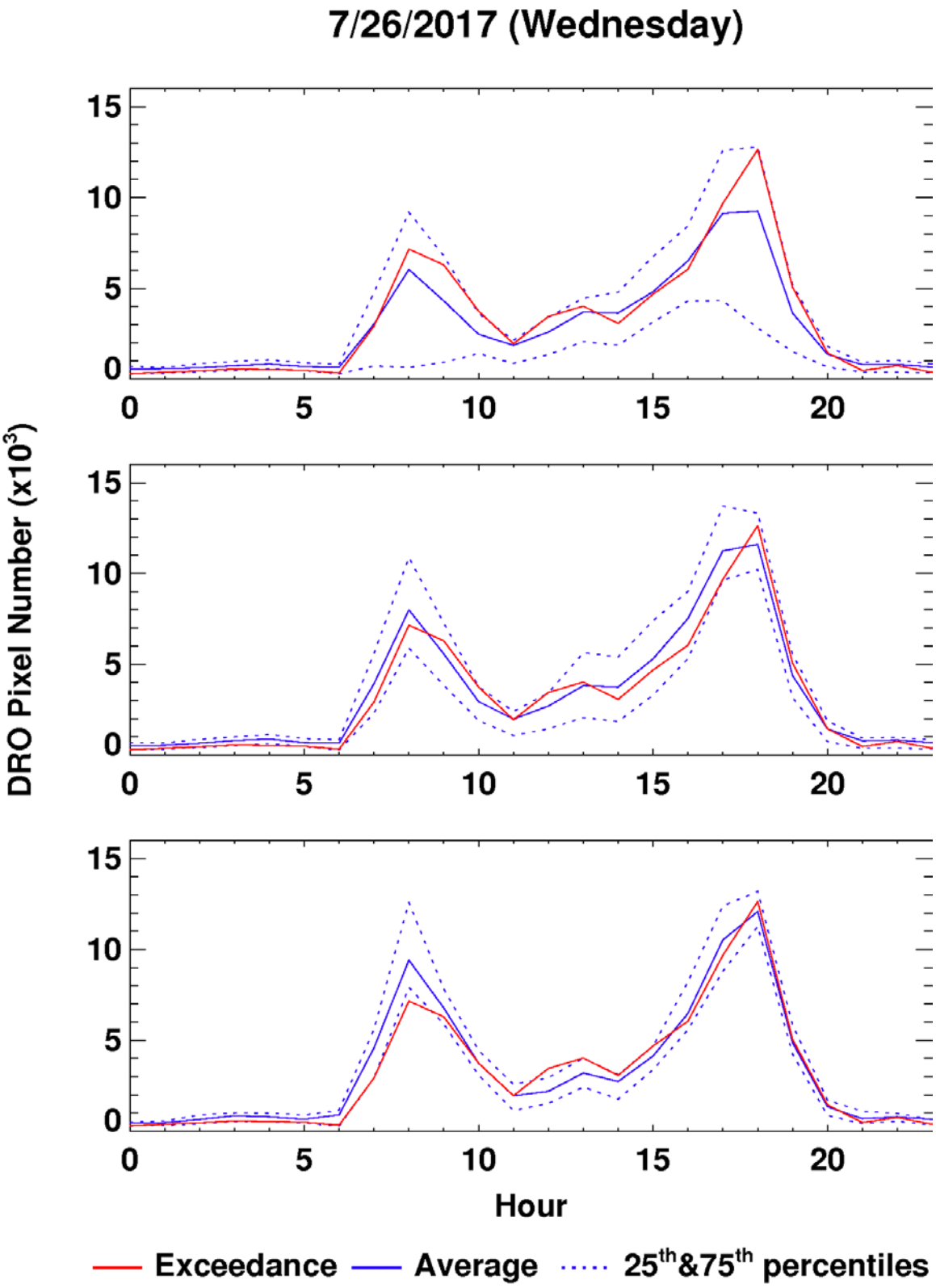

Figure 75. The hourly DRO pixel numbers on July 26, 2017, an ozone exceedance day (red line), and the hourly averages (blue solid line), 25th and 75th percentiles (blue dash lines) of DRO numbers on all days (top), weekdays (middle), and Wednesday (bottom).

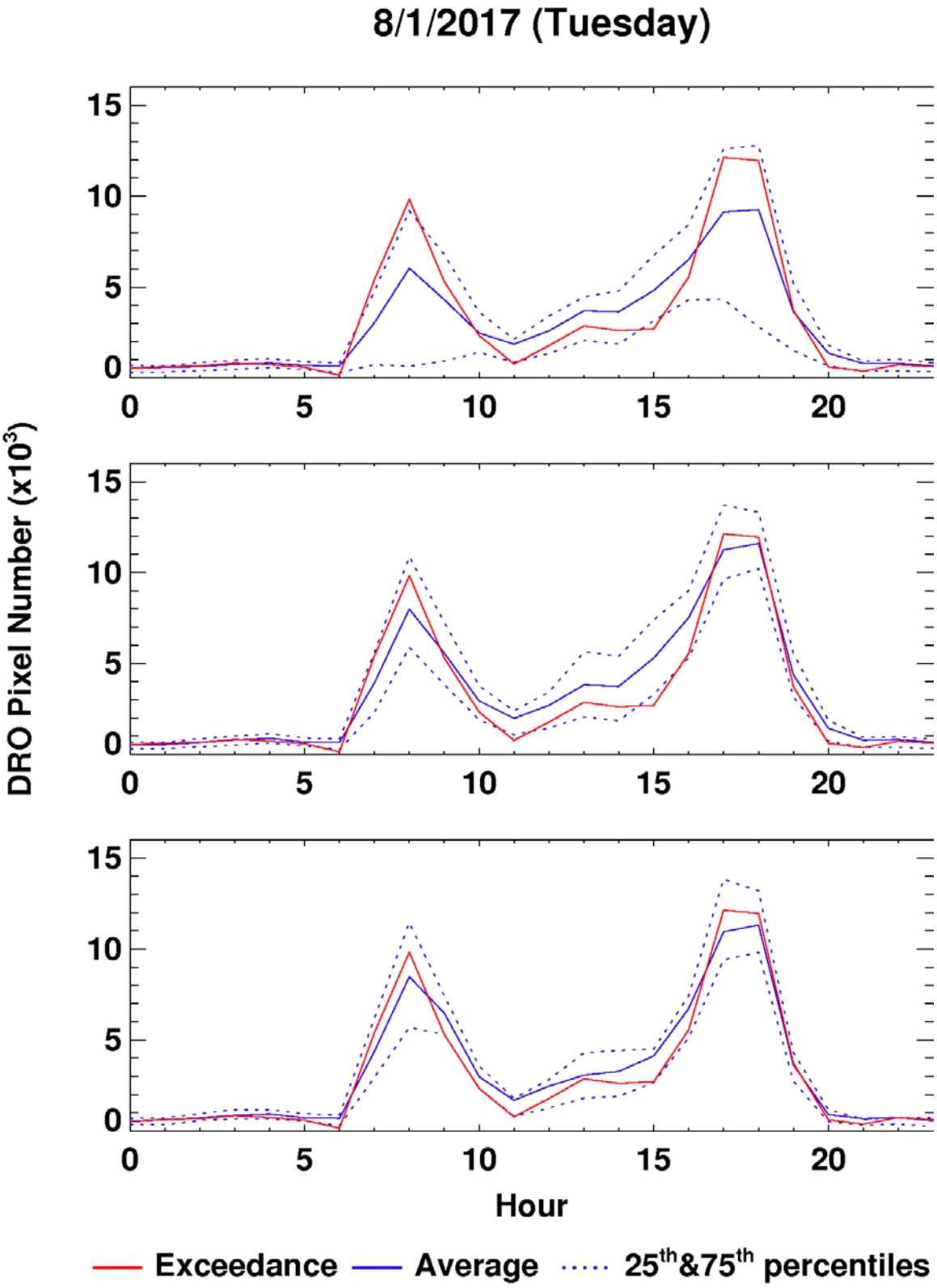

Figure 76. The hourly DRO pixel numbers on August 1, 2017, an ozone exceedance day (red line), and the hourly averages (blue solid line), 25th and 75th percentiles (blue dash lines) of DRO numbers on all days (top), weekdays (middle), and Tuesday (bottom).

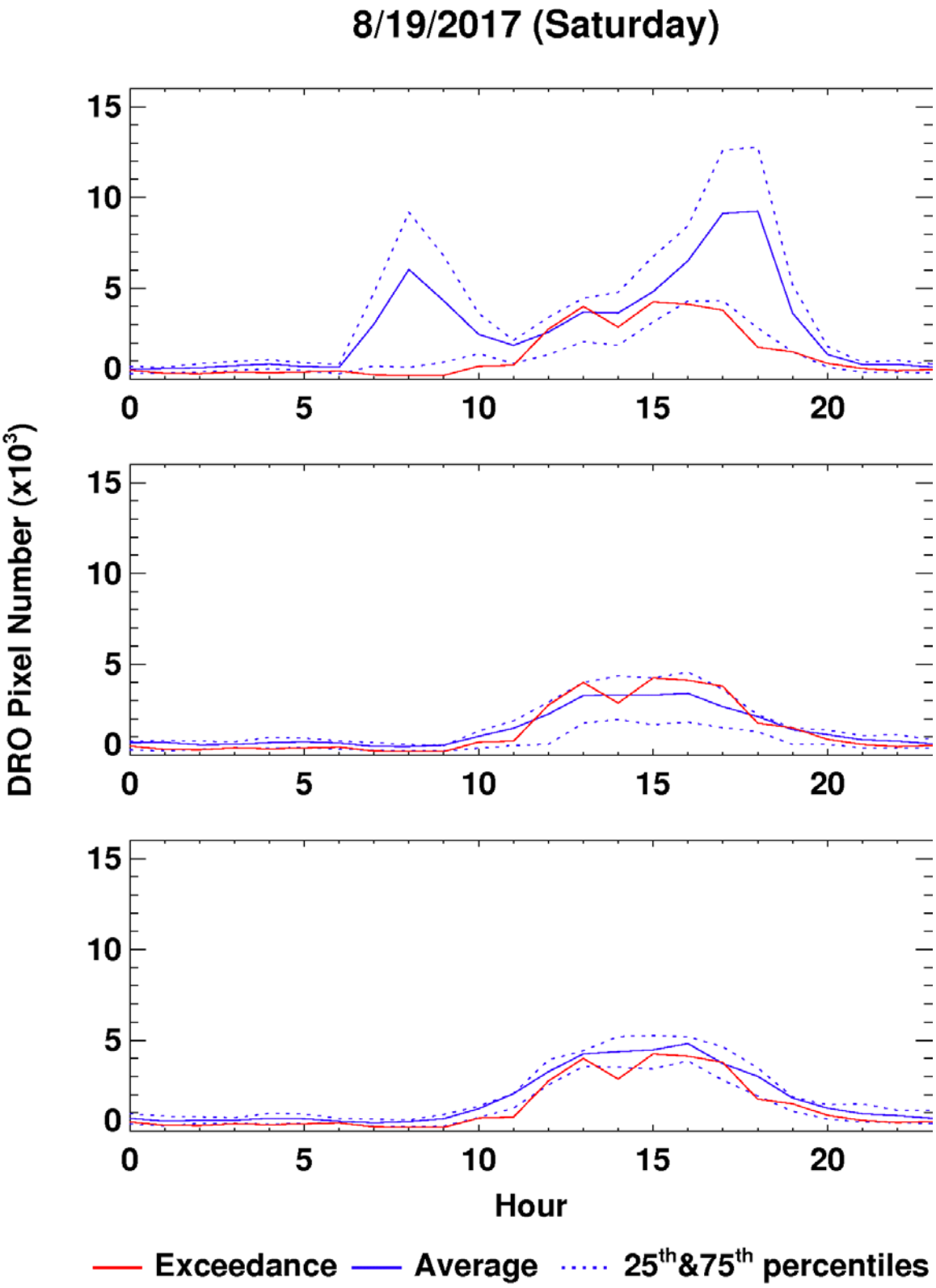

Figure 77. The hourly DRO pixel numbers on August 19, 2017, an ozone exceedance day (red line), and the hourly averages (blue solid line), 25th and 75th percentiles (blue dash lines) of DRO numbers on all days (top), weekends (middle), and Saturday (bottom).

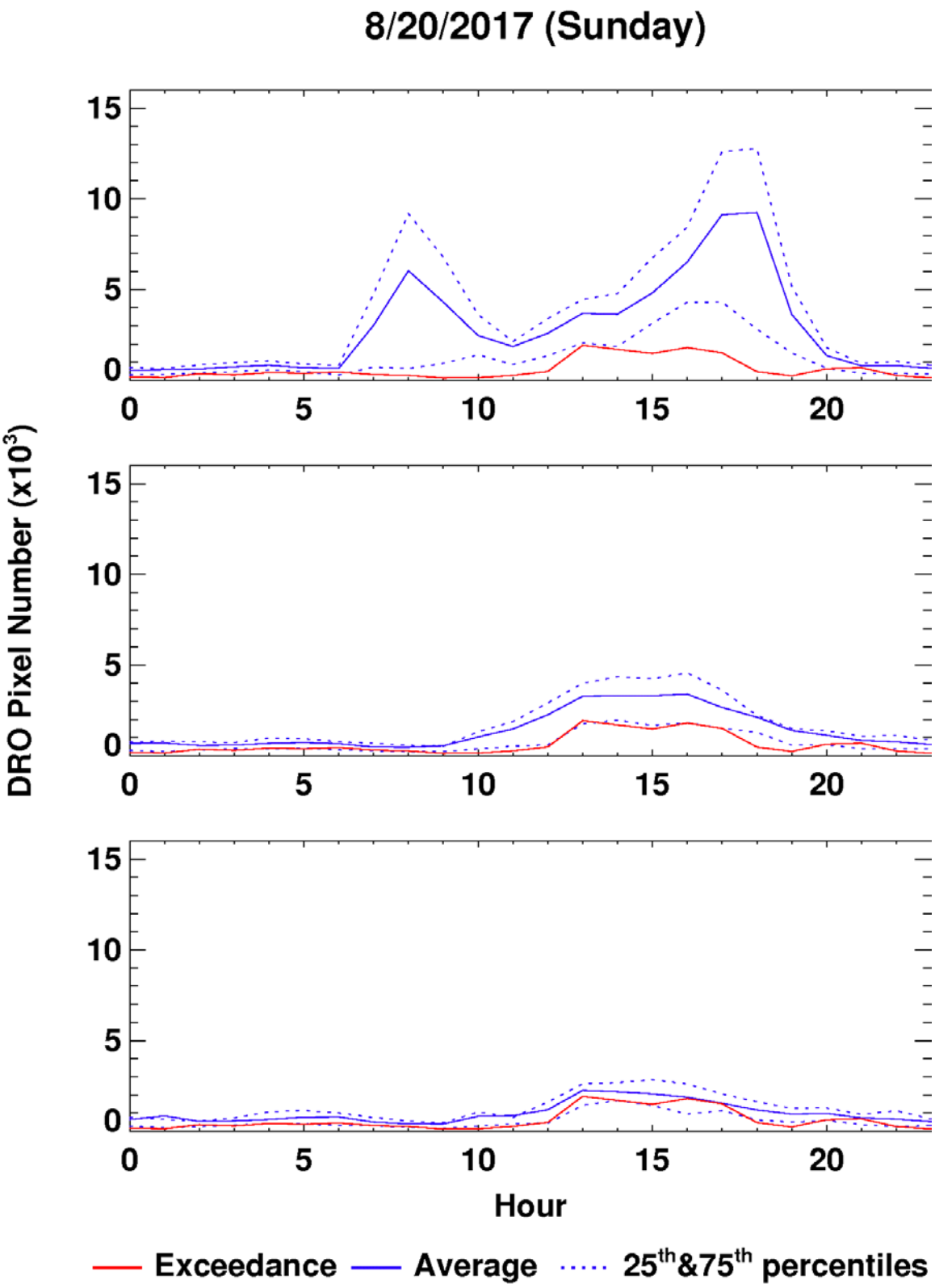

Figure 78. The hourly DRO pixel numbers on August 20, 2017, an ozone exceedance day (red line), and the hourly averages (blue solid line), 25th and 75th percentiles (blue dash lines) of DRO numbers on all days (top), weekends (middle), and Sunday (bottom).

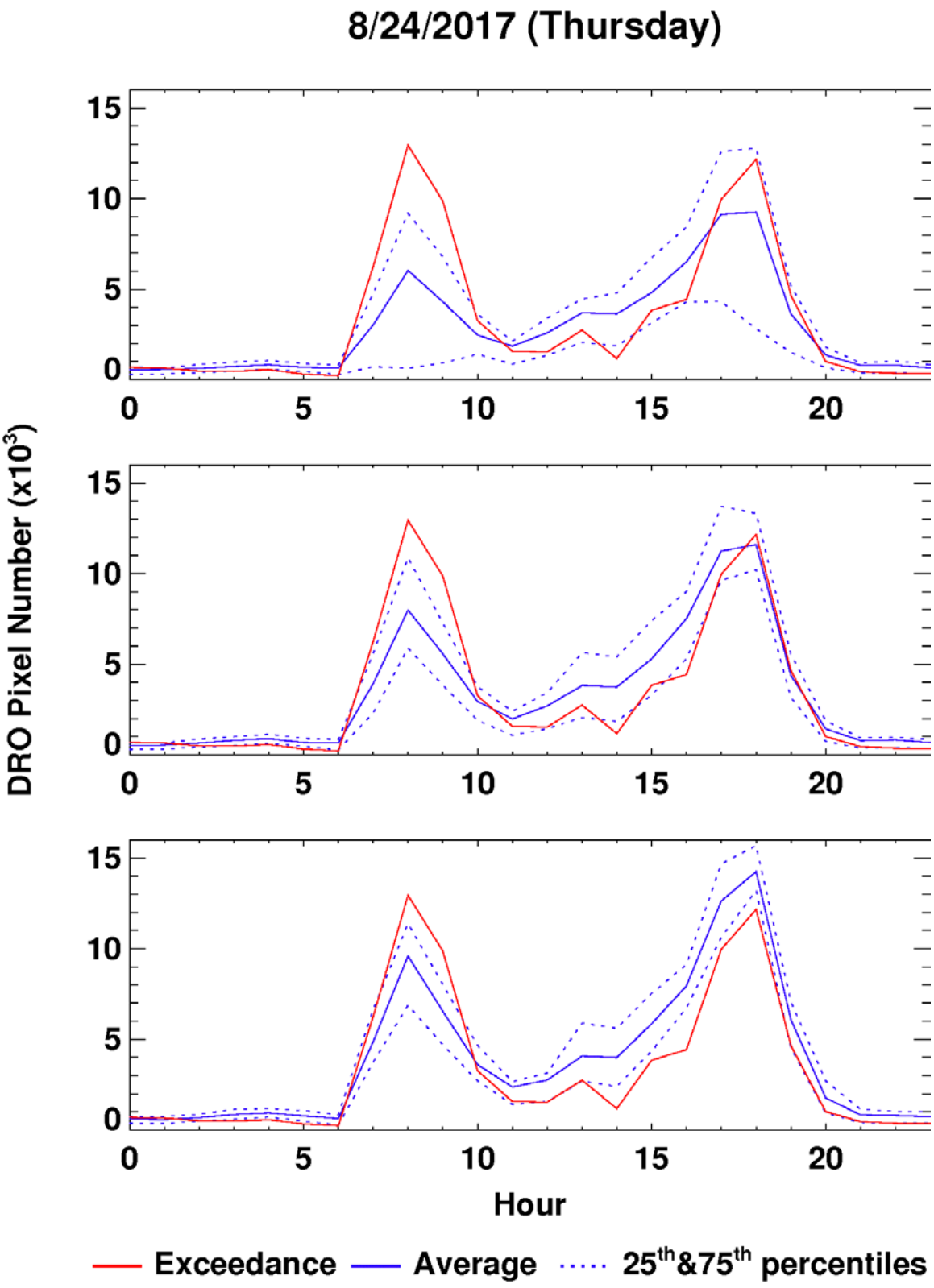

Figure 79. The hourly DRO pixel numbers on August 24, 2017, an ozone exceedance day (red line), and the hourly averages (blue solid line), 25th and 75th percentiles (blue dash lines) of DRO numbers on all days (top), weekdays (middle), and Thursday (bottom).

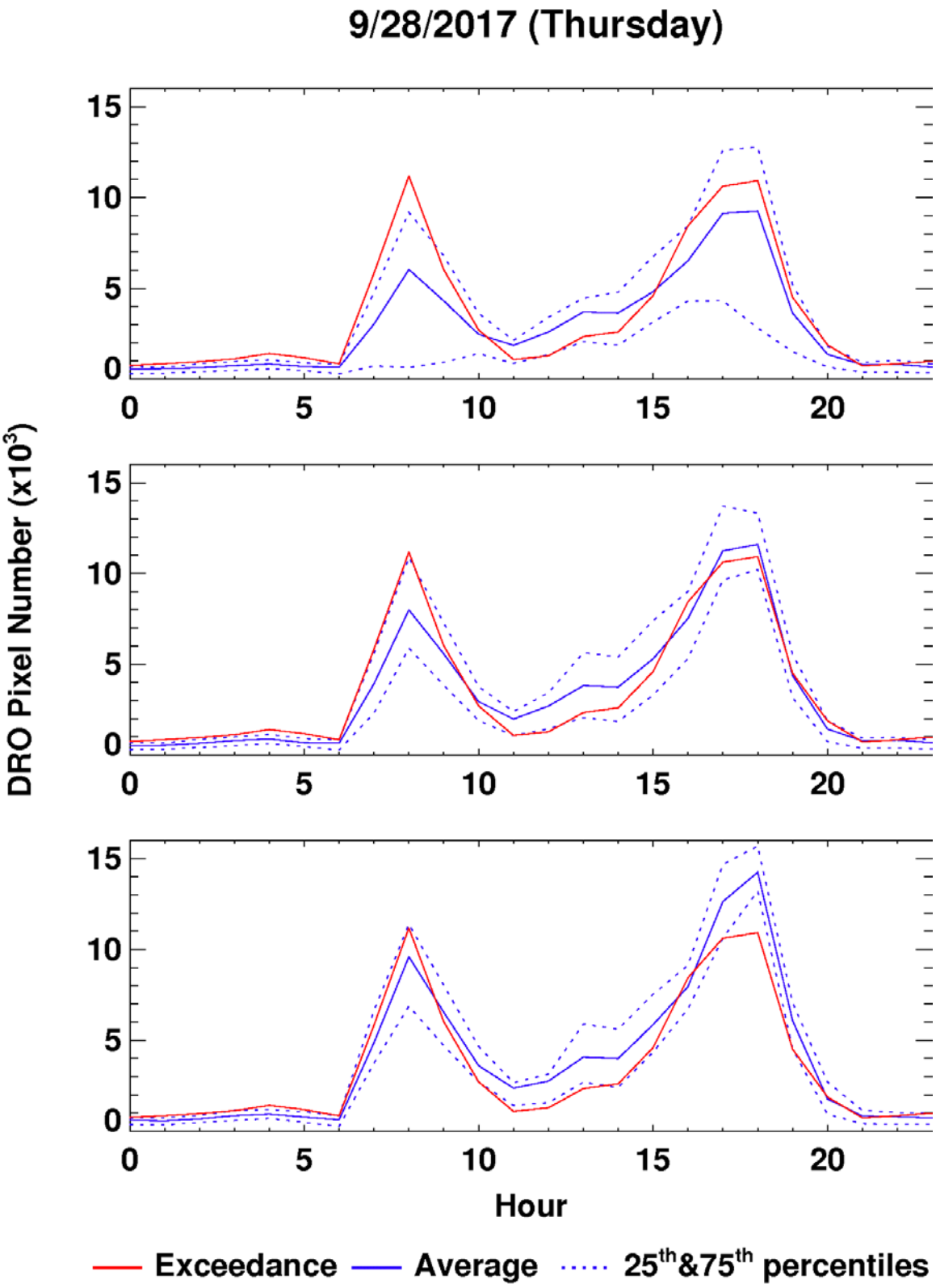

Figure 80. The hourly DRO pixel numbers on September 28, 2017, an ozone exceedance day (red line), and the hourly averages (blue solid line), 25th and 75th percentiles (blue dash lines) of DRO numbers on all days (top), weekdays (middle), and Thursday (bottom).

8. Ozone and VOCs precursors

Peak ozone concentrations in the Atlanta urban core can be sensitive to volatile organic compounds (VOCs), although the Metro Atlanta area is generally NOx-sensitive according to previous studies (Blanchard et al., 2010; Hidy et al., 2014). VOCs are emitted from a variety of sources, including motor vehicles, chemical manufacturing facilities, refineries, factories, consumer and commercial products, and natural (biogenic) sources (mainly trees). In the Metro Atlanta area during 2014, 68% of VOCs emissions are from biogenic sources, 16% from other sources (solvent, waste disposal, gas station, and bulk gasoline terminals), and 14% from mobile (onroad + nonroad) sources (Figure 81). Both anthropogenic VOCs emissions and ambient VOCs concentrations have been decreasing (Hidy and Blanchard, 2015). In this study, impacts of VOCs on 2017 ozone exceedances in the Metro Atlanta area are investigated using an observation-based method.

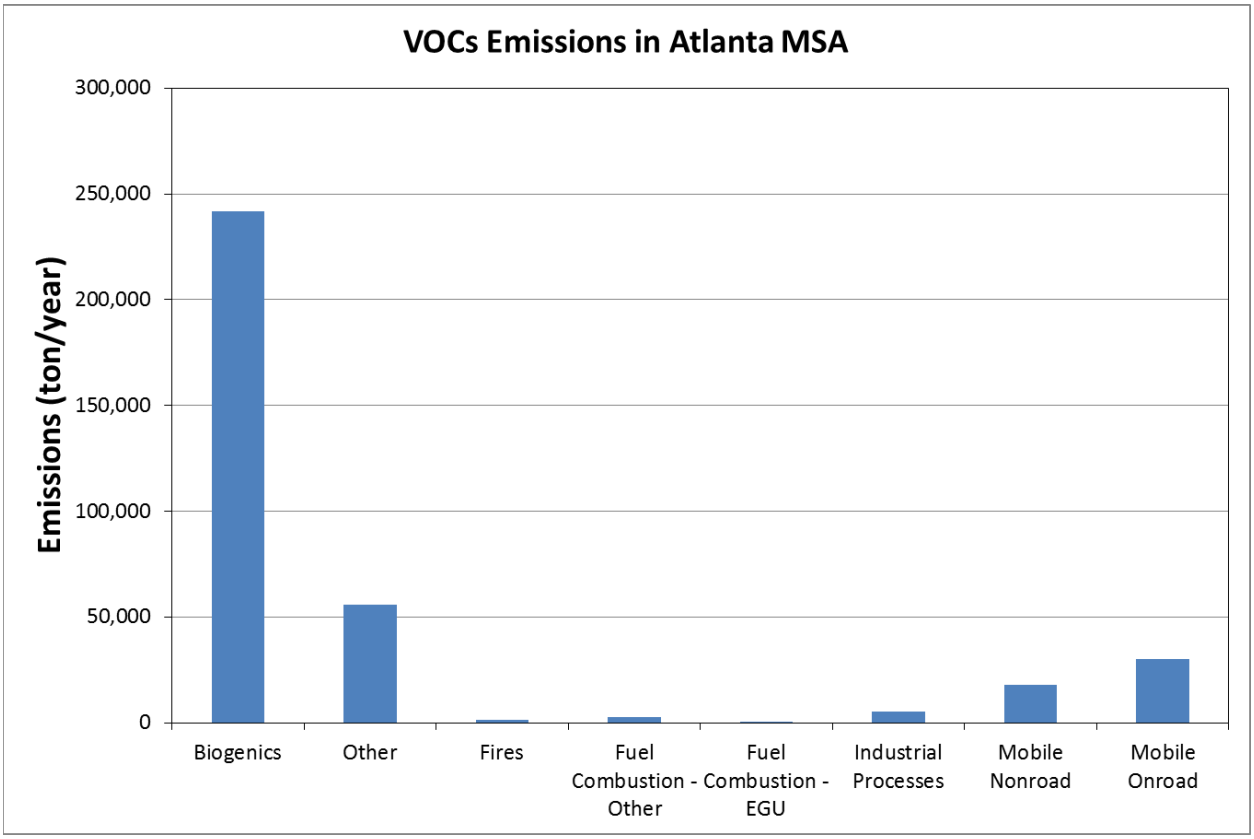

Figure 81. 2014 VOC emissions (tons/year) by source sectors in Metro Atlanta area.

Relationship between peak 8-hour ozone and anthropogenic VOCs

The relationship between MDA8O3 and anthropogenic VOCs was assessed using a linear regression model. In 2017, the South DeKalb monitor is the only Photochemical Assessment Monitoring Stations (PAMS) monitor (Figure 82) in the Metro Atlanta Area. Measurements at the South DeKalb monitor well represent urban air quality conditions because the monitor is located in the urban core. The annual summer time (June-August) average anthropogenic VOCs concentrations are calculated using 1-hour VOCs data measured daily at the South DeKalb monitor during 2010, 2011, 2013, 2014, 2106, and 2017. Significant data are missing in 2012

and 2015; therefore, data for these years are not used in this analysis. Anthropogenic VOCs are calculated by subtracting the isoprene concentration from the total non-methane organic carbon (NMOC) concentration since isoprene is mainly emitted from biogenic sources and referred to as "aNMOC" hereafter.

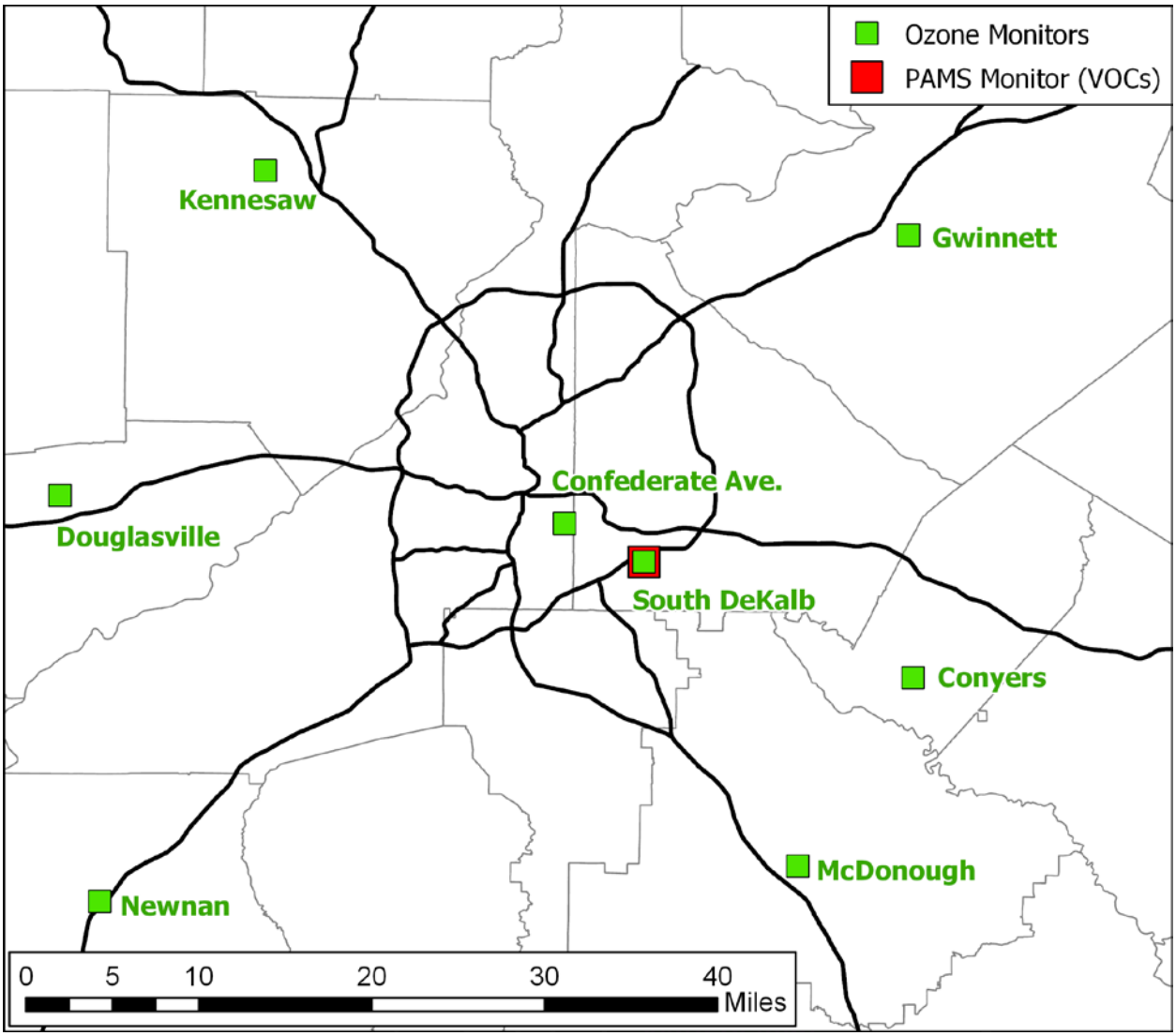

Figure 82. Locations of the ozone and PAMS monitors in the Metro Atlanta area.

Figure 83 shows a strong linear relationship between ozone and aNMOC except for year 2016. Coefficients of determination (R^2) values decreased from ~0.98 for regression without 2016 data to ~0.84 for regression with 2016 data. This strong correlation has also been found in previous work (Hidy and Blanchard, 2015). It is estimated that the annual 4th highest MDA8O3 can be reduced by 6 ppb if annual summertime average aNMOC concentrations are reduced by 10 ppbC assuming all photochemical conditions including reactivity of the total aNMOC and NOx concentrations are relatively constant during the period between 2011 and 2017. This result indicates that the Atlanta ozone may have become more sensitive to aNMOC than in past years. However, this analysis does not show any specific information about which VOCs are important

and, in turn, which anthropogenic sources are potentially important for controlling the Atlanta ozone.

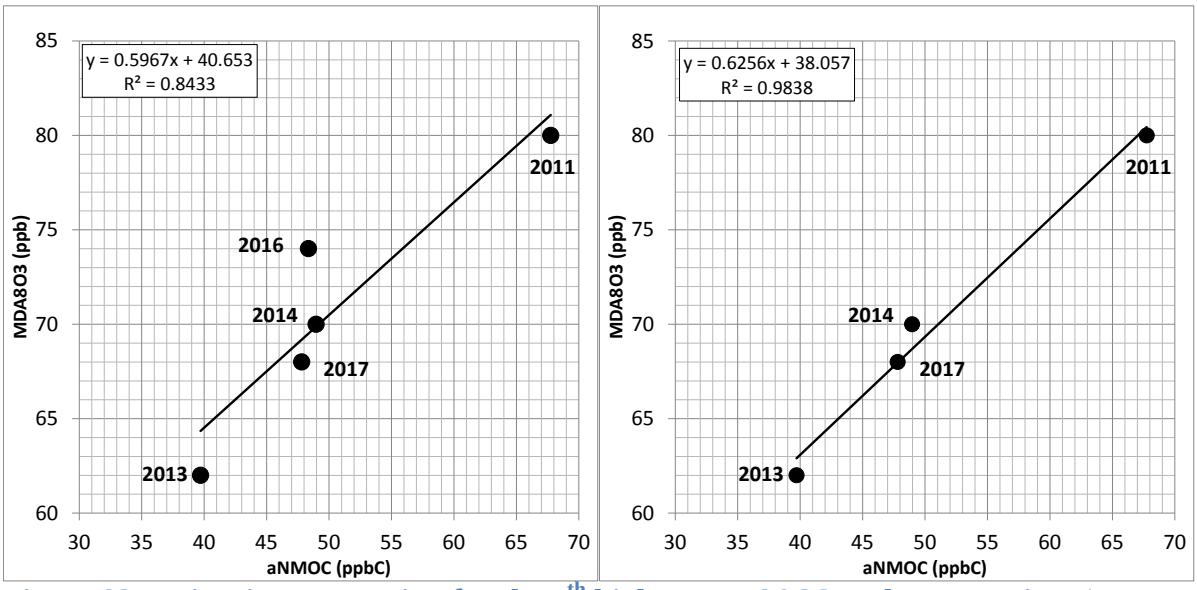

Figure 83. Univariate regression for the 4th highest MDA8O3 and summertime (June-August) average aNMOC concentrations at the South DeKalb monitor during 2011, 2013, 2014, and 2017 with (left) and without (right) 2016.

Comparison of reactivity-weighted concentrations of VOC species

Measurements of VOCs species at the South DeKalb monitor were weighted by corresponding reactivity which can describe their different effects on ozone formation, depending on ambient conditions. The higher reactivity-weighted concentrations indicate higher ozone effects. We reviewed different Incremental Reactivity (IR) scale for VOCS species developed by Bill Carter at the University of California at Riverside obtained from http://www.engr.ucr.edu/~carter/SAPRC/saprc07.xls. IR is the estimated number of additional ozone molecules formed per VOCs molecule added to the existing environment. Among different IR scales, we chose Equal Benefit Incremental Reactivity (EBIR) because EBIR is "for the conditions in which the sensitivity of ozone to VOCs is equal to that of NOx. Thus, the EBIR scale is calculated for conditions that lie midway between VOCs limitation and NOx limitation (the transitional regime)." The VOC-to-NOx ratio is relatively high in the Metro Atlanta area as found in previous work (Hidy and Blanchard, 2015). Reactivity-weighted concentrations (RWC) are calculated as follows:

$$\text{RWC in ppb} = \frac{(\text{VOC concentrations in ppbC})}{(\text{Carbon Number})} \times (\text{EBIR Scale})$$

Daily average measured VOCs concentrations were used to calculate reactivity-weighted concentrations. Though diurnal concentration patterns vary with VOC species which have different emissions characteristics and go through different photochemical reactions, correlation of MDA8O3 and VOC or VOC species with different average periods and types is similar. Table 14 lists daily average measured concentrations, number of carbons, EBIR scales, and reactivity-weighted concentrations of major PAMS VOCs species for the analysis period in 2016 and 2017.

It clearly shows that each VOCs species has difference in their abundance in the atmosphere (concentrations) and ozone forming capability per unit concentration (EBIR scale). Among all VOCs species measured at the South DeKalb PAMS monitor, isoprene has the highest reactivity-weighted concentrations, followed by ethylene, propylene, 1,2,3-trimethylbenzene, isopentane, and ethane. Isoprene is from biogenic sources. Ranking of VOCs for ozone contributions did not change between 2016 and 2017 for the top five anthropogenic species.

Table 14. Average concentrations, number of carbons, EBIR scale, and reactivity-weighted concentrations of major PAMS VOCS species at the South DeKalb PAMS monitor during summer (June-August) 2016 and 2017. Isoprene (biogenic) is shaded in green. The top five anthropogenic values are shaded in yellow.

VOCs Species	2016 Concentration (ppbC)	2017 Concentration (ppbC)	Carbon Number	EBIR Scale (mole O_3/ mole VOC)	2016 Reactivity-weighted Concentration (ppb)	2017 Reactivity-weighted Concentration (ppb)
isoprene	5.96	5.37	5	2.51	2.99	2.69
ethylene	1.53	1.78	2	2.49	1.91	2.22
propylene	0.85	0.92	3	2.95	0.84	0.91
1,2,3-trimethylbenzene	2.93	3.27	9	2.24	0.73	0.81
isopentane	2.86	3.56	5	0.66	0.38	0.47
ethane	4.23	2.32	2	0.14	0.29	0.33
propane	3.31	4.65	3	0.24	0.27	0.32
m-ethyltoluene	1.79	3.92	9	1.28	0.25	0.31
n-pentane	2.06	2.56	5	0.56	0.23	0.25
toluene	2.21	2.20	7	0.68	0.21	0.24
n-butane	1.43	1.69	4	0.52	0.19	0.22
1-butene	0.27	0.32	4	2.46	0.17	0.20
1,2,4-trimethylbenzene	0.50	0.85	9	1.74	0.10	0.11

Average reactivity-weighted concentrations of isoprene and ethylene, the two most ozone-contributing VOC species, during summertime (June-August) in 2011, 2013, 2014, 2016, and 2017 (Figure 84) show similar inter-annual variability as ozone concentrations (Figure 6). Isoprene was high in 2011 and 2016 when ozone concentrations were high; and lower in 2013, 2014 and 2017 when ozone concentrations were lower. This indicates a close correlation between ozone and isoprene concentrations. There is no clear correlation between ozone and ethylene concentrations.

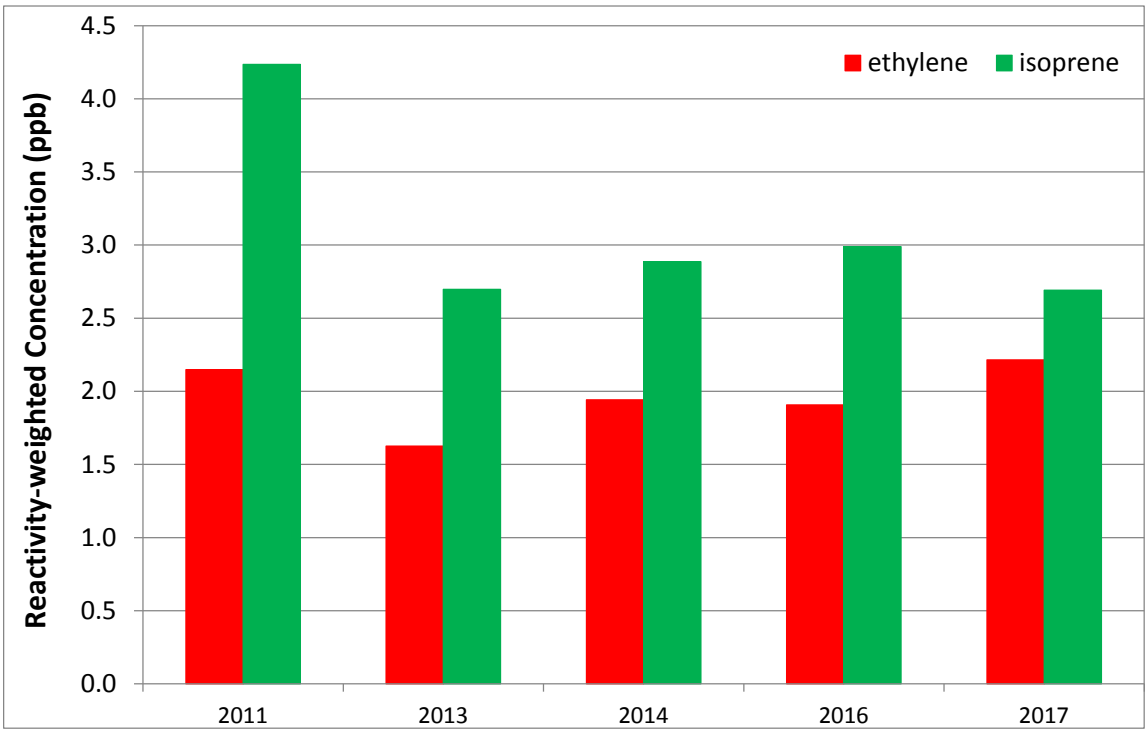

Figure 84. Average reactivity-weighted concentrations of isoprene and ethylene during summertime (June-August) in 2011, 2013, 2014, 2016, and 2017.

Ozone-VOCs Time Series Analysis

Time series of hourly ozone and reactivity-weighted VOCs concentrations during 2017 for the South DeKalb monitor were developed. Time series cover all exceedance days in July and August in the Metro Atlanta area when one or more ozone monitors exceeded the NAAQS and includes the data from one day before and the ending day of the exceedance event. The 2017 VOC measurements at the South DeKalb monitor are used in this study due to data availability and its existence in Atlanta urban core. These measurements are assumed to be representative of the photochemical conditions in the Metro Atlanta area. The representativeness can be partially verified by the high correlation of ozone measurements at the South DeKalb and Confederate Avenue monitors (Figure 85).

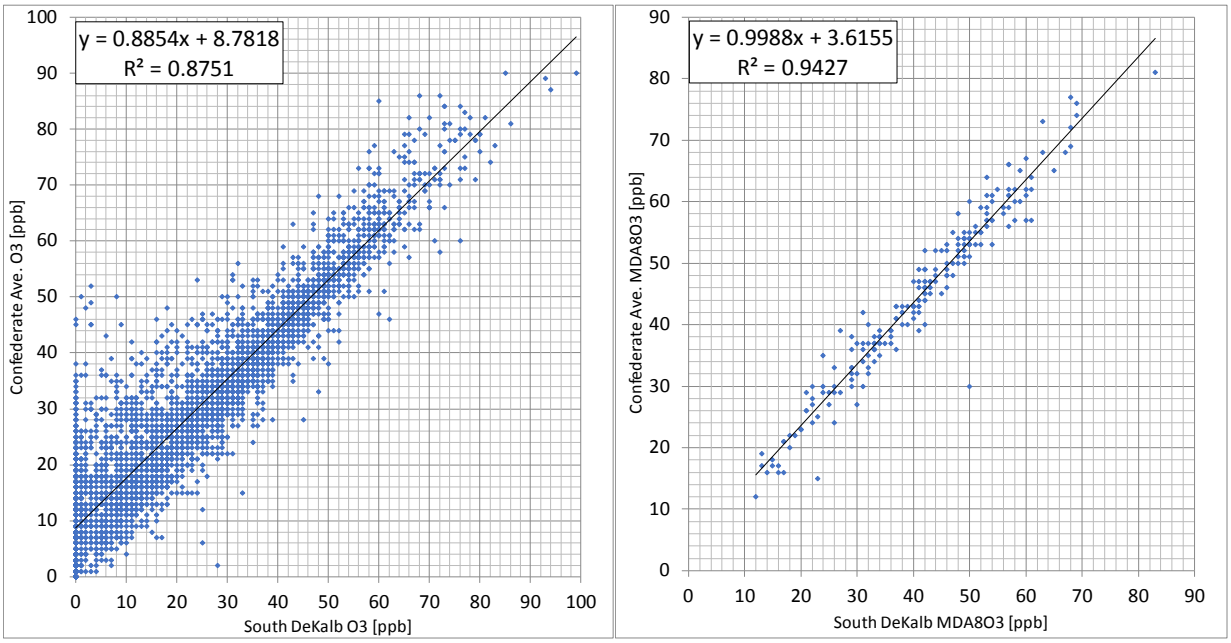

Figure 85. Correlation of 1-hour ozone concentrations (left) and MDA8O3 (right) between the South DeKalb and Confederate Ave. monitors.

Time series for five periods with ozone exceedance days at ozone monitors in the Metro Atlanta area show different conditions of anthropogenic VOCs species and isoprene during different periods (Figure 86-Figure 90). Isoprene levels during the daytime are significant on all days in July and August. Ethylene concentrations are high during the early morning and late evening hours on all ozone exceedance days in July and August, followed by propylene, 1,2,3-trimethylbenzene, isopentane, and ethane. These anthropogenic VOCs accumulate when the ozone concentrations are low and decrease rapidly as ozone is formed in the morning. Ethylene, propylene, 1,2,3-trimethylbenzene, isopentane, and ethane are mainly emitted from gasoline mobile sources and other sources that use gasoline (Nelson and Quigley, 1984; Conner et al., 1995; National Research Council, 1999). The impacts of isoprene and the anthropogenic VOCs on ozone exceedance days are in line with the ranking of reactivity-weighted VOCs concentrations shown in Table 14. This demonstrates the importance of both biogenic and anthropogenic VOCs emission sources on ozone exceedance days.

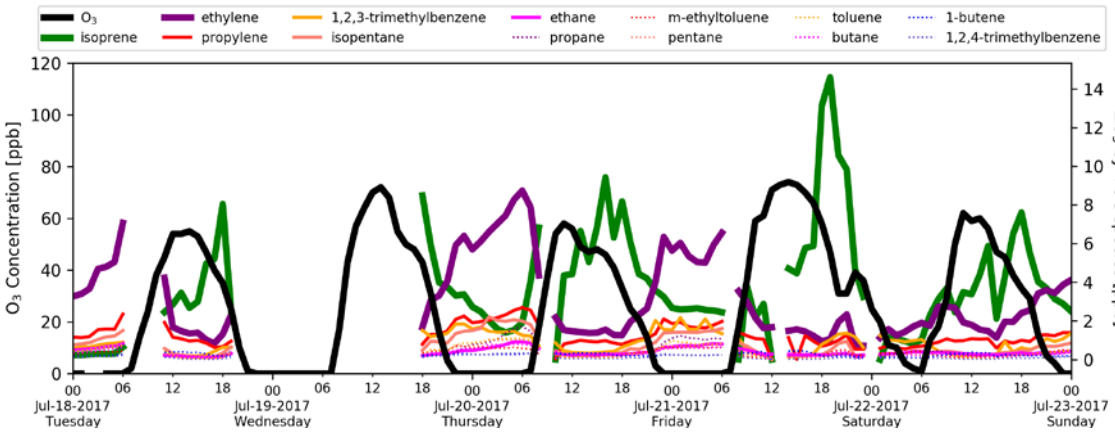

Figure 86. Time series of 1-hour ozone concentrations (left y-axis) and reactivity-weighted ozone concentration (right y-axis) for July 18-22, 2017.

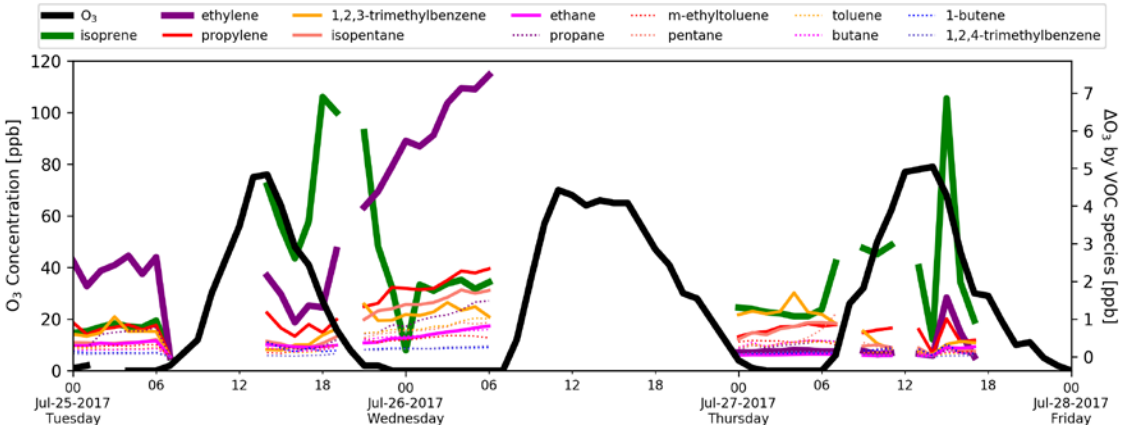

Figure 87. Time series of 1-hour ozone concentrations (left y-axis) and reactivity-weighted ozone concentration (right y-axis) for July 25-27, 2017.

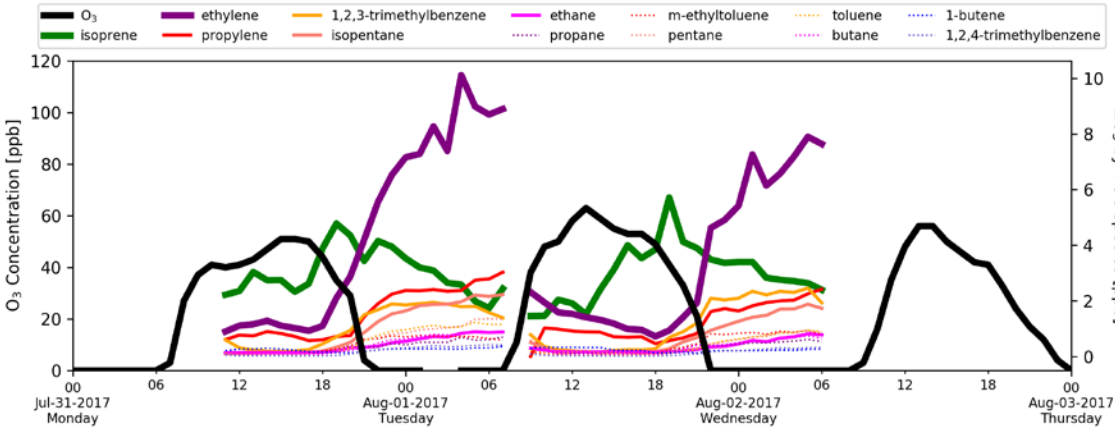

Figure 88. Time series of 1-hour ozone concentrations (left y-axis) and reactivity-weighted ozone concentration (right y-axis) for July 31-August 2, 2017.

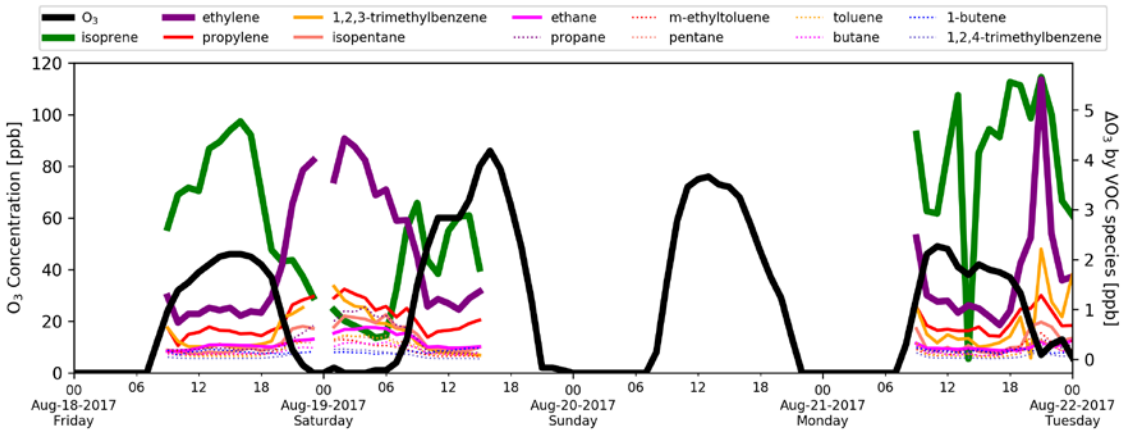

Figure 89. Time series of 1-hour ozone concentrations (left y-axis) and reactivity-weighted ozone concentration (right y-axis) for August 18-21, 2017.

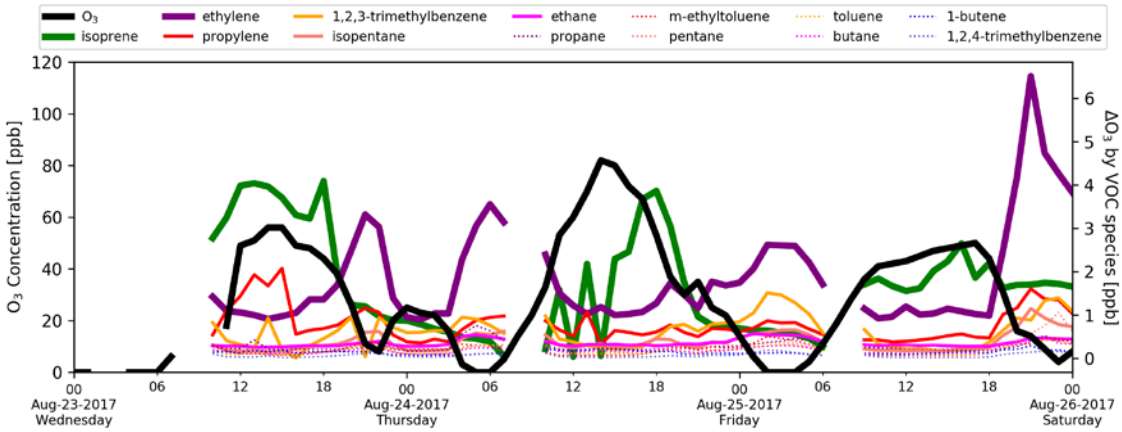

Figure 90. Time series of 1-hour ozone concentrations (left y-axis) and reactivity-weighted ozone concentration (right y-axis) for August 23-25, 2017.

HCHO trends Based on OMI Satellite Data

Formaldehyde (HCHO) has been widely used as a proxy of VOCs emissions. It is formed through the oxidation of VOCs to produce ozone in the atmosphere. Biogenic VOCs (mainly isoprene) is believed to be the main source of HCHO in the Southeastern U.S. with large forest coverage (Bauwens et al., 2016), although it can be emitted from anthropogenic sources.

Tropospheric HCHO columns derived at Belgian Institute for Space Aeronomy (BIRA) from the OMI observations were used in this study to HCHO trend. Level 3 monthly gridded vertical columns from 2005 to 2016 were downloaded from European TEMIS project (http://h2co.aeronomie.be/). 2017 data is not available yet. The monthly OMI HCHO has a global coverage with a spatial resolution of 0.25 degree.

The interannual variation of tropospheric HCHO columns is relatively small (Figure 91), ranging from 7.8 in 2015 to 10.2 molecules/cm^2 in 2006, implying the dominance of biogenic sources

whose emissions haven't changed much compared with anthropogenic sources. This is also consistent with VOCs emissions by source sectors (Figure 81). Tropospheric HCHO columns vary great by months following growing season of biogenic sources in the Southeast (Figure 92), peaking in June (15.6 molecules/cm^2) which is about 3 times of its January concentration (5.6 molecules/cm^2). The spatial difference of tropospheric HCHO columns is small over metro Atlanta (Figure 93) due to widespread biogenic emissions in the Southeast.

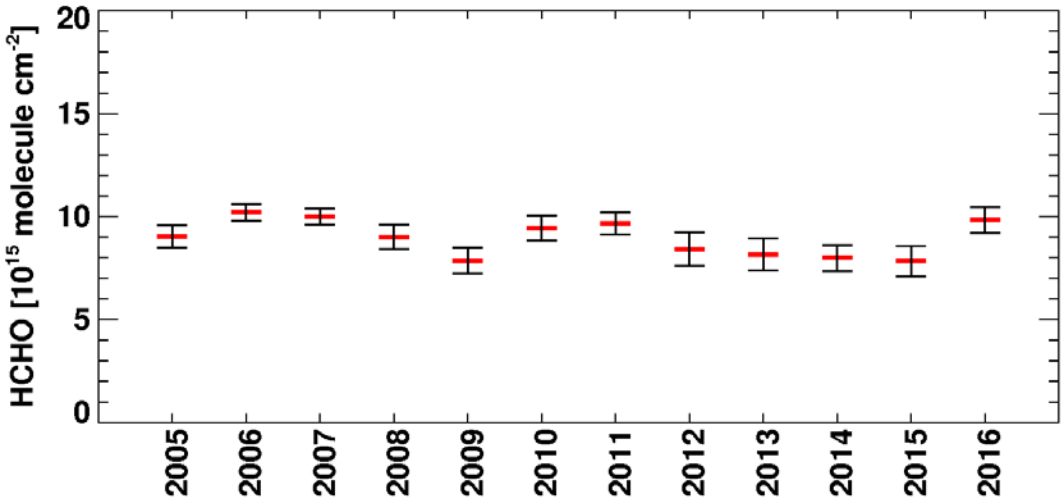

Figure 91. Annual spatial mean OMI HCHO tropospheric columns over the Metro Atlanta area in 2005-2016. The means (red bar) and its standard deviations (black bars) are shown.

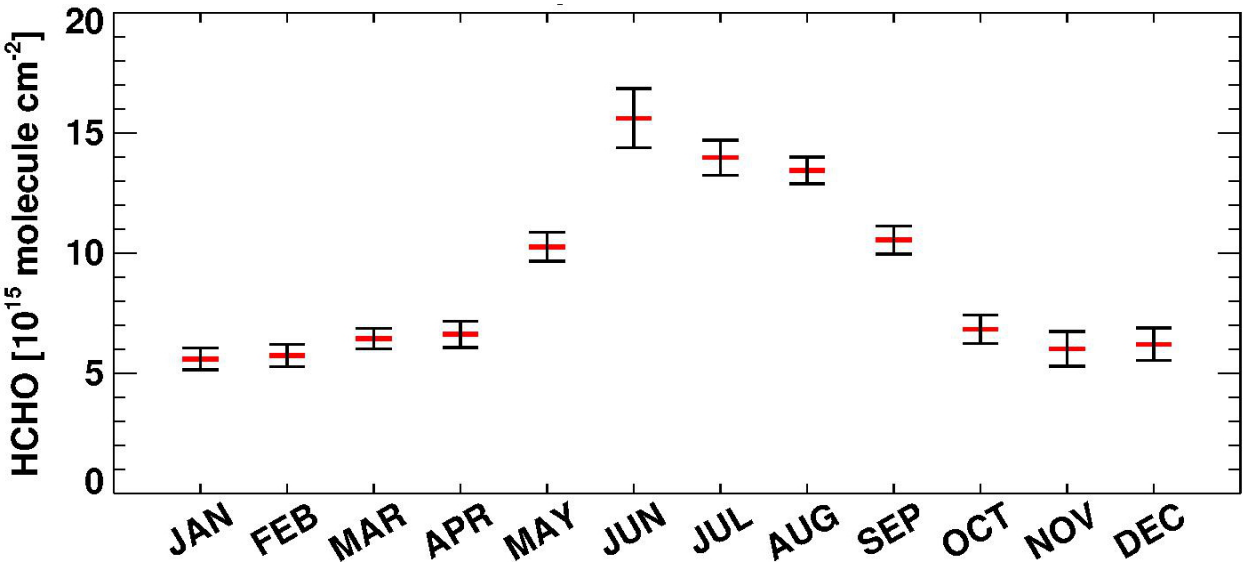

Figure 92. Monthly HCHO tropospheric columns in 2005-2016 over the Metro Atlanta area. The means (red bar) and its standard deviations (black bars) are shown.

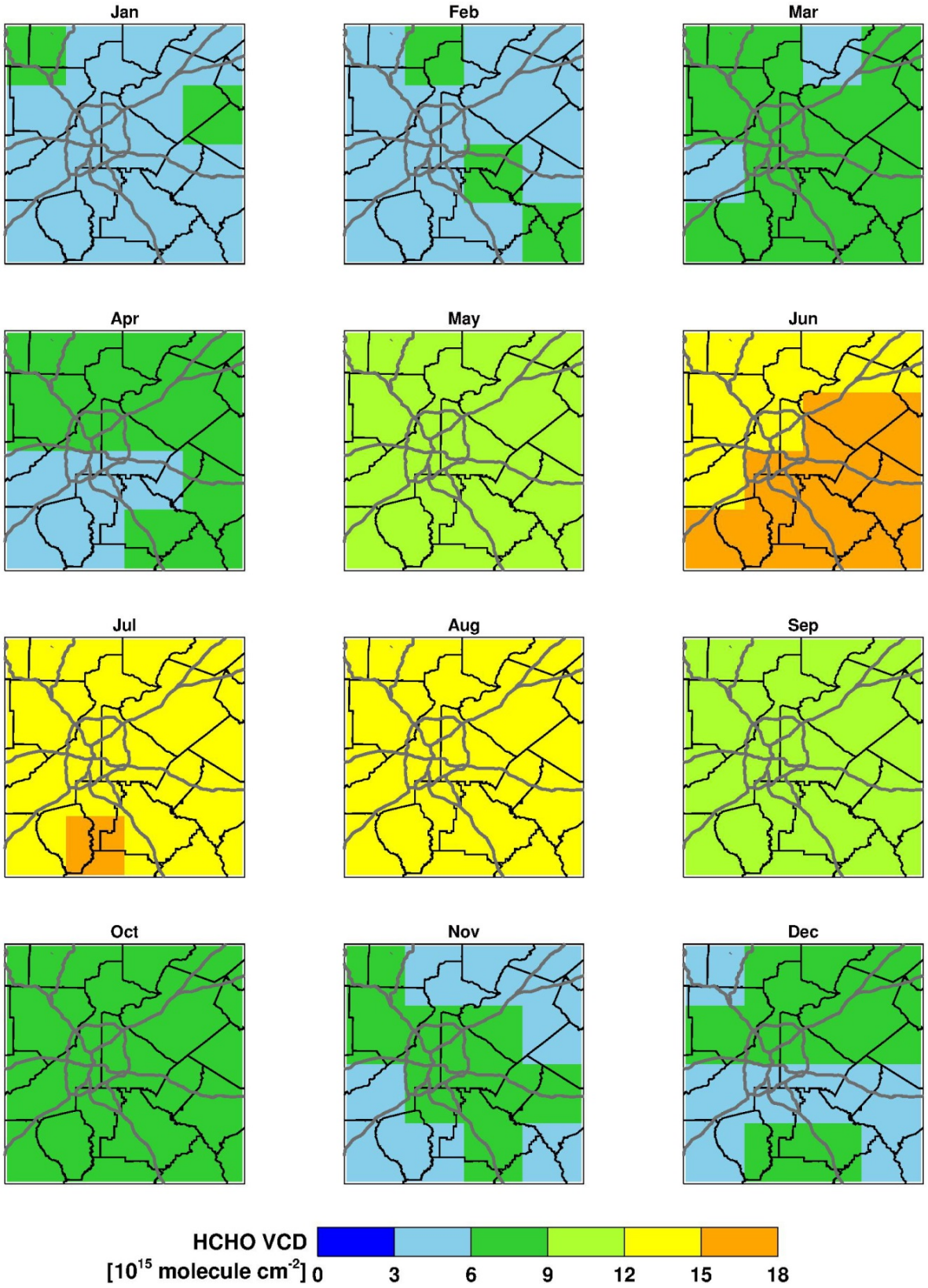

Figure 93. Monthly mean HCHO tropospheric columns over the Metro Atlanta area during 2005-2016.

The satellite derived HCHO and NO_2 ratios (FNR) were used to investigate the ozone production regime in Metro Atlanta (Martin et al, 2004, Jin et al., 2017). High HCHO and NO_2 were generally observed near its source regions due to their short lifetimes in the ambient condition. Its ratio represents the competition between OH reaction with VOC versus NO_2. Figure 94 compares the monthly means of OMI NO_2 and HCHO tropospheric columns over the urban core of Metro Atlanta. GEOS-Chem model derived ozone precursor results were applied to determine the threshold of NOx-limited and NOx-saturated regimes in each month (Jin et al., 2017). The OMI satellite data shows that ozone formation in Metro Atlanta was mostly in the NOx-limited regime except in some winter months when biogenic VOCs emission was very low.

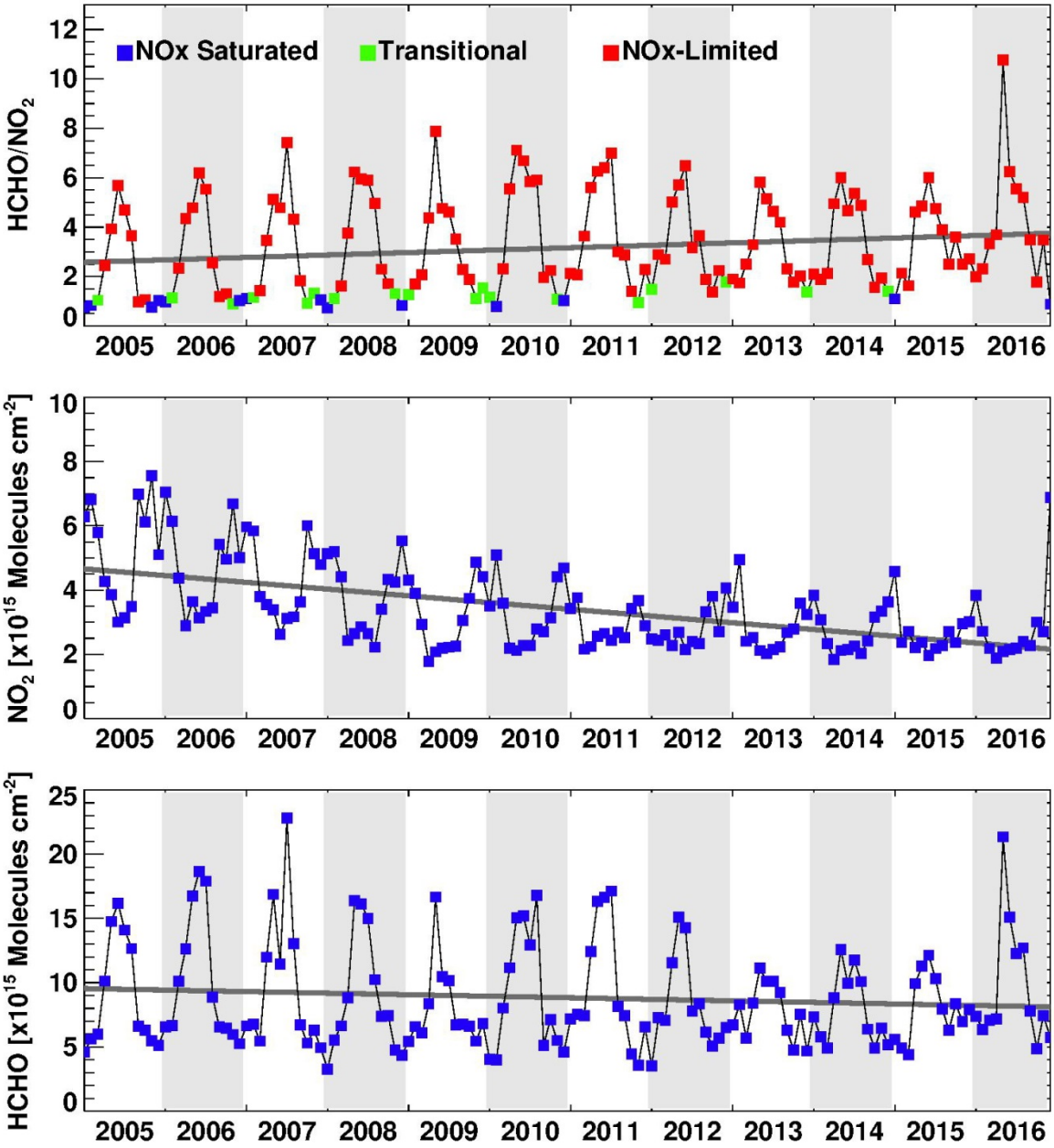

Figure 94. Monthly mean FNR (top), NO_2 (middle), and HCHO (bottom) over the Metro Atlanta area during 2005-2016. The linear trends are shown in dark grey.

9. Summary

Various in-depth analyses have been conducted to understand the causes of ozone exceedances in Atlanta during 2017. These analyses include: trend analysis of ozone exceedance and meteorological conditions in Atlanta during 1990-2017; multiple linear regression (MLR) analysis and classification and regression tree (CART) analysis to understand the relationship of Atlanta ozone and environmental variables; HYSPLIT back trajectory analysis to determine the origin of air masses and establish source-receptor relationships on ozone exceedance days; animation of ozone and wind conditions to illustrate ozone formation and transport; and analysis of VOCs and NOx measurements to understand the impacts of precursors on ozone exceedances. Also, a preliminary investigation of traffic congestion impacts on ozone exceedances was performed.

Both MLR and CART analyses have shown that ozone exceedances are likely to occur when relative humidity in the afternoon is low and daily maximum air temperature is high. These summertime meteorological conditions can occur in Atlanta under stable, stagnant conditions due to the presence of Bermuda and subtropical high pressure systems. The ozone exceedances are also associated with high ozone on previous days, low wind speed, and other meteorological variables with decreased correlation. HYSPLIT back trajectory analysis and combined analysis of ozone and wind conditions found that most 2017 ozone exceedances were linked to local air parcels. Also, the emissions from the Atlanta urban core area have been demonstrated to greatly impact local downwind monitors.

Analysis of NOx measurements in the Atlanta urban core area along with ozone measurements found that ozone exceedance occurred more often on weekdays when the NOx emissions from the dominant NOx source (on-road mobile) in the Metro Atlanta area are higher. The morning time NOx measurements on ozone exceedance days also tend to be higher due to commuter traffic. The ratio of ozone and NOx, an indicator of local ozone production efficiency, on exceedance days is close to previous studies, indicating a strong impact of NOx on ozone formation. In addition, OMI NO_2 column data have similarly shown high NO_2 concentration on weekdays and a downward trend consistent with the trend in ozone concentrations.

Analysis of VOCs measurements in the Atlanta urban core area found a strong correlation of elevated ozone concentrations with biogenic VOCs and a moderate correlation with anthropogenic VOCs. Isoprene (from biogenic sources) is the top VOC species with high reactivity-weighted concentrations. Ethylene, propylene, and isopentane (all associated with gasoline use and mobile engines) are the top three anthropogenic VOC species with high reactivity-weighted concentrations. In addition, the OMI HCHO data showed small interannual variation and large monthly variation of tropospheric HCHO from biogenic sources.

Preliminary analysis of Google traffic data and ozone exceedances in 2017 showed possible correlations on some exceedance days. However, additional analyses must be performed to more fully understand these correlations. GDOT “Navigator” speed and traffic data have been collected and will be used in future analysis.

In summary, the following factors likely contributed to 2017 ozone exceedances in Atlanta:

1) Low relative humidity in the afternoon;
2) High daily maximum air temperature;
3) Low cloud coverage;
4) High ozone on previous days;
5) Low wind speed;
6) NOx emissions, mainly from local on-road mobile sources;
7) VOC emissions, mainly from biogenic sources in the summer months with additional contributions from local on-road mobile sources in the evening and morning hours; and
8) Local transport of emissions from the Atlanta urban core to monitors outside the urban core.

The following studies and measurements are recommended to further understand the causes of future ozone exceedances in the Metro Atlanta area:

- Co-located measurements of NOx and VOC species at Confederate Ave.;
- Aircraft measurements (ozone, NOx, and CO) on elevated ozone days;
- Personal air sensors to understand spatial gradients;
- Ozone and NO_2 balloon soundings to understand vertical profiles;
- Ozone profiles from LIDAR;
- Geostationary satellite data from TEMPO (Tropospheric Emissions: Monitoring of Pollution) to be launched in 2019;
- Additional traffic studies using GPS speed data (Waze or Google maps) or GDOT "Navigator" speed and traffic data; and/or
- High resolution photochemical modeling (e.g., 1-km grid cells) to examine the impact of various emission control strategies on ozone concentrations.

Such information may help us explore new options to prevent future ozone exceedances in the Atlanta area.

10. References

Anderson, W.P., Pavlos, S.K., Miller, E.J., Buliung, R.N., 1996. Simulating automobile emissions in an integrated urban model. Transportation Research Record 1520,71-80.

Bauwens, M., T. Stavrakou, J.-F. Müller, et al. (2016). Nine years of global hydrocarbon emissions based on source inversion of OMI formaldehyde observations, Atmos. Chem. Phys., 16, 10133–10158, doi:10.5194/acp-16-10133-2016

Blanchard, C.L., Hidy, G.M., Tanenbaum, S. (2010). NMOC, ozone, and organic aerosol in the southeastern United States, 1999–2007: 2. Ozone trends and sensitivity to NMOC emissions in Atlanta, Georgia. Atmospheric Environment 44, 4840–4849. doi:10.1016/j.atmosenv.2010.07.030

Blanchard, C.L., G.M. Hidy, S. Tanenbaum (2014). Ozone in the southeastern United States: An observation-based model using measurements from the SEARCH network, Atmospheric Environment, 88 192-200.

Breiman, Leo, J. Friedman, R. Olshen, and C. Stone (1984). Classification and Regression Trees. Belmont, California: Wadsworth.

Bucsela, E. J., Krotkov, N. A., Celarier, et al. (2013). A new stratospheric and tropospheric NO2 retrieval algorithm for nadir-viewing satellite instruments: applications to OMI, Atmos. Meas. Tech., 6, 2607–2626, doi:10.5194/amt-6-2607-2013.

Cardelino, C., M. Chang, J. St. John, et al. (2011). Ozone Predictions in Atlanta, Georgia: Analysis of the 1999 Ozone Season, J. Air & Waste Manage. Assoc. 51:1227-1236.

Conner, T.L., Lonneman, W.A., Seila, R.L., 1995. Transportation-Related Volatile Hydrocarbon Source Profiles Measured in Atlanta. Journal of the Air & Waste Management Association 45, 383–394. doi:10.1080/10473289.1995.10467370

De Vlieger, I., De Keukeleere, D., Kretzschmar, J. (2000). Environmental effects of driving behavior and congestion related to passenger cars. Atmospheric Environment 34 (27), 4649-4655.

Heland, J., H. Schlager, A. Richter, and J. P. Burrows (2002). First comparison of tropospheric NO2 column densities retrieved from GOME measurements and in situ aircraft profile measurements, Geophys. Res. Lett., 29, 1983, doi:10.1029/2002GL015528, 2002.

Hidy, G.M., Blanchard, C.L., 2015. Precursor reductions and ground-level ozone in the Continental United States. Journal of the Air & Waste Management Association 65, 1261–1282. doi:10.1080/10962247.2015.1079564

Hidy, G.M., Blanchard, C.L., Baumann, K., Edgerton, E., Tanenbaum, S., Shaw, S., Knipping, E., Tombach, I., Jansen, J., Walters, J., 2014. Chemical climatology of the southeastern United States, 1999–2013. Atmospheric Chemistry and Physics 14, 11893–11914. doi:10.5194/acp-14-11893-2014

Jin, X. Fiore, A. M., Murray, L.T., et al. (2017). Evaluating space-based indicator of surface ozone-NO_x-VOC sensitivity over mid-latitude source regions and applications to decadal trends. J. Geophys. Res. Atmos, 122. https://doi.org/10.1002/2017JD026720

Lamsal, L. N., N. A. Krotkov, E. A. Celarier, et al. (2014). Evaluation of OMI operational standard NO2 column retrievals using in situ and surface-based NO2 observations, Atmos. Chem. Phys., 14, 11587–11609.
Laughner, J L., A. Zare, and R. C. Cohen (2016). Effects of daily meteorology on the interpretation of space-based remote sensing of NO2, Atmos. Chem. Phys., 16, 15247–15264.

Martin, R. V., D. D. Parrish, T. B. Ryerson, et al. (2004). Evaluation of GOME Satellite Measurements of Tropospheric NO2 and HCHO Using Regional Data from Aircraft Campaigns in the Southeastern United States. J. Geophysical Research 109 (D24): D24307. doi:10.1029/2004jd004869.

Martin, R. V., Fiore, A. M., & Van Donkelaar, A. (2004). Space-based diagnosis of surface ozone sensitivity to anthropogenic emissions. Geophys. Res. Lett., 31, L06120. https://doi.org/10.1029/2004GL019416

National Research Council, 1999. Ozone-Forming Potential of Reformulated Gasoline. National Academies Press, Washington.

Therneau, T. M., E. J. Atkinson, M. Foundation (2015). An Introduction to Recursive Partitioning Using the RPART Routines, https://cran.r-project.org/web/packages/rpart/vignettes/longintro.pdf

Timofeev, Roman (2004). Classification and Regression Trees (CART), Theory and Applications, Master Thesis. http://edoc.hu-berlin.de/master/timofeev-roman-2004-12-20/PDF/timofeev.pdf

Tonnesen, Gail S., and Robin L. Dennis. 2000. “Analysis of Radical Propagation Efficiency to Assess Ozone Sensitivity to Hydrocarbons and NO X : 1. Local Indicators of Instantaneous Odd Oxygen Production Sensitivity.” Journal of Geophysical Research 105(D7): 9213. http://apps.webofknowledge.com.proxy.lib.uiowa.edu/CitedFullRecord.do?product=WOS&colN

ame=WOS&SID=4CFNLHuzDcKBGOYfWrU&search_mode=CitedFullRecord&isickref=WOS:000086586400025\nhttp://dx.doi.org/10.1029/1999JD900371.

Seinfeld, J. H., S. N. Pandis (1998). Atmospheric chemistry and physics: from air pollution to climate change, Wiley.

Steinbacher, M., C. Zellweger, B. Schwarzenbach, et al. (2007). Nitrogen oxides measurements at rural sites in Switzerland: Bias of conventional measurement techniques, J. Geophys. Res., 112, D11307, doi:10.1029/2006JD007971.

Zhang, K., S. Batterman, F. Dion., 2011. Vehicle emissions in congestion: Comparison of work zone, rush hour and free-flow condition. Atmos. Environ., 45 1929-2939.

Zhang, Y., and Y. Wang (2016). Climate driven ground-level ozone extreme in the fall over the Southeast United States, Proc. Natl. Acad. Sci., 113, 10025-10030, doi: 10.1073/pnas.1602563113.